Plant Physiology Preview. Published on July 10, 2015, as DOI:10.1104/pp.15.00871

Running Head: Poplar undergoing short-term climate extremes

Corresponding author: Jörg-Peter Schnitzler
Email: jp.schnitzler@helmholtz-muenchen.de
Address: Helmholtz Zentrum München, Research Unit Environmental Simulation (EUS) at the Institute of Biochemical Plant Pathology (BIOP), Ingolstädter Landstraße 1, 85764 Neuherberg, Germany
Phone: +49 89 3187 2413
Fax: +49 89 3187 4431

Type of paper: Research Article
Research Area: Ecophysiology and Sustainability

Facing the future – Effects of short-term climate extremes on isoprene-emitting and non-emitting poplar

Elisa Vanzo[1], Werner Jud[2], Ziru Li[3*], Andreas Albert[1], Malgorzata A. Domagalska[4], Andrea Ghirardo[1], Bishu Niederbacher[1], Juliane Frenzel[5], Gerrit T. S. Beemster[4], Han Asard[4], Heinz Rennenberg[5], Thomas D. Sharkey[3], Armin Hansel[2], Jörg-Peter Schnitzler**[1]

1 Helmholtz Zentrum München, Research Unit Environmental Simulation (EUS) at the Institute of Biochemical Plant Pathology (BIOP), Ingolstädter Landstraße 1, 85764 Neuherberg, Germany

2 Institute for Ion Physics and Applied Physics, University of Innsbruck, Technikerstrasse 25, 6020 Innsbruck, Austria

3 Department of Biochemistry and Molecular Biology, Michigan State University, East Lansing, MI 48824, USA

4 Laboratory for Molecular Plant Physiology and Biotechnology, Department of Biology, University of Antwerp, Groenenborgerlaan 171, 2020 Antwerp, Belgium

5 Institute of Forest Sciences, Chair of Tree Physiology, University of Freiburg, Georges-Koehler-Allee 53/54, 79110 Freiburg, Germany

*Present address: Benson Hill Biosystems, 1100 Corporate Square Dr., MO 63132, USA

**Corresponding author: jp-schnitzler@helmholtz-muenchen.de

Summary:

The ability to emit isoprene does not protect poplar trees from realistic short-term and periodic drought and heat waves under proposed future conditions

Financial source:

The work was financially supported (HA, TDS, AH, and JPS) by the European Science Foundation (ESF) Eurocores programme 'EuroVOL' within the joint research project 'MOMEVIP'. Research of HR and JPS was financially supported by the German Ministry of Education and Research (BMBF, 'PROBIOPA' project). MD, GB and HA are supported by the Belgian Fund for Scientific Research (FWO, grant GA13511N) and WJ and AH by the Austrian Science Funds (project no. I655-B16).

Key words: climate change scenarios, isoprene, VOC, *Populus* x *canescens*, canopy-level versus leaf-level, phytotron

Abstract

Isoprene emissions from poplar plantations can influence atmospheric chemistry and regional climate. These emissions respond strongly to temperature, [CO_2] and drought but the superimposed effect of these three climate change factors are, for the most part, unknown. Performing predicted climate change scenario simulations (periodic and chronic heat and drought spells (HDS) applied under elevated [CO_2]), we analyzed volatile organic compound (VOC) emissions, photosynthetic performance, leaf growth and overall carbon (C) gain of poplar genotypes emitting (IE) and non-emitting (NE) isoprene. We aimed (i) to evaluate the proposed beneficial effect of isoprene emission on plant stress mitigation and recovery capacity and (ii) to estimate the cumulative net C gain under the projected future climate. During HDS, the chloroplastidic electron transport rate of NE plants became impaired, while IE plants maintained high values similar to unstressed controls. During recovery from HDS episodes, IE plants reached higher daily net CO_2 assimilation rates compared to NE genotypes. Irrespective of the genotype, plants undergoing chronic HDS showed the lowest cumulative C gain. Under control conditions simulating ambient [CO_2], the C gain was lower in the IE than NE plants. In summary, the data on the overall C gain and plant growth suggest that the beneficial function of isoprene emission in poplar might be of minor importance to mitigate predicted short-term climate extremes under elevated [CO_2]. Moreover, we demonstrate that an analysis of the canopy-scale dynamics of isoprene emission and photosynthetic performance under multiple stresses is essential to understand the overall performance under proposed future conditions.

Introduction

Climate change will lead to an increase in global temperatures of at least 2 °C in the near future (IPCC, 2014). There is nowadays substantial evidence that this climate change is leading to an increase in frequency and intensity of extreme events such as heat and drought waves (Feyen and Dankers, 2009; Fischer and Schär, 2010; Perkins et al., 2012; Thorton et al., 2014) creating a sequence of recurring stress and recovery cycles for plants. Coumou and Ramstorf (2012) showed that in the last fifteen years five extreme heat waves events have occurred worldwide, four of which were observed also in Europe. Interactions between heat and drought under predicted elevated [CO_2] (IPCC, 2014) generate complex, often nonadditive physiological responses. Such effects cannot be predicted by single-factor analyses and highlight the importance of carrying out controlled, multi-stress scenarios to investigate plant performance under future climate conditions (Clausen et al., 2011; Alemayehu et al., 2014).

Photosynthesis, respiration and photorespiration are the three dominating processes determining carbon (C) exchange and C metabolism in plants (Bauwe et al., 2010; Mahecha et al., 2010). In addition, the emission of biogenic volatile organic compounds (BVOCs) contributes to the overall C exchange of plants with isoprene being the most abundant volatile compound that is released by vegetation, in particular by forest ecosystems (Guenther et al., 2006). Due to its high reactivity, isoprene can significantly influence the oxidative capacity of the troposphere as well as cloud formation with important consequences for air quality, climate, ecosystem processes, and even human health (Bell et al., 2007; Ashworth et al., 2012).

From a plant's perspective, isoprene is an important bioactive hydrocarbon, participating in the mitigation of a wide range of abiotic stresses (Loreto and Schnitzler, 2010), in particular transient episodes of high temperature and light (Monson et al., 1992; Sharkey et al., 2001; Behnke et al., 2007, 2010b), oxidative stress (Loreto and Velikova, 2001; Affek and Yakir, 2002; Vickers et al., 2009) and drought (Brilli et al., 2007).

In terms of carbon and energy, isoprene biosynthesis is a costly investment for the plant (Sharkey and Yeh, 2001; Ghirardo et al., 2011), and is biochemically (Schnitzler et al., 2005; Rasulov et al., 2010; Way et al., 2011; Monson et al., 2012) and transcriptionally (Mayrhofer et al., 2005; Wiberley et al., 2009) under the control of environmental factors such as light, temperature and [CO_2]. Isoprene synthesis is light-dependent (Loreto and Sharkey, 1993); however, emissions can become uncoupled from photosynthesis under stress that impairs net CO_2 assimilation and makes plants rely on alternative ('old') carbon sources (Affek and Yakir, 2003; Brilli et al., 2007; Ghirardo et al., 2011; Trowbridge et al., 2012). While isoprene biosynthesis and emission correlate with fluctuations in leaf temperature (Monson et al., 1992; Singsaas and Sharkey, 1998), increases in atmospheric [CO_2] have a more ambiguous effect on isoprene emission. At the leaf-level, isoprene biosynthesis and its consequent emission in Populus is inhibited in elevated [CO_2] environments (Rosenstiel et al., 2003; Way et al., 2011), but the inhibitory effect is reduced at temperatures higher than 30 °C (Potosnak et al., 2014). Canopy-scale flux measurements report enhanced isoprene emission at high [CO_2] due to strongly enhanced canopy leaf dry mass, and leaf area index

(Sun et al., 2013). Thus, for predicting future isoprene emissions, one has to consider not only the direct effects of global drivers on the isoprene emission capacity (e.g., light, [CO_2], and temperature), but also indirect effects resulting from changes in the overall net primary productivity (Constable et al., 1999; Arneth et al., 2008) and the impact of stress (e.g., drought).

The impact of drought alone on the amount of isoprene emission depends on the timing and severity of the stress (Brüggemann and Schnitzler, 2002; Brilli et al., 2007; Fortunati et al., 2008; Brilli et al., 2013; Tattini et al., 2014) and the co-occurrence of other abiotic stressors (e.g., temperature; Centritto et al., 2011). Previous cuvette-based measurements demonstrated that under standard conditions (fixed light and leaf temperature), the capacity for isoprene formation is sustained under mild drought stress but begins to decline when water scarcity becomes more severe or prolonged (Pegoraro et al., 2004; Brilli et al., 2007; Fortunati et al., 2008). However, how these effects on isoprene emission emerge at the canopy-scale and under fluctuating ambient climatic conditions are unknown.

The predicted increases in climate extremes, such as summer droughts and concomitant heat spells, threaten plant growth and fitness (Rennenberg et al., 2006). This threat is particularly true when stressful climatic conditions recur within short intervals, as plant fitness depends not only on tolerance during the stress but also on the ability to recover rapidly and completely after these events. The rate and extent of photosynthetic recovery have been examined in several studies (Kirschbaum, 1988; Gallé and Feller, 2007; Correia et al., 2014). However, information regarding the recovery of VOC emission following environmental stress is scarce (Pegoraro et al., 2004; Fortunati et al., 2008; Centritto et al., 2011) and virtually lacking when plants experience multiple environmental stresses. Improved mitigation of oxidative stress (via anti-oxidants) and the capacity to preserve chloroplast membrane stability during stress phases are crucial for a fast and complete recovery (Mittler and Zilinskas, 1994; Sales et al., 2013). In this context, the ascribed anti-oxidative and membrane-stabilizing properties of isoprene (Vickers et al., 2009; Velikova et al., 2011) may abate membrane damage during the occurrence of stress, paving the way for a more rapid and complete recovery.

Poplar, a strong isoprene emitter, is a widely used woody model organism (Wullschleger et al., 2002; Brunner et al., 2004; Tuskan et al., 2006). Poplars are fast-growing tree species that are globally used in plantation forestry for cellulose production or more recently in intensive short rotation coppice for bioenergy generation (Aylott et al., 2008). In the context of climate change policy to reduce greenhouse gas emissions, the cultivation of poplar in short rotation coppice is close to 'carbon neutral' (Aylott et al., 2008). However, as a fast-growing pioneer tree species, poplars are hygrophilic plants with high transpiration rates (Allen et al., 1999) and their productivity depends strongly on water availability (Tschaplinski et al., 1998). In view of the predicted water scarcity (IPCC, 2014) and the increase in the poplar plantation area, an advanced understanding of the water-use efficiency (WUE) of poplar in water-limited environments is essential.

In this study, we aimed to assess the effects of predicted climate change on the photosynthetic performance, isoprene emission, plant growth and overall fitness of poplar grown in well-controlled phytotron chambers. We designed the experimental scenarios based on the 4th IPCC report (IPCC, 2007), being consistent with the latest report (IPCC, 2014) and focused on projections of the summer climate in the short-term (until 2050) in Central Europe: elevated atmospheric [CO_2], periodic (short-term) and chronic (long-term) high temperature episodes with concomitant reduction in precipitation and intermittent, short phases of recovery. Using Grey poplar (*Populus* × *canescens*) wild type and well-established transgenic genotypes, which are almost completely suppressed in isoprene emission (Behnke et al., 2007, 2012), we aimed to address the following questions: (i) What are the dynamics of photosynthesis and VOC emissions under the different climate scenarios? (ii) Is the ability to tolerate stress and to recover different between short-term and long-term heat and drought spells, and what are the costs (in terms of C gain) that poplars will pay under the projected future climate? Finally, (iii) is trait "isoprene emission" essential for poplar to adapt to fast changing environmental extremes and influences the recovery after stress?

RESULTS

Photosynthetic parameters under climate change scenarios measured at the plant scale

We studied the photosynthetic performance of IE and NE plants under averaged present day and projected future climates (Fig. 1) by measuring the net plant (canopy) CO_2 flux (= net ecosystem exchange, NEE) and evapotranspiration rate (Fig. 2) of the plants. NEE was equal in IE and NE poplars in the control scenarios (ambient and elevated [CO_2]); overall, elevated [CO_2] increased the NEE (P = 0.001). Heat and drought spells (HDS) significantly decreased (all P values are given in Supplemental Table S1) the NEE under periodic stress (PS) and chronic stress (CS) in both IE and NE (Fig. 2) compared to plants that were grown in the control chambers under ambient and enhanced [CO_2]. After three cycles (PS) or 22 days (CS) of heat and drought, the NEE decreased to 43% and 35%, respectively, compared to the ambient control, with no differences between IE and NE genotypes. At this time point (S3), the irrigation was the lowest (Supplemental Fig. S1C). HDS also affected the evapotranspiration rates, showing similar dynamics as those that were observed for NEE but with a much more pronounced decline (Fig. 2B).

During recovery, IE plants reached significantly higher NEE rates compared to those of NE plants under both stress scenarios (P = 0.016 in PS, P = 0.042 in CS). Compared to the NEE rates of poplars under control conditions, the NEE in PS was 95% and 53% higher in IE and NE, respectively. In CS, the increase during R3 was 36% higher in IE and 25% in NE (P < 0.05 for all).

The electron transport rate (ETR), a measure of the photosynthetic performance in the light-adapted state, was similar in IE and NE plants that were grown under present and future [CO_2] when no HDS was applied. The application of periodic HDS reduced the ETR in the NE poplars during each stress cycle, while the ETR of the IE plants was maintained at control levels (or even slightly increased) during the 1st and 2nd stress cycles and decreased in the last cycle (P = 0.001; Fig. 2). The ETR in the NE plants was significantly different from that of the IE plants during the 1st (P = 0.024), 2nd (P < 0.001) and 3rd stress cycle (P = 0.014). In CS, ETR began to decrease in NE plants at day 8 of HDS reaching a minimum value of 73 $\mu mol\ m^{-2}\ s^{-1}$ at day 22, while ETR in IE plants stayed at control level over the entire experiment. The difference in the ETR between IE and NE became statistically significant at day 14 of progressive drought (S2). Similar to the PS scenario a few days of re-watering and reduced temperature were sufficient to fully recover the ETR in the NE genotype, which reached the same value as that of the IE plants (approx. 82 μmol m^{-2} s^{-1}), irrespective of treatment.

Overall plant VOC fluxes under climate change scenarios

The simulation of extreme events (PS and CS) showed dramatically increased net isoprene fluxes per leaf area (nmol isoprene m^{-2} s^{-1}) during HDS at the plant-level from emitting plants (IE) (Fig. 3A). In both of these stress scenarios, during HDS, the daily sum of isoprene fluxes was 9 times greater than that of poplars growing under unstressed conditions, with a significant increase with each stress cycle (PS) and when the stress progressed in CS scenario. Under enhanced [CO_2], the isoprene fluxes from the IE plants were slightly lower compared to those of the plants that were grown throughout the entire experimental period under present day [CO_2] but statistically significantly lower when the measurements were performed at the leaf-level under standard conditions (P = 0.019; Table I). We also calculated the isoprene emission per plant (nmol isoprene s^{-1} $plant^{-1}$). This calculation did not change the picture we obtained from the leaf area base. Here, the increase in the isoprene flux during HDS was up to 7 times greater than that of controls. Under enhanced [CO_2], the isoprene flux per plant was also slightly lower than that under ambient [CO_2]. The isoprene emission in IE genotypes showed maximal emissions around mid-day (Supplemental Fig. S3), while the NE plants showed isoprene fluxes < 5% compared to IE plants (Fig. 3A).

The emission of LOX products (m99 and m101; Fig. S2), methyl vinyl ketone (MVK) and/or methacrolein (MACR) (both m71) could not be detected. In IE, we detected as m71 the double isotope ^{13}C of isoprene (i.e. $^{13}C_2{}^{12}C_3H_8$, m71), which represents 0.305% of the isoprene emissions at m69 (Supplemental Fig. S2A). Monoterpenes (m137), which are primarily emitted by young, immature poplar leaves (Ghirardo et al., 2011), were detected in trace amounts, particularly at the beginning of the experiment, whereas sesquiterpenes (m205) were never detected (data not shown).

In addition to isoprene, methanol (MeOH) was the 2nd most abundant VOC. We used the emission of this compound as an indicator of leaf growth (Hüve et al., 2007). Generally, the emission of MeOH decreased towards the end of the experiment (Fig. 3B) and showed no difference between the IE and NE plants. Immediately after the onset of periodic or chronic HDS, the MeOH emission started to decline in both IE and NE plants (Fig. 3B). In the PS scenario, MeOH emission recovered from HDS after the 1st and much weaker after the 2nd stress cycle. Under the CS scenario, the emission of MeOH decreased constantly (Fig. 3B).

At the diurnal time scale, MeOH emission always peaked in the morning hours (Supplemental Fig. S3), most likely as a consequence of stomatal opening (Niinemets et al., 2004; Hüve et al., 2007), and decreased constantly until the evening.

Because plant primary and secondary metabolism are both temperature dependent (Monson et al., 1992; Way and Yamori, 2014), we monitored the temperature of light exposed leaves in the scenarios weekly by infrared thermography (Supplemental Fig. S4). Under unstressed conditions (time point P, all scenarios), the leaf temperature was slightly lower than the scenario air temperature (Supplemental Fig. S4B; indicated by a black, dashed line). However, during HDS, when leaf cooling by transpiration diminishes as consequence of stomatal closure (Fig. 2, Table I), the leaf temperatures in both of the genotypes were 3-4 °C higher than the scenario air temperature (Supplemental Fig. S4).

Impact of climate change scenarios on the plant water status and cell growth

To non-invasively monitor the water status of the leaves under the different scenarios, we assessed the relative water content (RWC) in young (no. 4, from apex), fully emerged (no. 8) and older leaves (no. 12) throughout the duration of the experiment by measuring the leaf near-infrared reflectance (NIR) and calculating the moisture stress index (MSI) (Hunt, 1989; Ceccato et al., 2001). The MSI was well correlated with the RWC of Grey poplar leaves during drying ($r^2 = 0.73$, $P < 0.001$; Supplemental Fig. S5) and was thus a useful indicator of the leaf RWC. Both IE and NE plants had similar RWC across the scenarios and leaf age classes (Fig. 4A). At the time points R2, S3 and R3, the RWC was 5–10% higher under elevated [CO_2] compared to that under ambient [CO_2] atmosphere. Plants in the two stress scenarios displayed a remarkable difference in the time course of the RWC. The plants in the PS scenario maintained a high leaf RWC in each leaf age class with an increase from each recovery cycle to the next (R1, R2, and R3). In CS scenario, the RWC decreased in the young leaves (no. 4) as HDS continued or was maintained at pre-stress levels in leaves no. 8 and no. 12. Re-watering induced a distinctive increase in the RWC in all of the leaf age classes in both of the stress scenarios, but the rate of increase almost doubled in CS compared to PS (Fig. 4A). As classical measure of the water status, we also analyzed the shoot water potential (mid-day) on a subset of plants at S3 and R3 (Fig. 4B). At S3, both of the genotypes exhibited significantly reduced water potentials compared to those of control plants (P < 0.001, all). Compared to PS, the water potentials under chronic water scarcity were significantly lower (P = 0.002), indicative of more severe water stress in CS (Fig. 4B). The final recovery phase in both stress scenarios showed no difference in the RWC or mid-day water potential between IE and NE poplars.

To understand the impact of HDS on the leaf development of the IE and NE genotypes, we assessed the relative leaf expansion rates (RLER), leaf cell number and cell size. The RLER reflect the increasing total leaf area during the HDS periods. We observed a strong reduction of RLER, similar in both genotypes, during PS and CS (50% and 56%, respectively), compared to that of enhanced [CO_2] only (both $P < 0.001$; data not shown). The strong positive correlation between the leaf-level MeOH emission rates at time point S3 (Fig. 3) and the RLER ($r^2 = 0.76$, $P < 0.001$, Fig. 5A) clearly indicates the suitability of the MeOH emissions as a marker of plant cell growth.

Overall, in the span of periodic or chronic stress (day 1 – day 22), both genotypes developed fewer leaves than did the controls (leaves per plant: 16, 9, and 8 in ambient [CO_2], PS, and CS, respectively; $P < 0.001$, data not shown). Moreover, the leaf dimensions of trees that were exposed to periodic and chronic stress were smaller than were those of the control plants ($P = 0.002$, both; Fig. 5C) with no difference between PS and CS (Fig. 5C). These changes in the leaf dimensions coincide with a positive correlation between the size of the leaf blade area and the number of adaxial epidermal cells in ambient [CO_2] ($r^2 = 0.62$, $P < 0.001$), PS (r^2=0.63, $P < 0.001$), and CS (r^2=0.80, $P < 0.001$; Fig. 5B). Apparently, the leaves that were grown in different scenarios exhibited the same developmental program, i.e., the leaves of a specific size grown in different climates have a comparable number of cells (Fig. 5D). Thus, the difference in the leaf size must be attributed to a significant reduction in the cell area under stress, as observed (Fig. 5E; $P < 0.001$ for both of the scenarios).

Enclosed leaf-level measurements of photosynthetic parameters and isoprene emission

To compare plant-level (Fig. 2, 3) with leaf-level measurements, we analyzed the photosynthetic gas exchange and VOC emission rates at the leaf-scale under steady-state standard conditions (i.e., 30 °C leaf temperature and 1 000 µmol photons m^{-2} s^{-1}) at the time of maximum stress (S3) and after seven days of final recovery (R3) (Table I). At S3, the isoprene emission of fully developed IE leaves was 10% (35 nmol m^{-2} s^{-1}) higher in PS and 15% (26 nmol m^{-2} s^{-1}) lower in CS compared to that of the leaves of the ambient [CO_2] scenario (31 nmol m^{-2} s^{-1}). The lowest isoprene emission rate was observed under elevated [CO_2] (up to 40% decrease compared to ambient [CO_2]). In general, the stimulating effect of

HDS on isoprene emission was less pronounced at the leaf scale compare compared to the plant scale (Fig. 3, Table I).

At S3, the net CO_2 assimilation (A) of the leaves that were exposed to HDS decreased by approx. 55% in PS and 60% in CS (*P* < 0.001, both) compared to that of the control scenario under ambient [CO_2]. In accordance, the leaf stomatal conductance (g_s), transpiration (light and dark, E and E_d), leaf internal [CO_2] (c_i) and consequently the c_i c_a^{-1} ratio decreased during stress. The instantaneous WUE at the leaf-level, calculated as the ratio of A over E, increased under elevated [CO_2] (*P* = 0.033) and was greatest under stress scenarios (time point S3, *P* < 0.001, all). As expected, the plants that were grown under high [CO_2] generally exhibited a lower g_s and E than did the plants that were grown under ambient [CO_2] (*P* < 0.001). For the plants that were grown under ambient [CO_2], the A and g_s were higher in the IE genotype than in the NE genotype at S3 (*P* = 0.05) but not one week later (R3; *P* = 0.22). In general, the combination of temperature increase (+ 6 °C, daily maximum) and water limitation had minor effects on the basal isoprene emission capacity whilst photosynthesis was impaired. As a consequence, the fraction of carbon that was emitted as isoprene (expressed on the base of photosynthetic assimilated C) increased during HDS, being highest under CS conditions in the IE genotype (3.5%), whereas it was negligible in the NE plants (< 0.2%).

After seven days of recovery (R3), the leaves from the trees that were grown under the PS and CS scenarios reached the same g_s, E, $E_{d,}$ c_i and c_i c_a^{-1} ratio and WUE as those of the leaves of the untreated control plants (EC), whereas the A exceeded that of the control level (PS: + 15%, CS: + 20%). Overall, the leaves from the IE genotypes had higher net CO_2 assimilation rates (*P* < 0.001) in every scenario compared to NE.

Net carbon uptake and pigmentation

Based on the continuous reading of the plant net CO_2 (NEE) and net isoprene (NIE) fluxes throughout the experimental period, we calculated the net C uptake in each scenario based on the projected leaf area (NEE minus NIE; Fig. 6). Overall, there was no significant difference between the poplar genotypes within each scenario. At the end of the experiment, the net C uptake under elevated [CO_2] was approx. 22% higher in IE and 7% higher in NE compared to the ambient [CO_2] control scenario. The PS scenario reduced the uptake of C by approx. 20% and 23% in IE and NE, respectively, compared to that under enhanced [CO_2]. In the CS scenario, the plants fixed less C than in PS (IE: - 33%, NE: - 38%). Concurrently with the reduction of net C uptake, the amount of C lost as isoprene increased in the IE plants by 6-9 times during the periodic or chronic HDS compared to control conditions. The percentage of photosynthetic C lost as isoprene (daily) progressively increased as the water scarcity became more severe (Supplemental Fig. S6), finally reaching 5.8% at day 20 in the CS scenario.

As an additional measure of leaf performance under abiotic stress, we non-invasively monitored the anthocyanin, flavonol and chlorophyll contents in the leaves using an optical sensor. Cultivation under high [CO_2] resulted in higher contents of anthocyanins and flavonoids in both of the genotypes compared to cultivation under ambient [CO_2] ($P < 0.001$, Supplemental Fig. S7). The application of HDS reduced the anthocyanin and flavonoid content in the leaves that were grown under CS ($P < 0.001$, $P = 0.01$, respectively) but not in PS ($P = 0.34$, $P = 0.49$, respectively) compared to the enhanced [CO_2] control. The chlorophyll content in the leaves remained unchanged throughout the experiment within the four scenarios. However, under ambient [CO_2], the NE leaves had lower chlorophyll contents than that in the IE plants ($P < 0.05$).

Discussion

Online analysis at plant-level display the high fluctuation of gas exchange and VOC emissions under the different climate scenarios

While many studies have investigated leaf-level measurements of photosynthetic processes, transpiration and isoprene emission, most of these studies have only reported measurements from a single point in time and from one distinct leaf. In contrast, online measurements at the canopy (plant)-scale provide a dynamic, intrinsic view of the overall plant behavior under changing environmental conditions, herein climate scenarios, considering whole-ecosystem processes (such as microclimatic factors inside a canopy; Zhu et al., 2012) and allowing direct measurements of net CO_2 and VOC fluxes from entire plants. The interaction between rising temperatures, elevated [CO_2] and drought stress (during HDS) led to a strong increase in constitutive isoprene emission. This effect was less pronounced when analyzing the standard emission factor on leaf-level (1.5 times higher than in ambient [CO_2]), while the overall plant response was much stronger (9 times higher expressed based on the leaf area, 7 times higher expressed per plant). This increase in the overall plant isoprene fluxes is most likely a combination of the temperature and drought on isoprene emission. At the plant-scale, the measured air temperature (33 °C) and leaf temperature (33-37 °C, Supplemental Fig. S4) during HDS were higher than at the leaf-level (30 °C; leaf temperature). As temperature is the main driver of ISPS enzyme activity, the strong increase in the isoprene emission during HDS is probably a combined function of enhanced ISPS activity and higher substrate availability (Rasulov et al., 2010). Drought can also promote isoprene emission, albeit with a concomitant decrease in photosynthesis (Monson et al., 2007; Tattini et al., 2014), probably as a result of decreased leaf internal [CO_2] (c_i) (Table I). The ascent in canopy isoprene emission over time in the PS and CS scenarios reflects long-term acclimation to high temperatures. Here, gene activation may lead to higher ISPS amounts (Wiberley et al., 2005). Fortunati et al. (2008) showed in a combined temperature and drought experiment a decrease in leaf isoprene emission when drought was prolonged. There, the decrease in the isoprene emission was in concert with the mRNA transcript level, the protein amount and the ISPS activity and could not be offset by the elevated temperature (35 °C instead of 25 °C).

The reductions in isoprene emission capacity and overall plant emission at elevated [CO_2] are consistent with previous studies on different Populus species (e.g., *P. deltoides* in Rosenstiel et al., 2003, *P. × euroamericana* in Centritto et al., 2004, *P. deltoides* and *P. tremuloides* in Wilkinson et al., 2009, *P. × canescens* in Way et al., 2011). However, the repressive effect of elevated [CO_2] on the isoprene emission herein was more moderate, probably due to the lower experimental increase of [CO_2] (500 ppm) compared to the aforementioned studies or the high degree of species-specific variability (*P. alba* in Loreto et al., 2007) with some poplar genotypes even not showing any reduction (Eller et al., 2012).

Poplars pay for stress adaption by significant reductions in carbon gain

In the context of plant stress concepts (Lichtenthaler, 1996), the present climate change simulations effectively demonstrate plant stress resistance strategies; in other words, the ability of Grey poplar to tolerate 'unfavorable conditions' (Levitt et al., 1980) and adapt to them. The photosynthetic performance in the PS and CS scenarios shows features of eustress, which is per definition a mild, stimulating stress, strengthening plants resistance (Lichtenthaler, 1996). In this study, the NEE of poplar temporarily deviated from their normal physiological standard without exceeding the plant's limit of tolerance (= resistance minimum, Lichtenthaler, 1996) and leading to irreversible damage, as demonstrated by the fast and complete reversibility of the response, suggesting that the integrity of the photosynthetic machinery was maintained during HDS, another characteristic of drought resistance (Sofo et al., 2004; Gallé and Feller, 2007). Therefore, stomatal constraints were likely the main factors responsible for the decrease in NEE, as observed when water stress is moderate (Chaves et al., 2003), as in the PS and CS scenarios.

During recovery from HDS (short-term recoveries in PS and long-term recovery in PS and CS) the net C gain of both poplar genotypes returned to higher rates than the pre-stress and control values (AC, EC) (angle(R3) > angle(P); Fig. 7, Supplemental Table S2). Here, the experience of HDS stimulated cell metabolism and established a new physiological optimum with a higher daily NEE. Such an overcompensation of the net CO_2 assimilation during re-watering after drought stress has been reported several times (e.g. Correia et al., 2014). However, how long the priming effect in the Grey poplar plants is maintained remains to be elucidated.

We could not detect any inducible C6 volatiles that were produced from polyunsaturated fatty acids (LOX products; Feussner and Wasternack, 2002) throughout the experiment. LOX products are reliable stress markers of oxidative stress and indicate membrane damage (Beauchamp et al., 2005; Loreto et al., 2006). Thus, this result suggests that the threshold for oxidative membrane damage in Grey poplar was not exceeded during and after the stress events, and the emission of LOX products may not be a reliable feature of drought stress in poplar. The rapid and transient emission of LOX products has been reported in response to other abiotic factors including high temperature (Behnke et al., 2013), flooding (Copolovici and Niinemets, 2010) and ozone (Beauchamp et al., 2005), as well as biotic stimuli (e.g. Ghirardo et al., 2012). However, LOX emissions upon dehydration have been detected as early stress responses on cut grass (de Gouw et al., 1999; Brilli et al., 2012). These 'drought' treatments were, in contrast to our climate change scenarios, rather extreme and artificial and resulted in fast dehydration that normally does not occur in natural drought progression. It was proposed that under oxidative stress, a substantial fraction of isoprene is oxidized inside the leaf to MVK and/or MACR (Jardine et al., 2012). Here, we could not detect any isoprene oxidation products neither in measurements on the plant-level (with PTR-QMS), nor on the leaf-level (with PTR-ToF-MS).

While HDS positively triggered isoprene emission rates and NEE, we observed a long-lasting impairment of plant growth and leaf pigmentation (anthocyanins and flavonols) in both IE and NE during HDS and during the recovery phases. The strong correlation between methanol emission and RLER, clearly demonstrates that methanol is a suitable indicator of overall plant growth. The phylogenic emission of methanol is primarily associated with leaf expansion and cell elongation (Nemecek-Marshall et al., 1995; Fall and Benson, 1996; Hüve et al., 2007) and developing poplar leaves emit significantly more compared to mature ones (Ghirardo et al., 2011). The recovery of NEE in contrast to plant growth demonstrates that water limitation exerted a greater impact on cell growth (site of C use and sink activity) than on photosynthetic processes (site of carbon gain and source activity). It is common in many plant species that are exposed to moderate drought that C use (growth) decreases before the C source (photosynthesis) is impaired (Hummel et al., 2010). When stress limits resources, plants must balance primary and secondary metabolisms, investing in either plant growth or protective strategies. We did not observe an accumulation of polyphenols (anthocyanins and flavonols) in the leaves of either the IE or NE genotypes under stress exposure. However, the pool of polyphenols increased under elevated [CO_2] compared to ambient [CO_2] conditions (Fig. S7), as reported previously (Kuokkanen et al., 2001).

Isoprene emission is not essential for poplar to adapt to fast changing environmental extremes

In addition to the general physiological performance of Grey poplar under predicted future short-term extremes, we also aimed to quantify the environmental impact on transgenic poplar genotypes with an almost complete absence of isoprene emission (e.g., Behnke et al., 2007, 2010a). This interest is motivated by the proposed function of isoprene in plant stress mitigation (Loreto and Schnitzler, 2010) and the potential for biotechnological generation or the phenotyping of low-isoprene-emitting or NE poplars as a strategy to minimize the harmful effects of large poplar plantations on local air quality and human health (Ainsworth et al., 2012; Rosenkranz et al., 2014). The latter issue is especially important because the pollution of the atmosphere by isoprene is predicted to increase due to the promotion of new poplar plantations worldwide (International Poplar Commission, Synthesis of Country Progress Reports 2008).

Globally, the genotypes IE and NE performed similarly under the different stress scenarios, indicating that the absence of isoprene emission marginally influences physiology, even under periodic and chronic stress exposure. This result is in accordance with an earlier observation in which comparable growth rates, biomass yield and (projected) CO_2 uptake were reported in IE and NE plants grown for two vegetation periods under semi-natural conditions (Behnke et al., 2012). The authors presumed that the absence of any climate extreme in their field-trail might mask different sensitivities to abiotic stress and proposed experiments under more harsh environmental conditions to prove the potential stress-alleviating function of isoprene. Here, after HDS, we observed similar growth performance in both genotypes (Fig. 5). That IE plants somehow must ‘pay’ for the release of C as isoprene was recently reported for transgenic IE tobacco (Ryan et al., 2014). These authors showed that drought stress resulted in slower growth of IE plants relative to the NE wild type or vector control plants. In the control scenarios, we observed a lower cumulative net C gain in IE plants under ambient [CO_2] (Fig. 7). This difference, however, vanished under elevated [CO_2] conditions, in concomitance with decreases in the metabolic differences between IE and NE (Way et al., 2013), possibly due to the inhibitory effect of elevated [CO_2] on the MEP pathway flux (Ghirardo et al., 2014) and isoprene biosynthesis (Rosenstiel et al., 2003; Possell and Hewitt, 2011).

The strongest difference that was observed between the genotypes was an impaired ETR in the NE plants during each stress cycle (Fig. 2; PS) and when stress progressed (Fig. 2; CS). In contrast, the ETR in IE plants remained stable or became even slightly increased possibly due to increased leaf temperatures during HDS (Copolovici et al., 2005; Behnke et al., 2007). Different tolerance of ETR in IE and NE Grey poplar upon abiotic (heat and light) stress has been previously reported (Behnke et al., 2010b; Way et al., 2011). ETR reflects the quantum yield of PSII and provides information about the light reaction of photosynthesis and the CO_2 assimilation (Genty et al., 1990). Because ETR is a thylakoid-membrane-localized process, reduced ETR in heat-stressed NE plants may be explained as a consequence of altered membrane stability (Singsaas et al., 1997; Velikova et al., 2011) and/or of direct interaction of isoprene with reactive oxygen species resulting in lower oxidative damage and lipid peroxidation (Loreto and Velikova, 2001; Velikova et al., 2005; Vickers et al., 2009). Recent findings by Velikova et al. (2014, 2015) suggest that the lower ETR in NE plants may result from subcellular remodeling processes that occur in NE chloroplasts possibly as a consequence of the RNAi-mediated silencing of the ISPS. The analysis of the chloroplast ultrastructure, the proteome and the lipid composition of the thylakoid membrane of IE and NE poplars (Velikova et al., 2014; 2015) revealed a comprehensive structural and functional reorganization in the thylakoid-membranes of NE plants. The lower amount of unsaturated fatty acids (i.e. linolenic acid (18:3)) associated with a lower abundance of two oxygen-evolving complexes, PsbP, and PsbQ (subunits of PSII) and of the cytochrome b_6f complex may affect the electron flow under stress-conditions. During drought and heat, when the photo-inhibition of PSII often occurs (Murata et al., 2007), the reduced basic equipment of components of the electron transport chain in NE may be insufficient to maintain the same ETR as isoprene-emitting plants. Furthermore, in NE plants, several components of the PSII repair cycle are down-regulated (thylakoid formation protein, THF 1, thylakoid lumen protein TLP 18.3; Velikova et al., 2014), further promoting photo-inhibition, as the extent of photo-inhibition depends strongly on the plant's ability to repair PSII (Takahashi and Murata, 2008).

Despite these differences in the biochemical and biophysical properties, NE plants are not deterred in growth or CO_2 fixation in a future, high-[CO_2] climate with recurring heat and drought spells. Moreover, a recent phytotron study demonstrated that the long-term cultivation (9 months) under enhanced [CO_2] diminishes the physiological and metabolic differences between IE and NE plants (Way et al., 2011; Way et al., 2013), indicating that the beneficial function of isoprene emission via the enhanced abiotic stress tolerance of photosynthetic processes (Loreto and Schnitzler, 2010) under future climate conditions might be of lesser importance.

Conclusions

Overall we aimed to quantify the dynamics of the superposed effects of three global change factors (temperature, [CO_2], and water limitation) on the photosynthetic performance, VOC emissions, leaf growth, and C uptake by the woody model species poplar.

The use of highly controlled phytotron chambers allowed us to enclose the whole canopy of small Grey poplar trees to simultaneously measure single-leaf and whole-plant responses to the periodic and chronic heat and drought events that were predicted in the future climate (IPCC, 2014). The data clearly showed that whole-plant isoprene fluxes increased dynamically and strongly under the HDS, although the plants developed fewer and smaller leaves under these conditions. The poplars were able to tolerate periodic and chronic stress events but paid for their stress adaption with temporarily reduced net CO_2 assimilation and C gain. However, the higher photosynthesis rates at the end of the recovery phase suggests that the impact of periodic and chronic HDS on growth and biomass can be compensated under unstressed conditions in due time. The comparison of photosynthesis, growth and stress parameters in the IE and NE poplars suggests that isoprene emission does not enhance plant stress-mitigation under future climate in poplar.

Materials and Methods

Plant material and growth conditions

The experiments were conducted with four genotypes of *Populus* × *canescens* (Aiton.) Sm. (INRA clone 7171-B4; syn. *Populus tremula* x *Populus alba).* Two isoprene-emitting (IE) genotypes (WT and PcISPS:GUS/GFP genotypes in which the PcISPS (*P.* × *can.* isoprene synthase) promotor was fused to the β-glucuronidase (GUS) and green fluorescence protein (GFP) reporter genes; for details see Cinege et al., 2009) and two well-characterized non isoprene-emitting (NE), transgenic genotypes (35S::PcISPS-RNAi lines RA1 and RA2; see Behnke et al., 2007; Way et al., 2013). Plantlets were amplified by micropropagation under sterile conditions (Leplé et al., 1992) and rooted plantlets (approx. plant height 5 cm) were cultivated in the greenhouse in 2.2 L pots on a sandy soil (1:1 (v:v) silica sand and Fruhstorfer Einheitserde). For optimum fertilization the soil was initially mixed with a mixture of slow release-fertilizers (Triabon (Compo, Münster, Germany) and Osmocote (Scotts Miracle-Gro, Marysville, USA); 1:1, 10 g per L of soil). Furthermore, we applied a liquid fertilizer every two weeks for the duration of the experiment (0.1% (w/v) Hakaphos® Grün, Compo, Münster, Germany). Climate conditions in the greenhouse were maintained at a 16/8 h photoperiod with supplemental lighting (200-240 µmol photons m^{-2} s^{-1} at canopy level, photosynthetically active radiation (PAR)). The temperature was set to 22:18 °C (day:night), [CO_2] was ambient (380 µL L^{-1}). The plantlets were raised for 5 weeks in the greenhouse before they were moved to the phytotron chambers for the next 7 ½ weeks into different climatic scenarios and [CO_2] (see next chapter). When the plants were placed into the phytotron chambers they had reached a height of 40 ± 5 cm and leaf number of 12 ± 2. Before starting the stress scenarios (PS, CS), the plants were cultivated for 25 days to adapt growth and physiology under ambient and enhanced [CO_2] control conditions (AC, EC). At the start of 1st HDS the plants were 8 ½ weeks old. At the end of the experiment (after 52 in the phytotron chambers) the plant height was 125 ± 7 cm in the control scenarios (AC, EC) and 111 ± 7 cm in the stress scenarios (PS, CS). The leaf number was 39 ± 5 in AC and EC and 31 ± 4 in PS and CS scenarios.

Climate change scenarios

The simulation of the different environmental conditions was performed in four walk-in-size phytotron chambers at the Helmholtz Zentrum München (HMGU; for more details see Seckmeyer, 1993). Each phytotron chamber contained four sub-chambers made of acrylic glass (about 1 m^3 of volume). In each sub-chamber one genotype (WT, GUS/GFP, RA1, RA2; 12 plants from each) was accommodated. Each sub-chamber was equipped with combined air-temperature- and relative-humidity-sensors and were flushed (40 m^3 h^{-1}) by purified air (charcoal filtered) adjusted in temperature, humidity and [CO_2]. To achieve irradiation regimes very close to solar outdoor conditions from the ultraviolet (UV) to the near-infrared, the phytotron facility uses a combination of different lamps and filters which enables the simulation of the daily course of solar radiation from sunrise to sunset (Thiel et al., 1996). Details of climate conditions and plant arrangement in the sub-chambers are shown in Supplemental Fig. S1.

We simulated four environmental scenarios with the first two (1, 2) as present and future controls (daily maximum temperature of 27 °C, no stress episodes) and two stress scenarios (3, 4) with periodic and chronic exposure of increased temperatures (T = control temperature + 6 °C, daily maximum temperature of 33 °C) and water limitation (see next paragraph). The scenarios are termed as follows (see also Fig. 1). 1. (AC): Control with ambient [CO_2] = 380 µL L^{-1}. 2. (EC): Control with elevated [CO_2] = 500 µL L^{-1}. 3. (PS): Periodic stress containing three cycles (each 6 days) with increased temperature and concomitant, acute drought (hereafter referred as 'heat and drought spell', HDS). Between the 1^{st} and 2^{nd} and the 2^{nd} and 3^{rd} HDS a recovery time of two days was implemented, where temperature declined to control level (27 °C) and plants were irrigated to pot capacity. 4. (CS): Chronic stress with slowly developing drought progressing over 22 days (d) from d0 to d22 (during these days temperature was increased as in PS). The HDS in the PS and CS scenarios are followed by a final recovery time of seven days (from d22 to d29) where temperature decreased to control level and pots were irrigated to saturation. The [CO_2] in the PS and CS scenario was elevated as in EC (500 µL CO_2 L^{-1}). The CO_2 concentrations in all scenarios followed natural occurring diurnal variations. The elevated CO_2 environment in the EC, PS and CS scenarios was created by injection of pure CO_2 (+ 120 µL L^{-1}) into the air stream of the ambient [CO_2]. In our analysis, AC scenario is the direct control of PS and CS scenarios, while EC scenario was performed to compare the reported inhibitory effect of elevated [CO_2] on leaf-level isoprene emission (Wilkinson et al., 2009; Way et al., 2011) to canopy-scale dynamics (Sun et al., 2013). There was no attempt to separate temperature and drought factors in this study.

The experiment was repeated twice with exchanging the scenarios between the phytotron chambers and the position of each genotype in the sub-chambers to avoid position effects. Genotypes were pooled according to their isoprene-emission capability: WT and GUS/GFP genotypes to isoprene-emitters (IE) and RA1 and RA2 to non-emitters (NE). The start of the 1st HDS (PS) and beginning of the progressive drought (CS) is termed as day 1 (d1) of the experiment, at this time point, IE and NE poplar plants exhibited a mean height ± SE of 74 cm ± 4 cm and 72 cm ± 3 cm, respectively. Also the mean number of leaves did not differ between IE and NE (IE: 28 ± 0.4; NE: 28 ± 1).

Plant irrigation and simulation of water scarcity

The controlled water regime was obtained using automated drip irrigation systems placed in each pot half way between the stem and the edge of the pot. Plants were exposed to the short-term (in PS) and long-term drought (in CS) by reducing the amount of irrigation water gradually during each HDS (Supplemental Fig. S1C). In the PS scenario, three drought cycles were imposed to mimic natural wet–dry cycles in the field. In the 1st, 2nd and 3rd cycle the amount of water was reduced by 50%, 60% and 70% compared to AC and EC, respectively. To slow down the progression of drought in the CS scenario, in the first 5 days the irrigation amount was reduced by only 30% compared to fully watered controls in AC and EC. Every 5 days water amount in CS was reduced by 10% reaching a reduction of 70% compared to the controls.

Sampling protocol and measurements

On a weekly base we monitored non-invasively the leaf relative water content, leaf temperature, chlorophyll fluorescence of PSII and leaf pigmentation. Measurements were performed on 6 random plants of each scenario and genotype at 5-7 time points throughout the experiment, reflecting physiological important time points of PS scenario: pre-stress (P), stress 1 (S1), recovery 1 (R1), stress 2 (S2), recovery 2 (R2), stress 3 (S3) and recovery 3 (R3) (see also Fig. 7). Measurements were performed directly in the sub-chambers and always between 10:00-14:00 MEZ, when irradiation and chamber air temperature were at their maxima.

Overall plant-level gas exchange and VOC measurements were performed online with an hourly resolution from inlet and outlet air of the sub-chambers. Moreover, we measured both parameters on the leaf-level under constant conditions at the time points S3 and R3 (see below). Destructive samplings were taken at the maximum stress (S3) and after the final recovery (R3).

Overall plant leaf area estimation

The daily canopy leaf area (LA) was estimated from the total number of leaves, plant height (both assessed twice a week) and LA obtained from pictures taken on three reference plants per genotype and scenario at the time points P and S3. The number of leaves lost during the experiment (aging) was taken into account. At the two destructive samplings (S3, R3), the area of all leaves was measured (approx. 25), except the upper leaves harvested for biochemical and molecular biological analysis. The overall LA of 12 (6 plants during R3) plants was used to calculate gas exchange and VOC emission fluxes at the plant-level.

Growth analysis of leaves

For growth analysis of leaves, photos and leaf discs of three plants per genotype and scenario were taken before (P) and after the stress treatments (S3). Photos were used to calculate relative leaf expansion rates (RLER) from the formula: RLER = $\ln(LA_{S3}) - \ln(LA_P)/\Delta t$, where LA is total leaf area before (P) or after the stress (S3) treatment, and Δt is duration of the HDS (22 days). LAs were calculated for each individual plant using photos from each leaf. For cell number and cell area analysis, small discs cut out from the middle part of each photographed leaf were immediately placed in ethanol, followed by lactic acid. Samples with high starch levels were cleared and mounted in Hoyer's solution on microscope slides (Wuyts et al., 2010). Microscopic images of the adaxial epidermal cells (ca. 30-40 cells) were used to draw cells (using ImageJ software) and from the obtained drawings the cell size and cell number were calculated (Andriankaja et al., 2012). These values, together with the respective LAs, were used to calculate the cell number in each leaf. For growth analysis, data were not available for EC scenario.

Plant water status

To monitor the plant water status over time, leaf water content was measured non-invasively using the spectroradiometer HR-1024 (Spectra Vista Corporation, Poughkeepsie, New York, USA). Reflectance (R) of the upper leaf surface was recorded from 350 to 2500 nm using the leaf probe equipped with an internal tungsten halogen lamp illuminating either the reference plate (white disk of R > 99%) or the leaf upon a black disk (R < 5%). Two measurements were taken at leaf no. 4, four measurements at leaf no. 8 and 12 (from the apex). From the R measurements, the moisture stress index (MSI) = R(1600 nm)/R(820 nm) was calculated according to (Hunt, 1989) and linearly correlated to the relative water content (RWC) of the leaves. In order to calculate RWC, a drying experiment was performed: intact leaves were cut and transferred to sealed tubes containing water, allowing them to hydrate to a constant level overnight, defined as weight (W) at full turgor (W_{FT}). The next day, leaves were placed on a bench to desiccate. Reflectance spectra and W were measured every 30 min. Finally, leaf samples were oven-dried at 90 °C for 24 h to determine the dry W (W_{DW}). RWC was calculated according RWC = $(W-W_{DW})/(W_{FT}-W_{DW})$.

The water potential of the plants was determined at mid-day (ψ_{md}) using the Scholander pressure chambers (Scholander et al., 1965). Measurements of ψ_{md} were performed only at the time points S3 and R3 when destructive sampling was performed.

Online plant-level gas exchange and VOC analysis

[CO_2] and [H_2O] in the ambient air were measured with two infrared gas analyzers (IRGA) (one for two scenarios; Rosemount 100/4P, Heinz Walz GmbH, Effeltrich, Germany) continuously and sequentially throughout the entire experiment by switching to the outlet of each sub-chamber (4 per scenario) every 5 min. Every 20 min the inlet air of the chambers was measured. From the difference between outlet and inlet [CO_2]/[H_2O] of each sub-chamber the whole plant (canopy) net ecosystem exchange (NEE) and evapotranspiration were calculated according the equation of (von Caemmerer and Farquhar, 1981). These fluxes of CO_2 and H_2O were then normalized to LA unit using the canopy LA estimation of every given day (see section above).

Online determination of isoprene (m69), methanol (m33), m71, lipoxygenase (LOX) products (m99 and m101), and mono- and sesquiterpenes (m137, m205, respectively) were conducted simultaneously to the gas-exchange measurements by using a high-sensitivity proton-transfer-reaction-quadrupole mass spectrometer (PTR-QMS; Ionicon Analytik GmbH, Innsbruck, Austria) at a sampling flow rate of 200 mL min^{-1}. The PTR-QMS switched between the two IRGAs every second day. The details of the PTR-QMS operating parameters and the calibration procedures are given elsewhere (Ghirardo et al., 2010; Kreuzwieser et al., 2014). In addition, the sum of isoprene oxidation products methyl-vinyl-ketone (MVK) and methacrolein (MACR) were calculated at m/z 71, after subtracting the amount of isoprene occurring as stable ^{13}C isotope (i.e. $^{13}C_2{}^{12}C_3H_8$, 0.305% of m69). The first minute of each measurement after switching the sub-chambers was always discarded in order to avoid any memory effects. VOC concentrations in inlet air of the sub-chambers were used as background and therefore subtracted from the outlet concentrations every 20 min. In general, VOC emission rates were expressed per unit leaf area (m^2); for isoprene we calculated also the isoprene emission rate per plant.

Leaf-level gas exchange and VOC analysis

Leaf-level gas exchange measurements were performed under constant light and temperature using two GFS-3000 instruments (Heinz Walz GmbH, Effeltrich, Germany) with an 8 cm^2 clip-on-type cuvette connected online with a proton transfer reaction time of flight mass spectrometer (PTR-ToF-MS). The measurements were performed on attached leaves (no. 9 from the apex) under standard conditions (30 °C, 1,000 µmol photons m^{-2} s^{-1}, air humidity of 10,000 ppmv). The cuvette was flushed with synthetic air with growth [CO_2] (AC: 380 µL CO_2 L^{-1}; EC, PS and CS: 500 µL CO_2 L^{-1}). The measurements were carried out on the time points S3 and R3 on four plants per genotype and scenario. Each measurement cycle took 40 min per plant and was split into three time ranges: 10 min light in the cuvette, 20 min (25 min in 2nd experiment) dark in the cuvette, 10 min (5 min in 2nd experiment) background of the empty cuvette (blank for PTR-ToF-MS). While sampling from one cuvette, a plant for the subsequent measurement could be installed in the other cuvette and was allowed to acclimatize for 40 min before the measurement cycle begun.

A Teflon-bypass (heated) was inserted at the cuvettes outlet and a PTR-ToF-MS (Graus et al., 2010) drew air from the back stream lines (Supplemental Fig. S1E). The PTR-ToF-MS was operated under standard conditions, 60 °C drift-tube temperature, 540 V drift voltage and 2.3 mbar drift pressure, corresponding to an E/N of 120Td (E being the electric field strength and N the gas number density; 1Td = 10^{-17} V c^2). The instrument was calibrated once a week by dynamic dilution of VOC using a gas standard (Apel Riemer Environmental Inc., Broomfield, USA). Full PTR-ToF-MS mass spectra were recorded up to m315 with a one second time resolution. Raw data analysis was performed using the routines and methods described in Müller et al. (2010).

PSII fluorescence

Fluorescence was determined by a pulse modulation fluorometer (MiniPAM, Heinz Walz GmbH, Effeltrich, Germany) for six plants per genotype and scenario. On the basis of the measured quantum yield and PAR, the electron transport rate (ETR) was calculated according the following equation: yield x PAR x 0.5 x 0.8, where 0.5 represents the fraction of light to PSII and 0.8 accounts for the leaf absorptivity (Genty et al., 1990).

Statistics

Each sub-chamber was treated as one biological replicate and contained plants of the same genotype (either WT, GUS/GFP, RA1, or RA2). Non-destructive measurements conducted on 6 plants per sub-chamber (4 plants for leaf-level gas exchange) were first averaged to one measurement per sub-chamber and the statistics were performed on the means of each sub-chamber. Mean values of $n = 4 \pm SE$ were calculated for isoprene-emitters (IE) and non-emitters (NE) by pooling together the two repetitions of the experiment and WT with GUS/GFP (IE), and RA1 with RA2 (NE). ANOVAs were performed for each measurement time point (P, S1, R1, S2, R2, S3, R3) using the two factors "Scenarios" (AC, EC, PS, CS) and "Genotypes" (IE, NE). Post-hoc test (with Bonferroni correction) followed the ANOVA to assess pairwise comparisons between particular scenarios and the poplar genotypes. Genotype effects were always tested between IE and NE.

Online gas exchange and VOC emission data were tested based on integrated daily fluxes averaged over the above described measurement time points (P, S1, R1, S2, R2, S3, or R3). Pearson correlation tests were performed to identify relationships between the RWC and MSI (Supplemental Fig. S5) and between methanol emission (leaf-level) and RLER (Fig. 3). In all cases, results were considered significant at $P < 0.05$. All analyses were performed in SPSS (v22.0, SPSS Inc., Chicago, IL, USA).

Supplemental Material

Supplemental Table S1. Results of two-way ANOVAs and Bonferroni post-hoc tests for all measured parameters. Significant differences are marked in red when $P < 0.05$.

Supplemental Table S2. Calculated angles of different stress phases of cumulative net C gain.

Supplemental Figure S1. Time courses of air temperature, relative humidity, irrigation, and plant appearance in the four scenarios.

Supplemental Figure S2. Time course of (a) m71 and (b) LOX products (i.e. m99 + m101) emission rates of isoprene-emitting (IE, black circles) and non-emitting (NE, red circles) Grey poplar genotypes in the four scenarios (AC, EC, PS, CS).

Supplemental Figure S3. Representative day (day 20) showing the overall plant isoprene emission, MeOH emission and net ecosystem exchange (NEE) in the four scenarios.

Supplemental Figure S4. Infra-red thermography to measure leaf temperature of isoprene-emitting (IE, black) and non-emitting (NE, red) Grey poplar in the four scenarios.

Supplemental Figure S5. Drying experiment to assess the moisture stress index and the relative water context of Grey poplar leaves.

Supplemental Figure S6. Time course showing the daily percentage of the photosynthetic C loss as isoprene in the four scenarios.

Supplemental Figure S7. Effect of four scenarios on the anthocyanin index, flavonol index, nitrogen balance index (NBI®) and chlorophyll index of isoprene-emitting (IE, black circles) and non-emitting (NE, red circles) poplar genotypes.

Acknowledgements

We wish to thank the phytotron staff of HMGU for helping to maintain the experiment. We also thank Violeta Velikova and Amy Trowbridge for constructive comments on the manuscript.

Literature cited

Affek HP, Yakir D (2002) Protection by isoprene against singlet oxygen in leaves. Plant Physiol **129:** 269-277

Affek HP, Yakir D (2003) Natural abundance carbon isotope composition of isoprene reflects incomplete coupling between isoprene synthesis and photosynthetic carbon flow. Plant Physiol **131:** 1727-1736

Ainsworth EA, Yendrek CR, Sitch S, Collins WJ, Emberson LD (2012) The effects of tropospheric ozone on net primary productivity and implications for climate change. Annu Rev Plant Biol **63:** 637-661

Alemayehu FR, Frenck G, van der Linden L, Mikkelsen TN, Jorgensen RB (2014) Can barley (*Hordeum vulgare* L.) adapt to fast climate changes? A controlled selection experiment. Genetic Resources and Crop Evolution **61:**151-161

Allen SJ, Hall RL, Rosier PTW (1999) Transpiration by two poplar varieties grown as coppice for biomass production. Tree Physiol **19:** 493-501

Andriankaja M, Dhondt S, De Bodt S, Vanhaeren H, Coppens F, De Milde L, Mühlenbock P, Skirycz A, Gonzalez N, Beemster GT, Inzé D (2012) Exit from proliferation during leaf development in *Arabidopsis thaliana*: a not-so-gradual process. Dev Cell **22:** 64-78

Arneth A, Schurgers G, Hickler T, Miller PA (2008) Effects of species composition, land surface cover, CO_2 concentration and climate on isoprene emissions from European forests. Plant Biol **10:** 150-162

Ashworth K, Folberth G, Hewitt CN, Wild O (2012) Impacts of near-future cultivation of biofuel feedstocks on atmospheric composition and local air quality. ACP **12:** 919-939

Aylott MJ, Casella E, Tubby I, Street NR, Smith P, Taylor G (2008) Yield and spatial supply of bioenergy poplar and willow short-rotation coppice in the UK. New Phytol **178:** 358-370

Bauwe H, Hagemann M, Fernie AR (2010) Photorespiration: players, partners and origin. Trends Plant Sci **15:** 330-336

Beauchamp J, Wisthaler A, Hansel A, Kleist E, Miebach M, Niinemets Ü, Schurr U, Wildt J (2005) Ozone induced emissions of biogenic VOC from tobacco: relationships between ozone uptake and emission of LOX products. Plant Cell Environ **28:** 1334-1343

Behnke K, Ehlting B, Teuber M, Bauerfeind M, Louis S, Hänsch R, Polle A, Bohlmann J, Schnitzler J-P (2007) Transgenic, non-isoprene emitting poplars don't like it hot. Plant J **51:** 485-499

Behnke K, Grote R, Bruggemann N, Zimmer I, Zhou GW, Elobeid M, Janz D, Polle A, Schnitzler J-P (2012) Isoprene emission-free poplars - a chance to reduce the impact from poplar plantations on the atmosphere. New Phytol **194:** 70-82

Behnke K, Ghirardo A, Janz D, Kanawati B, Esperschütz J, Zimmer I, Schmitt-Kopplin P, Niinemets Ü, Polle A, Schnitzler JP, Rosenkranz M (2013) Isoprene function in two contrasting poplars under salt and sunflecks. Tree Physiol **33:** 562-578

Behnke K, Kaiser A, Zimmer I, Brüggemann N, Janz D, Polle A, Hampp R, Hänsch R, Popko J, Schmitt-Kopplin P, Ehlting B, Rennenberg H, Barta C, Loreto F, Schnitzler J-P (2010a) RNAi-mediated suppression of isoprene emission in poplar transiently impacts phenolic metabolism under high temperature and high light intensities: a transcriptomic and metabolomic analysis. Plant Mol Biol **74:** 61-75

Behnke K, Loivamäki M, Zimmer I, Rennenberg H, Schnitzler J-P, Louis S (2010b) Isoprene emission protects photosynthesis in sunfleck exposed Grey poplar. Photosynth Res **104:** 5-17

Bell ML, Goldberg R, Hogrefe C, Kinney PL, Knowlton K, Lynn B, Rosenthal J, Rosenzweig C, Patz JA (2007) Climate change, ambient ozone, and health in 50 US cities. Clim Chang **82:** 61-76

Brilli F, Barta C, Fortunati A, Lerdau M, Loreto F, Centritto M (2007) Response of isoprene emission and carbon metabolism to drought in white poplar (*Populus alba*) saplings. New Phytol **175**: 244-254

Brilli F, Hörtnagl L, Bamberger I, Schnitzhofer R, Ruuskanen TM, Hansel A, Loreto F, Wohlfahrt G (2012) Qualitative and quantitative characterization of volatile organic compound emissions from cut grass. Environ Sci Technol **46:** 3859-3865

Brilli F, Tsonev T, Mahmood T, Velikova V, Loreto F, Centritto M (2013) Ultradian variation of isoprene emission, photosynthesis, mesophyll conductance, and optimum temperature sensitivity for isoprene emission in water-stressed *Eucalyptus citriodora* saplings. J Exp Bot **64:** 519-528

Brüggemann N, Schnitzler J-P (2002) Comparison of isoprene emission, intercellular isoprene concentration and photosynthetic performance in water-limited oak (*Quercus pubescens* Willd. and *Quercus robur* L.) saplings. Plant Biol **4**: 456-463

Brunner AM, Busov VB, Strauss SH (2004) Poplar genome sequence: functional genomics in an ecologically dominant plant species. Trends Plant Sci **9:** 49-56

Ceccato P, Flasse S, Tarantola S, Jacquemoud S, Gregoire JM (2001) Detecting vegetation leaf water content using reflectance in the optical domain. Remote Sens Environ **77:** 22-33

Centritto M, Brilli F, Fodale R, Loreto F (2011) Different sensitivity of isoprene emission, respiration and photosynthesis to high growth temperature coupled with drought stress in black poplar (*Populus nigra*) saplings. Tree Physiol **31:** 275-286

Centritto M, Nascetti P, Petrilli L, Raschi A, Loreto F (2004) Profiles of isoprene emission and photosynthetic parameters in hybrid poplars exposed to free-air CO_2 enrichment. Plant Cell Environ **27:** 403-412

Chaves MM, Maroco JP, Pereira JS (2003) Understanding plant responses to drought - from genes to the whole plant. Funct Plant Biol **30:** 239-264

Cinege G, Louis S, Hänsch R, Schnitzler J-P (2009) Regulation of isoprene synthase promoter by environmental and internal factors. Plant Mol Biol **69:** 593-604

Clausen SK, Frenck G, Linden LG, Mikkelsen TN, Lunde C, Jorgensen RB (2011) Effects of single and multifactor treatments with elevated temperature, CO_2 and ozone on oilseed rape and barley. J Agron Crop Sci **197:** 442-453

Constable JVH, Guenther AB, Schimel DS, Monson RK (1999) Modelling changes in VOC emission in response to climate change in the continental United States. Global Change Biol **5:** 791-806

Copolovici L, Niinemets Ü (2010) Flooding induced emissions of volatile signalling compounds in three tree species with differing waterlogging tolerance. Plant Cell Environ **33:** 1582-1594

Copolovici LO, Filella I, Llusia J, Niinemets Ü, Peñuelas J (2005) The capacity for thermal protection of photosynthetic electron transport varies for different monoterpenes in *Quercus ilex*. Plant Physiol **139:** 485-496

Correia B, Pinto-Marijuan M, Neves L, Brossa R, Dias MC, Costa A, Castro BB, Araújo C, Santos C, Chaves MM, Pinto G (2014) Water stress and recovery in the performance of two *Eucalyptus globulus* clones: physiological and biochemical profiles. Physiol Plant **150:** 580-592

Coumou D, Rahmstorf S (2012). A decade of weather extremes. Nature Climate Change **2:** 491-496

de Gouw JA, Howard CJ, Custer TG, Fall R (1999) Emissions of volatile organic compounds from cut grass and clover are enhanced during the drying process. Geophys Res Lett **26:** 811-814

Eller AS, de Gouw JA, Graus M, Monson RK (2012) Variation among different genotypes of hybrid poplar with regard to leaf volatile organic compound emissions. Ecol Appl **7:** 1865-1875

Fall R, Benson AA (1996) Leaf methanol - The simplest natural product from plants. Trends Plant Sci **1:** 296-301

Feussner I, Wasternack C (2002) The lipoxygenase pathway. Annu Rev Plant Biol **53:** 275-297

Feyen L, Dankers R (2009) Impact of global warming on streamflow drought in Europe. J Geophys Res: Atmospheres **114:** D17116

Fischer EM, Schär C (2010) Consistent geographical patterns of changes in high-impact European heatwaves. Nat Geosci **3:** 398-403

Fortunati A, Barta C, Brilli F, Centritto M, Zimmer I, Schnitzler J-P, Loreto F (2008) Isoprene emission is not temperature-dependent during and after severe drought-stress: a physiological and biochemical analysis. Plant J **55:** 687-697

Gallé A, Feller U (2007) Changes of photosynthetic traits in beech saplings (*Fagus sylvatica*) under severe drought stress and during recovery. Physiol Plant **131:** 412-421

Genty B, Wonders J, Baker NR (1990) Non-photochemical quenching of Fo in leaves is emission wavelength dependent: consequences for quenching analysis and its interpretation. Photosynth Res **26:** 133-139

Ghirardo A, Gutknecht J, Zimmer I, Brüggemann N, Schnitzler J-P (2011) Biogenic volatile organic compound and respiratory CO_2 emissions after ^{13}C-labeling: online tracing of C translocation dynamics in poplar plants. PLoS One **6:** e17393

Ghirardo A, Heller W, Fladung M, Schnitzler J-P, Schröder H (2012) Function of defensive volatiles in pedunculate oak (*Quercus robur*) is tricked by the moth *Tortrix viridana*. Plant Cell Environ **35**: 2192-2207

Ghirardo A, Koch K, Taipale R, Zimmer I, Schnitzler J-P, Rinne J (2010) Determination of de novo and pool emissions of terpenes from four common boreal/alpine trees by $^{13}CO_2$ labelling and PTR-MS analysis. Plant Cell Environ **33:** 781-792

Ghirardo A, Wright LP, Bi Z, Rosenkranz M, Pulido P, Rodríguez-Concepción M, Niinemets Ü, Brüggemann N, Gershenzon J, Schnitzler J-P (2014) Metabolic flux analysis of plastidic isoprenoid biosynthesis in poplar leaves emitting and nonemitting isoprene. Plant Physiol **165:** 37-51

Graus M, Müller M, Hansel A (2010) High resolution PTR-TOF: quantification and formula confirmation of VOC in real time. J Am Soc Mass Spectrom **21:** 1037-1044

Guenther A, Karl T, Harley P, Wiedinmyer C, Palmer PI, Geron C (2006) Estimates of global terrestrial isoprene emissions using MEGAN (Model of Emissions of Gases and Aerosols from Nature). ACP **6**: 3181-3210

Hummel I, Pantin F, Sulpice R, Piques M, Rolland G, Dauzat M, Christophe A, Pervent M, Bouteillé M, Stitt M, Gibon Y, Muller B (2010) Arabidopsis plants acclimate to water deficit at low cost through changes of carbon usage: An integrated perspective using growth, metabolite, enzyme, and gene expression analysis. Plant Physiol **154:** 357-372

Hunt ERJr, Rock BN (1989) Detection of changes in leaf water content using near- and middle-infrared reflectances. Rem Sens Environ **30**: 43-54

Hüve K, Christ MM, Kleist E, Uerlings R, Niinemets Ü, Walter A, Wildt J (2007) Simultaneous growth and emission measurements demonstrate an interactive control of methanol release by leaf expansion and stomata. J Exp Bot **58:** 1783-1793

IPCC (2007) Summary for policymakers. In: Climate Change 2007: Impacts, Adaptation and Vulnerability. Contribution of Working Group II to the Fourth Assessment Report of the Intergovernmental Panel on Climate Change (eds Parry ML, Canziani OF, Palutikof JP, Van der Linden PJ, Hanson CE). Cambridge University Press, Cambridge

IPCC (2014) Near-term Climate Change: Projections and Predictability. In: Climate Change 2013: The Physical Science Basis. Contribution of Working Group I to the Fifth Assessment Report of the Intergovernmental Panel on Climate Change (eds Stocker, TF, Qin D, Plattner GK, Tignor M, Allen SK, Boschung J,Nauels A, Xia Y, Bex V, Midgley PM). Cambridge University Press, Cambridge

Jardine KJ, Monson RK, Abrell L, Saleska SR, Arneth A, Jardine A, Ishida FY, Yanez Serrano AM, Artaxo P, Karl T et al. (2012) Within-plant isoprene oxidation confirmed by direct emissions of oxidation products methyl vinyl ketone and methacrolein. Global Change Biol **18:** 973-984

Kirschbaum MUF (1988) Recovery of photosynthesis from water stress in *Eucalyptus pauciflora* - a process in two stages. Plant Cell Environ **11:** 685–694

Kreuzwieser J, Scheerer U, Kruse J, Burzlaff T, Honsel A, Alfarraj S, Georgiev P, Schnitzler J-P, Ghirardo A, Kreuzer I, Hedrich R, Rennenberg H (2014) The Venus flytrap attracts insects by the release of volatile organic compounds. J Exp Bot **65:** 755-766

Kuokkanen K, Julkunen-Tiitto R, Keinanen M, Niemela P, Tahvanainen J (2001) The effect of elevated CO_2 and temperature on the secondary chemistry of *Betula pendula* seedlings. Trees: Structure and Function **15:** 378-384

Leplé J, Brasileiro A, Michel M, Delmotte F, Jouanin L (1992) Transgenic poplars: expression of chimeric genes using four different constructs. Plant Cell Rep **11:** 137-141

Levitt J (1980) Stress concepts. In: Kozlowski, TT ed, Responses of plants to environmental stresses, Ed 2, Vol 2. Academic Press, Inc, New York, pp 3 - 20

Lichtenthaler HK (1996) Vegetation stress: An introduction to the stress concept in plants. J Plant Physiol **148:** 4-14

Loreto F, Barta C, Brilli F, Nogues I (2006) On the induction of volatile organic compound emissions by plants as consequence of wounding or fluctuations of light and temperature. Plant Cell Environ **29:** 1820-1828

Loreto F, Centritto M, Barta C, Calfapietra C, Fares S, Monson RK (2007) The relationship between isoprene emission rate and dark respiration rate in white poplar (*Populus alba* L.) leaves. Plant Cell Environ **30:** 662-669

Loreto F, Schnitzler J-P (2010) Abiotic stresses and induced BVOCs. Trends Plant Sci **15:** 154-166

Loreto F, Sharkey TD (1993) Isoprene emission by plants is affected by transmissible wound signals. Plant Cell Environ **16:** 563-570

Loreto F, Velikova V (2001) Isoprene produced by leaves protects the photosynthetic apparatus against ozone damage, quenches ozone products, and reduces lipid peroxidation of cellular membranes. Plant Physiol **127:** 1781-1787

Mahecha MD, Reichstein M, Carvalhais N, Lasslop G, Lange H, Seneviratne SI, Vargas R, Ammann C, Arain MA, Cescatti A, Janssens IA, Migliavacca M, Montagnani L, Richardson AD (2010) Global convergence in the temperature sensitivity of respiration at ecosystem level. Science **329:** 838-840

Mayrhofer S, Teuber M, Zimmer I, Louis S, Fischbach RJ, Schnitzler J-P (2005) Diurnal and seasonal variation of isoprene biosynthesis-related genes in Grey poplar leaves. Plant Physiol **139:** 474-484

Mittler R, Zilinskas BA (1994) Regulation of pea cytosolic ascorbate peroxidase and other antioxidant enzymes during the progression of drought stress and following recovery from drought. Plant J **5:** 397-405

Monson RK, Grote R, Niinemets Ü, Schnitzler J-P (2012) Modeling the isoprene emission rate from leaves. New Phytol **195:** 541-559

Monson RK, Jaeger CH, Adams WW, Driggers EM, Silver GM, Fall R (1992) Relationships among isoprene emission rate, photosynthesis, and isoprene synthase activity as influenced by temperature. Plant Physiol **98:** 1175-1180

Monson RK, Trahan N, Rosenstiel TN, Veres P, Moore D, Wilkinson M, Norby RJ, Volder A, Tjoelker MG, Briske DD, Karnosky DF, Fall R (2007) Isoprene emission from terrestrial ecosystems in response to global change: minding the gap between models and observations. Philosophical transactions. Series A, Mathematical, physical, and engineering science **365**: 1677-1695

Müller M, Graus M, Ruuskanen TM, Schnitzhofer R, Bamberger I, Kaser L, Titzmann T, Hörtnagl L, Wohlfahrt G, Karl T, Hansel A (2010) First eddy covariance flux measurements PTR-TOF. Atmos Meas Tech **3**: 387-395

Murata N, Takahashi S, Nishiyama Y, Allakhverdiev SI (2007) Photoinhibition of photosystem II under environmental stress. Biochim Biophys Acta-Bioenergetics **1767:** 414-421

Nemecek-Marshall M, MacDonald RC, Franzen JJ, Wojciechowski CL, Fall R (1995) Methanol Emission from Leaves (Enzymatic Detection of Gas-Phase Methanol and Relation of Methanol Fluxes to Stomatal Conductance and Leaf Development). Plant Physiol **108:** 1359-1368

Niinemets Ü, Loreto F, Reichstein M (2004) Physiological and physicochemical controls on foliar volatile organic compound emissions. Trends Plant Sci **9:** 180-186

Pegoraro E, Rey A, Bobich EG, Barron-Gafford G, Grieve KA, Malhi Y, Murthy R (2004) Effect of elevated CO_2 concentration and vapour pressure deficit on isoprene emission from leaves of *Populus deltoides* during drought. Funct Plant Biol **31**: 1137-1147

Perkins SE, Alexander LV, Naim JR (2012) Increasing frequency, intensity and duration of observed global heatwaves and warm spells. Geophys Res Lett **39:** L20714, doi:10.1029/2012GL053361

Possell M, Hewitt CN (2011) Isoprene emissions from plants are mediated by atmospheric CO_2 concentrations. Global Change Biol **17:** 1595–1610

Potosnak MJ, Lestourgeon L, Nunez O (2014) Increasing leaf temperature reduces the suppression of isoprene emission by elevated CO_2 concentration. Sci Total Environ **481:** 352-359

Rasulov B, Huve K, Bichele I, Laisk A, Niinemets Ü (2010) Temperature response of isoprene emission in vivo reflects a combined effect of substrate limitations and isoprene synthase activity: a kinetic analysis. Plant Physiol **154:** 1558-1570

Rennenberg H, Loreto F, Polle A, Brilli F, Fares S, Beniwal RS, Gessler A (2006) Physiological responses of forest trees to heat and drought. Plant Biol **8:** 556-571

Rosenkranz M, Pugh TAM, Schnitzler J-P, Arneth A (2014) Effect of land-use change and management on BVOC emissions - selecting climate-smart cultivars. Plant Cell Environ doi: 10.1111/pce.12453

Rosenstiel TN, Potosnak MJ, Griffin KL, Fall R, Monson RK (2003) Increased CO_2 uncouples growth from isoprene emission in an agriforest ecosystem. Nature **421:** 256-259

Ryan AC, Hewitt CN, Possell M, Vickers CE, Purnell A, Mullineaux PM, Davies WJ, Dodd IC (2014) Isoprene emission protects photosynthesis but reduces plant productivity during drought in transgenic tobacco (*Nicotiana tabacum*) plants. New Phytol **201:** 205-216

Sales CR, Ribeiro RV, Silveira JA, Machado EC, Martins MO, Lagoa AM (2013) Superoxide dismutase and ascorbate peroxidase improve the recovery of photosynthesis in sugarcane plants subjected to water deficit and low substrate temperature. Plant Physiol Biochem **73**: 326-336

Schnitzler J-P, Zimmer I, Bachl A, Arend M, Fromm J, Fischbach RJ (2005) Biochemical properties of isoprene synthase in poplar (*Populus* x *canescens*). Planta **222:** 777-786

Scholander PF, Bradstreet ED, Hemmingsen EA, Hammel HT (1965) Sap pressure in vascular plants: Negative hydrostatic pressure can be measured in plants. Science **148:** 339-346

Seckmeyer GP, Payer HD (1993) A new sunlight simulator for ecological research on plants. J Photochem Photobiol B: Biology **21:** 175-181

Sharkey TD, Chen XY, Yeh SS (2001) Isoprene increases thermotolerance of fosmidomycin-fed leaves. Plant Physiol **125:** 2001-2006

Sharkey TD, Yeh SS (2001) Isoprene emission from plants. Annu Rev Plant Physiol and Plant Mol Biol **52:** 407-436

Singsaas EL, Lerdau M, Winter K, Sharkey TD (1997) Isoprene increases thermotolerance of isoprene-emitting species. Plant Physiol **115:** 1413-1420

Singsaas EL, Sharkey TD (1998) The regulation of isoprene emission responses to rapid leaf temperature fluctuations. Plant Cell Environ **21:** 1181-1188

Sofo A, Dichio B, Xiloyannis C, Masia A (2004) Effects of different irradiance levels on some antioxidant enzymes and on malondialdehyde content during rewatering in olive tree. Plant Sci **166:** 293-302

Sun ZH, Niinemets Ü, Hüve K, Rasulov B, Noe SM (2013) Elevated atmospheric CO_2 concentration leads to increased whole-plant isoprene emission in hybrid aspen (*Populus tremula* x *Populus tremuloides*). New Phytol **198:** 788-800

Takahashi S, Murata N (2008) How do environmental stresses accelerate photoinhibition? Trends Plant Sci **13:** 178-182

Tattini M, Velikova V, Vickers C, Brunetti C, Di Ferdinando M, Trivellini A, Fineschi S, Agati G, Ferrini F, Loreto F (2014) Isoprene production in transgenic tobacco alters isoprenoid, non-structural carbohydrate and phenylpropanoid metabolism, and protects photosynthesis from drought stress. Plant Cell Environ **37:** 1950-1964

Thiel S, Döhring T, Köfferlein M, Kosak A, Martin P, Seidlitz HK (1996) A phytotron for plant stress research: How far can artificial lighting compare to natural sunlight? J Plant Physiol **148:** 456-463

Thornton PK, Ericksen PJ, Herrero M, Challinor AJ (2014) Climate variability and vulnerability to climate change: a review. Glob Change Biol **10:** 3313-3328

Trowbridge AM, Asensio D, Eller ASD, Way DA, Wilkinson MJ, Schnitzler J-P, Jackson RB, Monson RK (2012) Contribution of various carbon sources toward isoprene biosynthesis in poplar leaves mediated by altered atmospheric CO_2 concentrations. PLoS One **7:** e32387

Tschaplinski TJ, Tuskan GA, Gebre GM, Todd DE (1998) Drought resistance of two hybrid Populus clones grown in a large-scale plantation. Tree Physiol **18:** 653-658

Tuskan GA, DiFazio S, Jansson S, Bohlmann J, Grigoriev I, Hellsten U, Putnam N, Ralph S, Rombauts S, Salamov A et al. (2006) The genome of black cottonwood, *Populus trichocarpa* (Torr. and Gray). Science **313:** 1596-1604

Velikova V, Ghirardo A, Vanzo E, Merl J, Hauck SM, Schnitzler JP (2014) Genetic manipulation of isoprene emissions in poplar plants remodels the chloroplast proteome. J Prot Res **13:** 2005-2018

Velikova V, Müller C, Ghirardo A, Rock TM, Aichler M, Walch A, Schmitt-Kopplin P, Schnitzler J-P (2015) Knocking down of isoprene emission modifies the lipid matrix of thylakoid membranes and influences the chloroplast ultrastructure in poplar. Plant Physiol DOI:10.1104/pp.15.00612, preview

Velikova V, Pinelli P, Loreto F (2005) Consequences of inhibition of isoprene synthesis in *Phragmites australis* leaves exposed to elevated temperatures. Agric Ecosyst and Environ **106:** 209-217

Velikova V, Varkonyi Z, Szabo M, Maslenkova L, Nogues I, Kovács L, Peeva V, Busheva M, Garab G, Sharkey TD, Loreto F et al. (2011) Increased thermostability of thylakoid membranes in isoprene-emitting leaves probed with three biophysical techniques. Plant Physiol **157:** 905-916

Vickers CE, Possell M, Cojocariu CI, Velikova VB, Laothawornkitkul J, Ryan A, Mullineaux PM, Hewitt CN (2009) Isoprene synthesis protects transgenic tobacco plants from oxidative stress. Plant Cell Environ **32:** 520-531

von Caemmerer S, Farquhar GD (1981) Some relationships between the biochemistry of photosynthesis and the gas exchange of leaves. Planta **153:** 376-387

Way DA, Ghirardo A, Kanawati B, Esperschutz J, Monson RK, Jackson RB, Schmitt-Kopplin P, Schnitzler JP (2013) Increasing atmospheric CO_2 reduces metabolic and physiological differences between isoprene- and non-isoprene-emitting poplars. New Phytol **200:** 534-546

Way DA, Schnitzler J-P, Monson RK, Jackson RB (2011) Enhanced isoprene-related tolerance of heat- and light-stressed photosynthesis at low, but not high, CO_2 concentrations. Oecologia **166:** 273-282

Way DA, Yamori W (2014) Thermal acclimation of photosynthesis: on the importance of adjusting our definitions and accounting for thermal acclimation of respiration. Photosynth Res **119:** 89-100

Wiberley AE, Donohue AR, Westphal MM, Sharkey TD (2009) Regulation of isoprene emission from poplar leaves throughout a day. Plant Cell Environ **32:** 939-947

Wiberley AE, Linskey AR, Falbel TG, Sharkey TD (2005) Development of the capacity for isoprene emission in kudzu. Plant Cell Environ **28:** 898-905

Wilkinson MJ, Monson RK, Trahan N, Lee S, Brown E, Jackson RB, Polley HW, Fay PA, Fall R (2009) Leaf isoprene emission rate as a function of atmospheric CO_2 concentration. Global Change Biol **15:** 1189-1200

Wullschleger SD, Jansson S, Taylor G (2002) Genomics and forest biology: Populus emerges as the perennial favorite. Plant Cell **14:** 2651-2655

Wuyts N, Palauqui JC, Conejero G, Verdeil JL, Granier C, Massonnet C (2010) High-contrast three-dimensional imaging of the Arabidopsis leaf enables the analysis of cell dimensions in the epidermis and mesophyll. Plant Methods **6:** 17

Zhu XG, Song QF, Ort DR (2012) Elements of a dynamic systems model of canopy photosynthesis. Curr Opin Plant Biol **15:** 237-244

Figure legends

Table I. Leaf-level measurements of photosynthetic parameters and isoprene emission. Transpiration rate in the light (E), CO_2 assimilation rate (A), water-use efficiency (WUE), stomatal water vapor conductance (g_s), intercellular [CO_2] (c_i), ratio intracellular to extracellular [CO_2] ($c_i\ c_a^{-1}$), transpiration rate in the dark (E_d), mitochondrial respiration in the dark (R_d), isoprene emission rate (I) and percentage of photosynthetic carbon emitted as isoprene (C%) in IE and NE poplar plants grown at the four different scenarios (AC, EC, PS, CS). Gas exchange measurements were performed at maximum stress (S3) and after seven days of recovery (R3). IE = isoprene-emitting, NE = non-emitting.

Figure 1. Schematic overview of the 4 climate change scenarios and measurement time points. Scenarios are: AC = ambient [CO_2], EC = elevated [CO_2], PS = periodic stress, CS = chronic stress. Time points of measurements are: P = pre-stress, S1 = stress cycle 1, R1 = recovery cycle 1, etc. Relative time is indicated along the bottom of the figure and spans from day 0 (d0) to day 29 (d29), where d0 represents the day prior to the start of the 1st HDS (PS) and beginning of the progressive drought (CS). Before day 0, the plants were cultivated for 25 days (-d25) under ambient and elevated [CO_2] (AC and EC) control climate to adjust growth and physiology. At d0 the plants were 8 ½ weeks-old.

Figure 2. A, Net ecosystem exchange (NEE), (B) evapotranspiration and (C) electron transport rate (ETR) in isoprene-emitting (IE, black circles) and non-emitting (NE, red circles) poplar genotypes. Plant-level NEE and evapotranspiration values for each scenario are given as hourly mean of n = 4 ± SE. ETR was measured on leaf no. 8 below the apex on the indicated time points. Heat and drought spells are highlighted in red. Asterisk indicates significant differences ($P < 0.05$) between IE and NE within each scenario (in addition, *P* values are given in Supplemental Table S1) and n/d = no data. Time points of measurements are: P = pre-stress, S1 = stress cycle 1, R1 = recovery cycle 1, etc. The Scenarios are: AC = ambient [CO_2], EC = elevated [CO_2], PS = periodic stress, CS = chronic stress. PS and CS scenarios were performed under elevated [CO_2].

Figure 3. Overall plant (A) isoprene emission and (B) methanol (MeOH) emission from isoprene-emitting (IE, black circles) and non-emitting (NE, red circles) poplars in the four scenarios. Heat and drought spells are highlighted in red. The data are presented as hourly

means of n = 4 ± SE. The Scenarios are: AC = ambient [CO_2], EC = elevated [CO_2], PS = periodic stress, CS = chronic stress. PS and CS scenarios were performed under elevated [CO_2].

Figure 4. Plant water status. Effect of four scenarios on the (A) relative water content (RWC) and (B) mid-day stem water potential (Ψ_{md}) in isoprene-emitting (IE, black) and non-emitting (NE, red) poplars. A, The measurement of RWC was performed on leaf no. 4, 8 and 12 (counting from the apex) based on near-infrared reflectance. Values represent means of n = 4 ± SE; dashed lines indicate the reference value of 80% RWC. Highlighted areas represent the periods of drought and heat. B, The Ψ_{md} measurements were performed during the last day of the third stress cycle in the PS scenario (S3) and after seven days of recovery (R3). Values represent means of n = 4 ± SE, dashed lines indicate Ψ_{md} = -1.0 MPa. Scenarios: AC = ambient [CO_2], EC = elevated [CO_2], PS = periodic stress, CS = chronic stress. n/d = no data. PS and CS scenarios were performed under elevated [CO_2].

Figure 5. The effect of climate scenarios on the relative leaf expansion rate (RLER), mean area per leaf, leaf cell number and cell area. A, The relationship between leaf-level MeOH emission and the RLER in the AC (black circles), PS (white circle) and CS (grey triangle) scenarios. IE and NE poplar plants were combined within each scenario. The linear regression line was generated using the values at stress time point S3: y = 90.227x - 0.6703, r^2 = 0.76, P < 0.001. B, The correlation of the LA with the corresponding cell number of leaves developed during heat and drought spells (time point P until S3) in the scenarios AC, PS and CS. Linear regression line is shown: y = 185630.591x + 6045519.819, r^2 = 0.66, P < 0.001. C to E, Measurements of mean area per leaf (C), mean cell number (D) and mean cell area of leaves (E) that developed during stress. Values represent means of n = 4 ± SE. Significant differences between control (AC) and stress scenarios (PS, CS) with ** P < 0.001; ANOVA, LSD-test. Scenarios: AC = ambient [CO_2], PS = periodic stress, CS = chronic stress. PS and CS scenarios were performed under elevated [CO_2].

Figure 6. Net carbon (C) uptake in isoprene-emitting (IE, black bars) and non-emitting (NE, red bars) poplars in the four scenarios (AC, EC, PS, and CS) at the end of the experiment. Net C uptake was calculated based on overall plant fluxes of CO_2 and isoprene (see material and method), values for IE and NE of each scenario are given as mean of 4 sub-chambers ± SE.

Dashed line indicates the reference value of 87 g C m^{-2} (= mean in AC scenario, IE). AC = ambient [CO_2], EC = elevated [CO_2], PS = periodic stress, CS = chronic stress. PS and CS scenarios were performed under elevated [CO_2].

Figure 7. Cumulative net carbon (C) gain in isoprene-emitting (IE, black lines) and non-emitting (NE, red lines) Grey poplars in the four scenarios (AC, EC, PS, and CS). Dashed lines represent auxiliary lines to calculate the angles between the x-axis and the linear slope of each indicated phase. Different phases are indicated exemplary for IE poplars and are: P = pre-stress, S1 = stress cycle 1, R1 = recovery phase 1, S2 = stress cycle 2, R2 = recovery phase 2, S3 = stress cycle 3, R3 = recovery phase 3. In CS scenario, the phases are named as follows: P = pre-stress, S_{IN} = stress initial, S_{SEV} = stress severe, R = recovery. The scenarios are: AC = ambient [CO_2], EC = elevated [CO_2], PS = periodic stress, CS = chronic stress. Grey area illustrates the C that the plants were not able to gain due to stress incidence.

Table I. Leaf-level measurements[a] of photosynthetic parameters and isoprene emission. Transpiration rate in the light (E), CO_2 assimilation rate (A), water-use efficiency (WUE), stomatal water vapor conductance (g_s), intercellular [CO_2] (c_i), ratio intracellular to extracellular [CO_2] (c_i c_a^{-1}), transpiration rate in the dark (E_d), mitochondrial respiration in the dark (R_d), isoprene emission rate (I) and percentage of photosynthetic carbon emitted as isoprene (C%) in IE and NE poplar plants grown at the 4 different scenarios (AC, EC, PS, and CS). Gas exchange measurements were performed at maximum stress (S3) and after seven days of recovery (R3). IE = isoprene-emitting, NE = non-emitting.

Timepoint	Scenario	Line	E (mmol m^{-2} s^{-1})	A (µmol m^{-2} s^{-1})	WUE (µmol $mmol^{-1}$)	g_s (mol m^{-2} s^{-1})	c_i (ppm)	c_i c_a^{-1}	E_d (mmol m^{-2} s^{-1})	R_d (µmol m^{-2} s^{-1})	I (nmol m^{-2} s^{-1})	C%
S3	AC	IE	3.79 ± 0.5a	**13.09 ± 2.2a**	3.69 ± 0.4a	**0.125 ± 0.020a**	172 ± 19ab	0.45 ± 0.0a	1.58 ± 0.6a	0.96 ± 0.2a	**30.99 ± 8.4ab**	**1.13 ± 0.1a**
		NE	2.76 ± 0.6A	**9.50 ± 0.4A**	3.88 ± 0.6A	**0.088 ± 0.02A**	168 ± 23AB	0.45 ± 0.1A	1.25 ± 0.5A	0.57 ± 0.1A	**1.26 ± 0.4A**	**0.07 ± 0.0A**
	EC	IE	2.32 ± 0.4b	12.53 ± 1.4a	5.05 ± 0.4a	0.072 ± 0.012b	213 ± 23b	0.44 ± 0.0a	0.92 ± 0.3ab	0.82 ± 0.2a	**19.00 ± 7.0a**	**0.73 ± 0.2a**
		NE	2.19 ± 0.4A	9.51 ± 1.3A	4.68 ± 0.4AB	0.068 ± 0.015AB	222 ± 22B	0.45 ± 0.0A	1.12 ± 0.3A	0.81 ± 0.2A	**0.65 ± 0.1A**	**0.04 ± 0.0A**
	PS	IE	0.73 ± 0.1c	5.64 ± 0.6b	7.34 ± 0.3b	0.021 ± 0.002c	119 ± 6a	0.24 ± 0.0b	0.15 ± 0.0b	0.83 ± 0.1a	**34.45 ± 5.1b**	**3.16 ± 0.6b**
		NE	0.71 ± 0.1B	4.51 ± 0.6B	6.22 ± 0.5BC	0.021 ± 0.002BC	147 ± 26A	0.30 ± 0.1B	0.26 ± 0.0A	1.03 ± 0.2A	**1.28 ± 0.4A**	**0.14 ± 0.0B**
	CS	IE	0.69 ± 0.2c	4.85 ± 1.3b	7.46 ± 0.7b	0.020 ± 0.007c	132 ± 9a	0.25 ± 0.0b	0.22 ± 0.0b	0.68 ± 0.2a	**26.08 ± 1.4ab**	**3.47 ± 1.1b**
		NE	0.48 ± 0.1B	3.38 ± 1.1B	6.76 ± 0.2C	0.014 ± 0.004C	117 ± 9A	0.23 ± 0.0B	0.25 ± 0.1A	0.70 ± 0.1A	**0.74 ± 0.2A**	**0.13 ± 0.0B**
R3	AC	IE	2.32 ± 0.3a	9.15 ± 1.5a	4.07 ± 0.3a	0.071 ± 0.008a	148 ± 17a	0.44 ± 0.0a	0.35 ± 0.1a	0.75 ± 0.1a	**25.51 ± 4.3a**	**1.40 ± 0.1a**
		NE	1.73 ± 0.2A	6.94 ± 0.5A	4.11 ± 0.3A	0.052 ± 0.005A	145 ± 14A	0.42 ± 0.0A	0.40 ± 0.1A	0.54 ± 0.1A	**0.88 ± 0.3A**	**0.06 ± 0.0A**
	EC	IE	2.62 ± 0.6a	12.92 ± 2.2ab	4.69 ± 0.5a	0.083 ± 0.020a	231 ± 24b	0.51 ± 0.0a	0.87 ± 0.2a	1.15 ± 0.1ab	**16.66 ± 3.4a**	**0.64 ± 0.1a**
		NE	1.91 ± 0.2A	9.60 ± 0.6AB	4.75 ± 0.3A	0.058 ± 0.006A	226 ± 18B	0.48 ± 0.0A	0.81 ± 0.1AB	0.85 ± 0.1AB	**0.66 ± 0.2A**	**0.03 ± 0.0A**
	PS	IE	2.62 ± 0.3a	14.47 ± 1.3b	5.50 ± 0.4a	0.081 ± 0.011a	189 ± 23a	0.41 ± 0.0a	1.28 ± 0.1a	0.99 ± 0.1ab	**26.47 ± 3.5a**	**0.97 ± 0.2a**
		NE	2.16 ± 0.3A	12.20 ± 0.4B	5.31 ± 0.4A	0.074 ± 0.008A	197 ± 20AB	0.44 ± 0.0A	1.59 ± 0.0BC	1.40 ± 0.2B	**1.05 ± 0.2A**	**0.04 ± 0.0A**
	CS	IE	3.45 ± 0.6a	**15.83 ± 1.7b**	5.10 ± 0.4a	0.113 ± 0.022a	211 ± 21a	0.47 ± 0.0a	2.60 ± 0.4b	1.44 ± 0.1b	**24.29 ± 2.4a**	**0.79 ± 0.1a**
		NE	2.51 ± 0.4A	**11.55 ± 1.0AB**	4.76 ± 0.3A	0.078 ± 0.014A	227 ± 17B	0.49 ± 0.0A	1.90 ± 0.3C	1.40 ± 0.1B	**0.59 ± 0.1A**	**0.03 ± 0.0A**

[a] Leaf-level (LL) cuvette measurements of gas exchange and isoprene emission performed under steady-state standard condition (30 °C leaf temperature and 1000 µmol photons m^{-2} s^{-1}). [CO_2] in the cuvette was set as in the respective scenario. Main scenario effects were tested with one-way ANOVA within each time point (S3 or R3) and are indicated by different letters (IE = small letters, NE = capital letters). Bold values indicate significant differences between the lines at the same scenario and time point. All effects were regarded as significant at $P < 0.05$. Abbreviations are: AC = control with ambient [CO_2], EC = control with elevated [CO_2], PS = periodic stress, CS = chronic stress. PS and CS scenarios were also performed under elevated [CO_2].

Figure 1. Schematic overview of the 4 climate change scenarios and measurement time points. Scenarios are: AC = ambient [CO_2], EC = elevated [CO_2], PS = periodic stress, CS = chronic stress. Time points of measurements are: P = pre-stress, S1 = stress cycle 1, R1 = recovery cycle 1, etc. Relative time is indicated along the bottom of the figure and spans from day 0 (d0) to day 29 (d29), where d0 represents the day prior to the start of the 1st HDS (PS) and beginning of the progressive drought (CS).

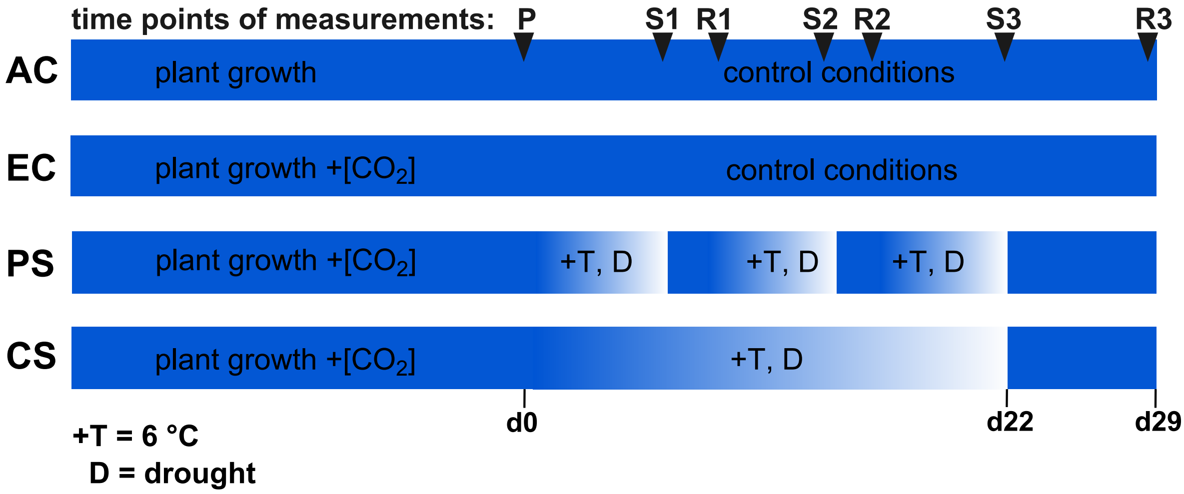

Figure 2. A, Net ecosystem exchange (NEE), (B) evapotranspiration and (C) electron transport rate (ETR) in isoprene-emitting (IE, black circles) and non-emitting (NE, red circles) poplar genotypes. Plant-level NEE and evapotranspiration values for each scenario are given as hourly mean of n = 4 ± SE. ETR was measured on leaf no. 8 below the apex on the indicated time points. Heat and drought spells are highlighted in red. Asterisk indicates significant differences ($P < 0.05$) between IE and NE within each scenario (in addition, *P* values are given in Supplemental Table S1) and n/d = no data. Time points of measurements are: P = pre-stress, S1 = stress cycle 1, R1 = recovery cycle 1, etc. The Scenarios are: AC = ambient [CO_2], EC = elevated [CO_2], PS = periodic stress, CS = chronic stress. PS and CS scenarios were performed under elevated [CO_2].

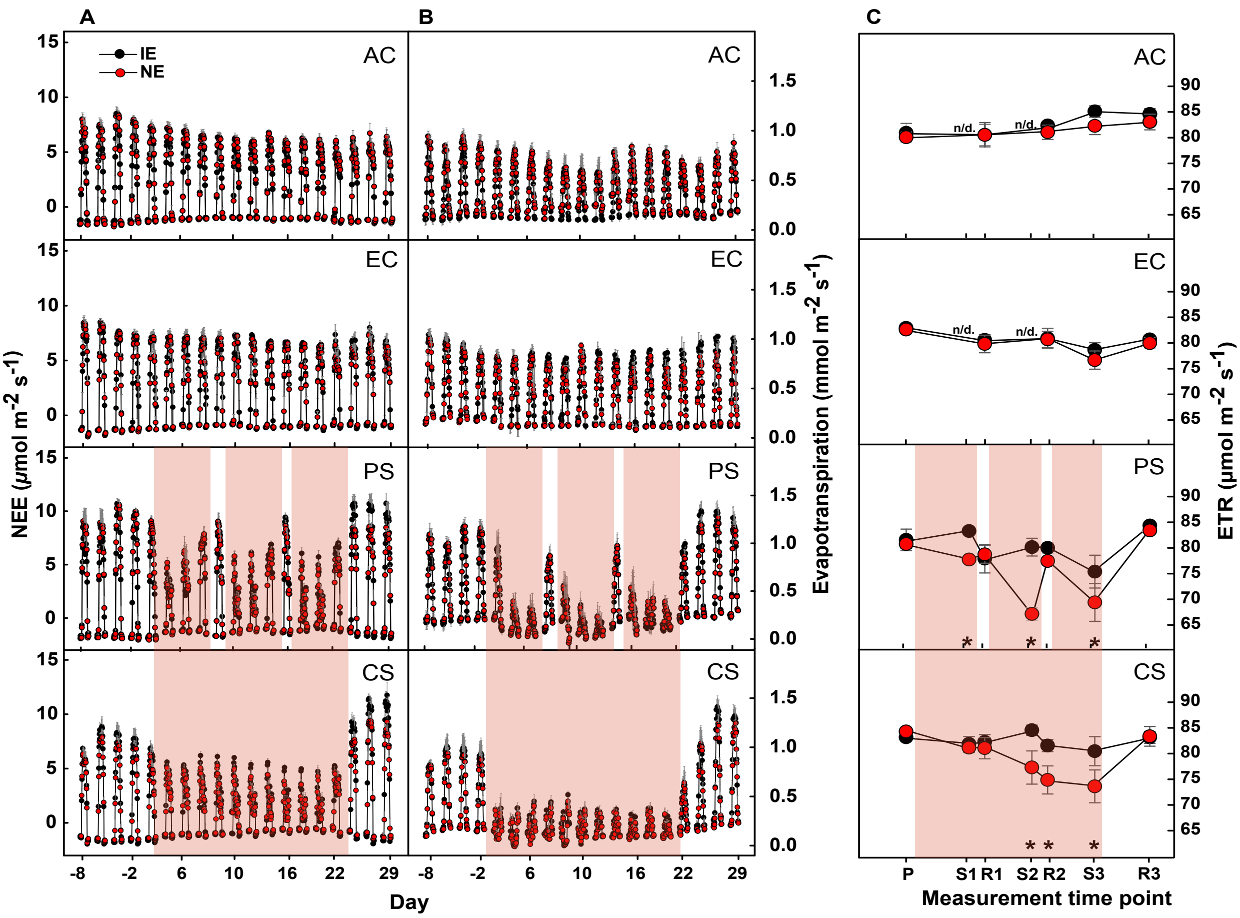

Figure 3. Overall plant (A) isoprene emission and (B) methanol (MeOH) emission from isoprene-emitting (IE, black circles) and non-emitting (NE, red circles) poplars in the four scenarios. Heat and drought spells are highlighted in red. The data are presented as hourly means of n = 4 ± SE. The Scenarios are: AC = ambient [CO_2], EC = elevated [CO_2], PS = periodic stress, CS = chronic stress. PS and CS scenarios were performed under elevated [CO_2].

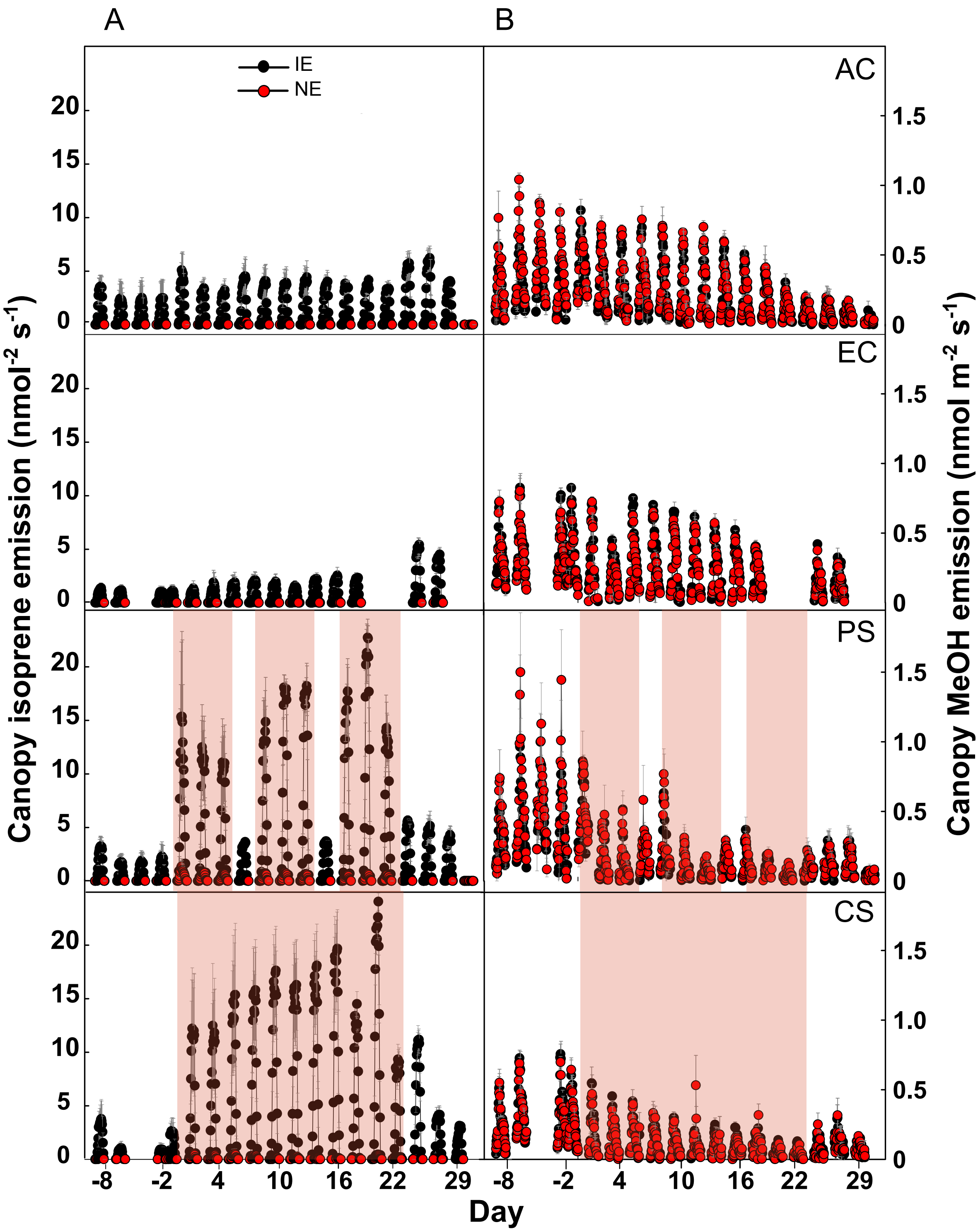

Figure 4. Plant water status. Effect of four scenarios on the (A) relative water content (RWC) and (B) mid-day stem water potential (Ψ_{md}) in isoprene-emitting (IE, black) and non-emitting (NE, red) poplars. A, The measurement of RWC was performed on leaf no. 4, 8 and 12 (counting from the apex) based on near-infrared reflectance. Values represent means of n = 4 ± SE; dashed lines indicate the reference value of 80% RWC. Highlighted areas represent the periods of drought and heat. B, The Ψ_{md} measurements were performed during the last day of the third stress cycle in the PS scenario (S3) and after seven days of recovery (R3). Values represent means of n = 4 ± SE, dashed lines indicate Ψ_{md} = -1.0 MPa. Scenarios: AC = ambient [CO_2], EC = elevated [CO_2], PS = periodic stress, CS = chronic stress. n/d = no data. PS and CS scenarios were performed under elevated [CO_2].

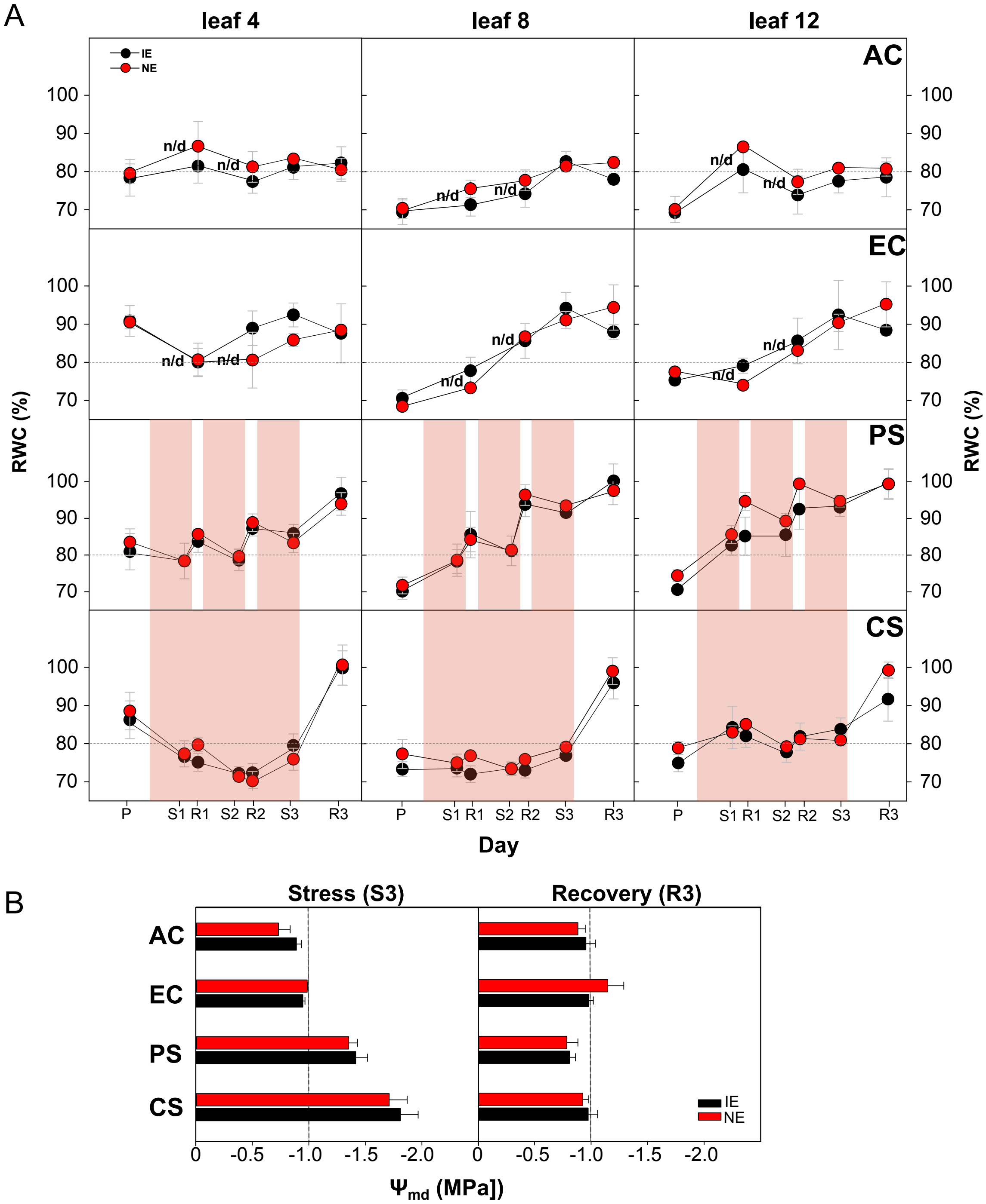

Figure 5. The effect of climate scenarios on the relative leaf expansion rate (RLER), mean area per leaf, leaf cell number and cell area. A, The relationship between leaf-level MeOH emission and the RLER in the AC (black circles), PS (white circle) and CS (grey triangle) scenarios. IE and NE poplar plants were combined within each scenario. The linear regression line was generated using the values at stress time point S3: y = 90.227x - 0.6703, $r^2 = 0.76$, $P < 0.001$. B, The correlation of the LA with the corresponding cell number of leaves developed during heat and drought spells (time point P until S3) in the scenarios AC, PS and CS. Linear regression line is shown: y = 185630.591x + 6045519.819, $r^2 = 0.66$, $P < 0.001$. C to E, Measurements of mean area per leaf (C), mean cell number (D) and mean cell area of leaves (E) that developed during stress. Values represent means of n = 4 ± SE. Significant differences between control (AC) and stress scenarios (PS, CS) with ** $P < 0.001$; ANOVA, LSD-test. Scenarios: AC = ambient [CO_2], PS = periodic stress, CS = chronic stress. PS and CS scenarios were performed under elevated [CO_2].

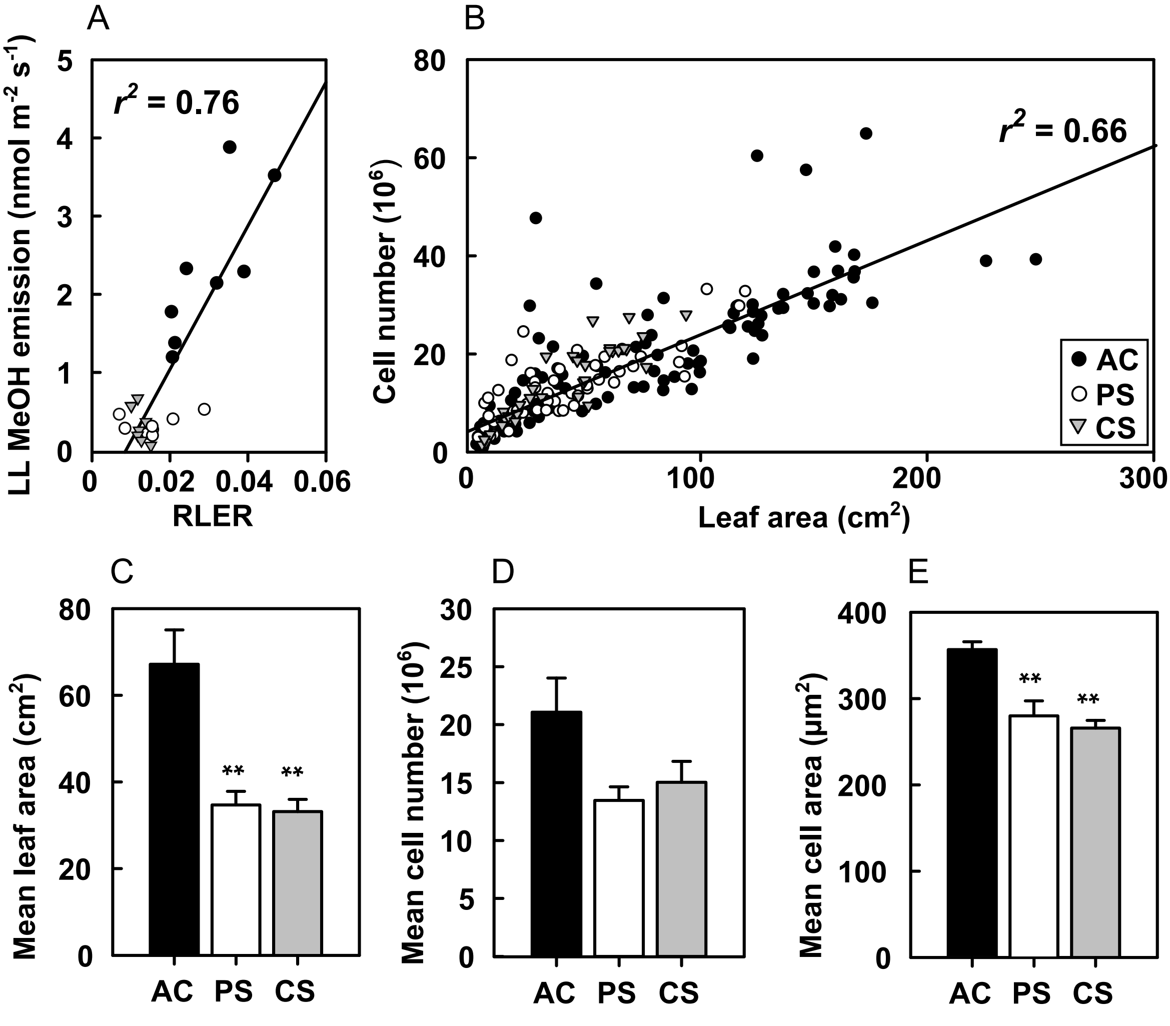

Figure 6. Net carbon (C) uptake in isoprene-emitting (IE, black bars) and non-emitting (NE, red bars) poplars in the four scenarios (AC, EC, PS, and CS) at the end of the experiment. Net C uptake was calculated based on overall plant fluxes of CO_2 and isoprene (see material and method), values for IE and NE of each scenario are given as mean of 4 sub-chambers ± SE. Dashed line indicates the reference value of 87 g C m^{-2} (= mean in AC scenario, IE). AC = ambient [CO_2], EC = elevated [CO_2], PS = periodic stress, CS = chronic stress. PS and CS scenarios were performed under elevated [CO_2].

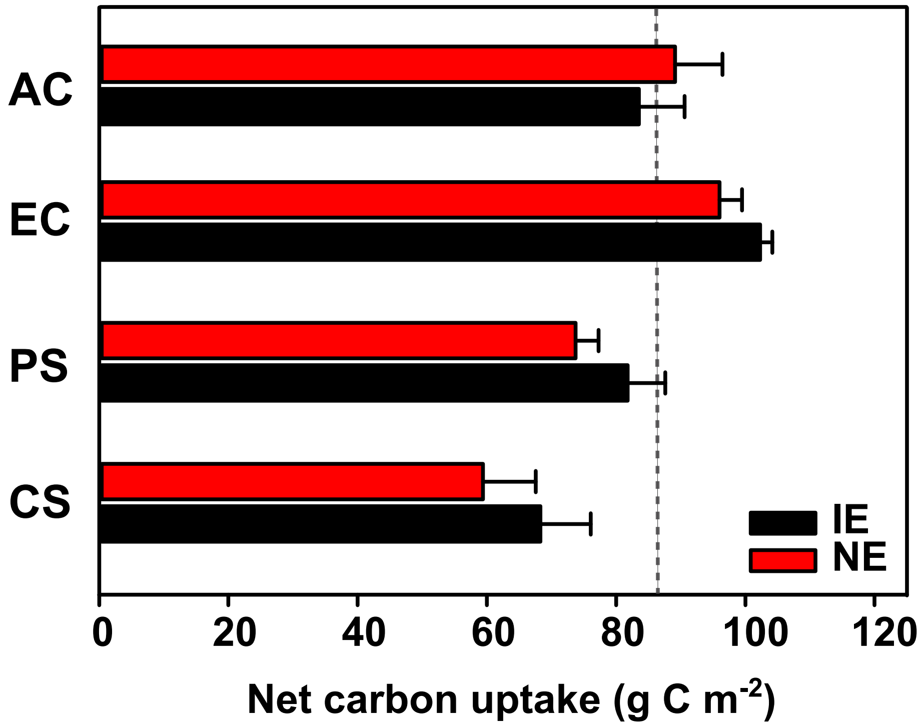

Figure 7. Cumulative net carbon (C) gain in isoprene-emitting (IE, black lines) and non-emitting (NE, red lines) Grey poplars in the four scenarios (AC, EC, PS, and CS). Dashed lines represent auxiliary lines to calculate the angles between the x-axis and the linear slope of each indicated phase. Different phases are indicated exemplary for IE poplars and are: P = pre-stress, S1 = stress cycle 1, R1 = recovery phase 1, S2 = stress cycle 2, R2 = recovery phase 2, S3 = stress cycle 3, R3 = recovery phase 3. In CS scenario, the phases are named as follows: P = pre-stress, S_{IN} = stress initial, S_{SEV} = stress severe, R = recovery. The scenarios are: AC = ambient [CO_2], EC = elevated [CO_2], PS = periodic stress, CS = chronic stress. Grey area illustrates the C that the plants were not able to gain due to stress incidence.

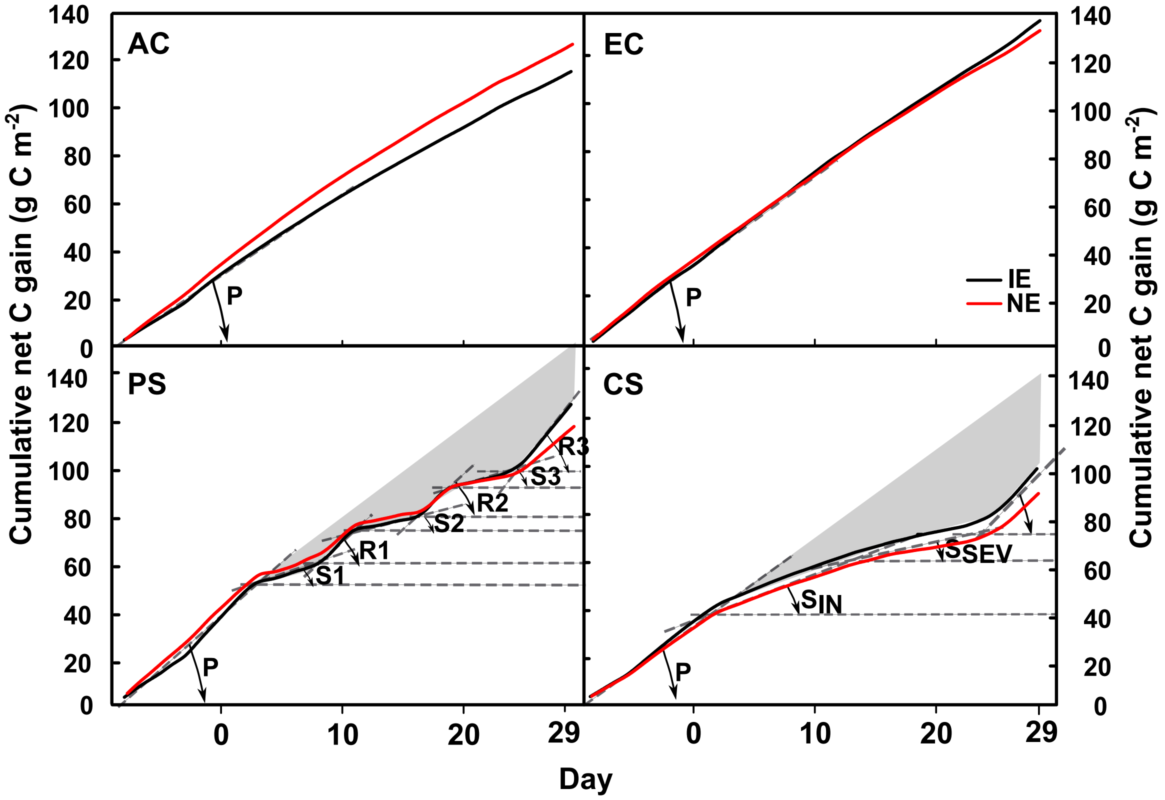

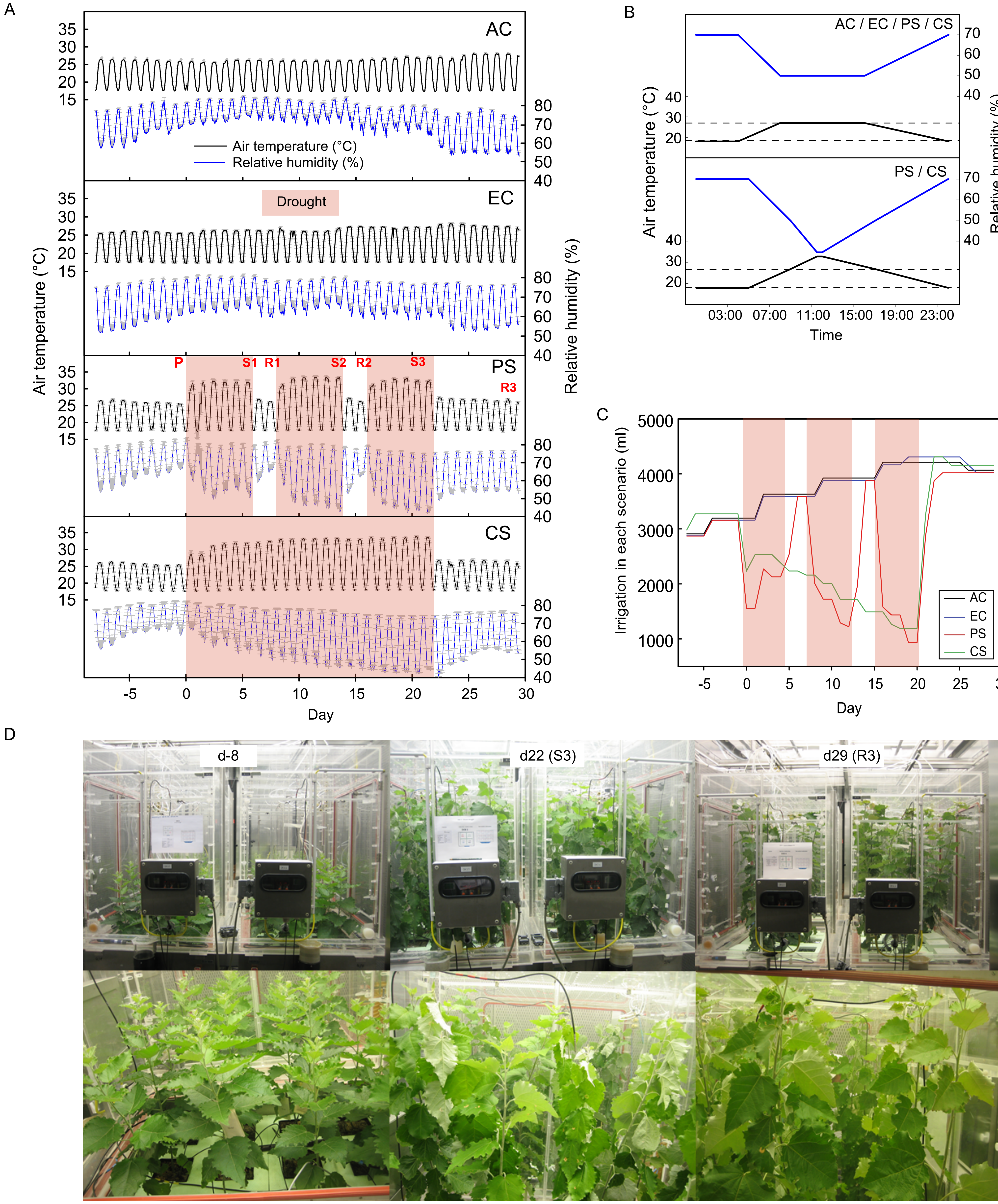

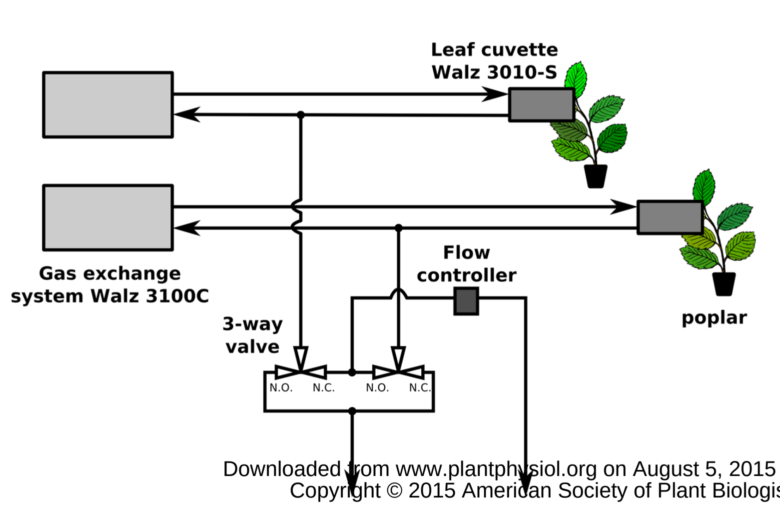

Figure S1. Time courses of air temperature, relative humidity, irrigation and plant appearance in the four scenarios. A, Diurnal course of air temperature and relative humidity during the experiment. The given values are the means of 4 sub-chambers (± SE). B, Theoretical values of daily air temperature and relative humidity when maximum air temperature was set to 27 °C (pre-stress and recovery, above) and to 33 °C during stress in PS and CS (below). Dashed lines indicate mean night temperature (18 °C) and light hour air temperature under unstressed conditions (27 °C). C, Irrigation profile of the experiment. Water amount (in ml) is given to the pots by automated drip irrigation systems. Values represent means of the 4 sub-chambers (representing each genotype) within each scenario (AC, EC, PS, CS). D, Front view of 2 sub-chambers (scenario PS) with12 Grey poplar plants arranged within 1 sub-chamber. E, Schematic of the setup used for the leaf-level gas exchange and VOC emission measurements. The PTR-ToF-MS was sampling from the leaf cuvette back-stream line and could be switched to sample from either gas exchange system. AC = control ambient [CO_2], EC = control elevated [CO_2], PS = periodic stress, CS = chronic stress.

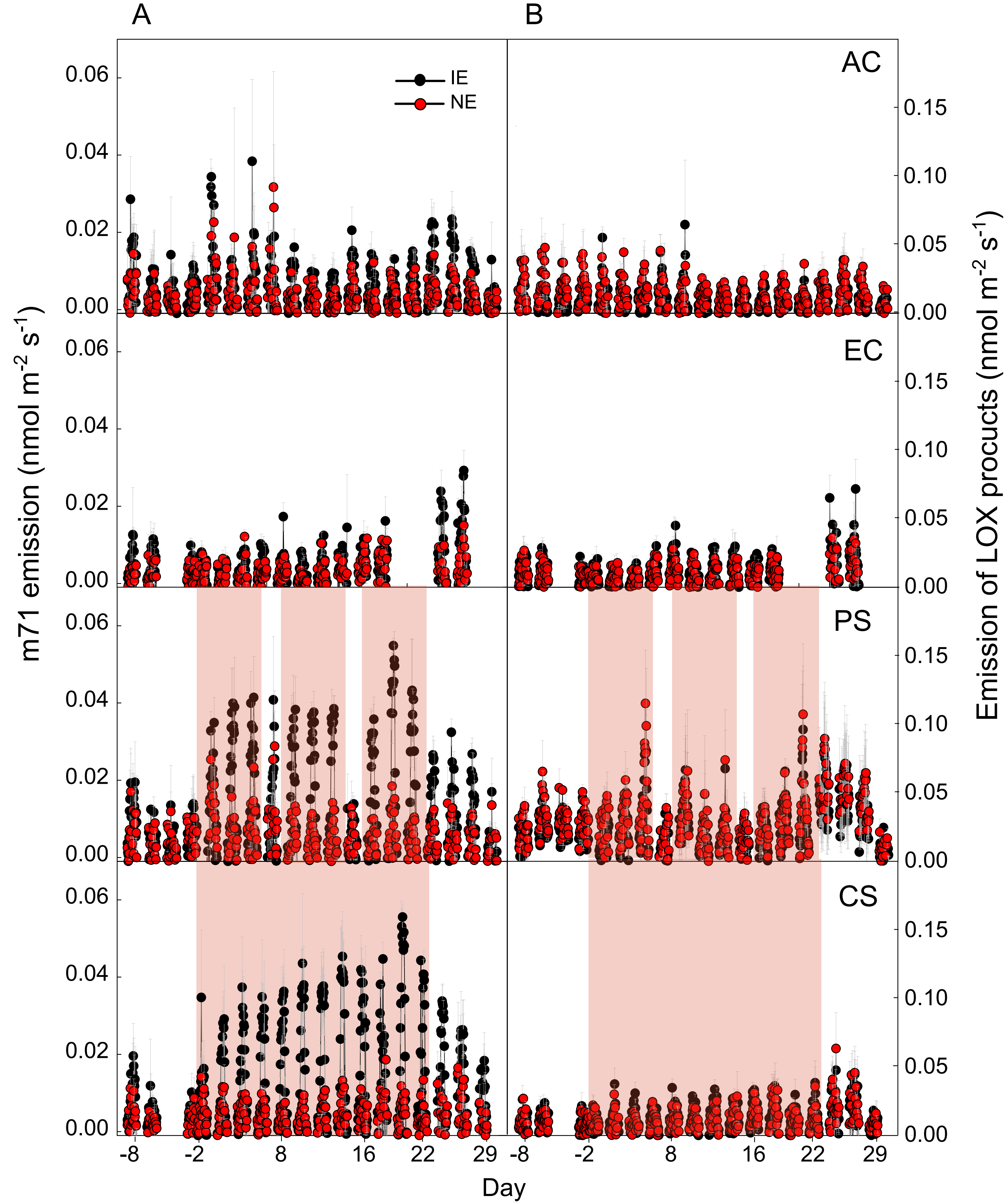

Figure S2. Time course of m71 (A) and LOX (B) products (i.e. m99 + m101) emission rates of isoprene-emitting (IE, black circles) and non-emitting (NE, red circles) Grey poplar genotypes in the four scenarios (AC, EC, PS, CS). Measurements were performed at the canopy-level. Periods of heat and drought spells are highlighted in red. Values represent means of n = 4 ± SE.

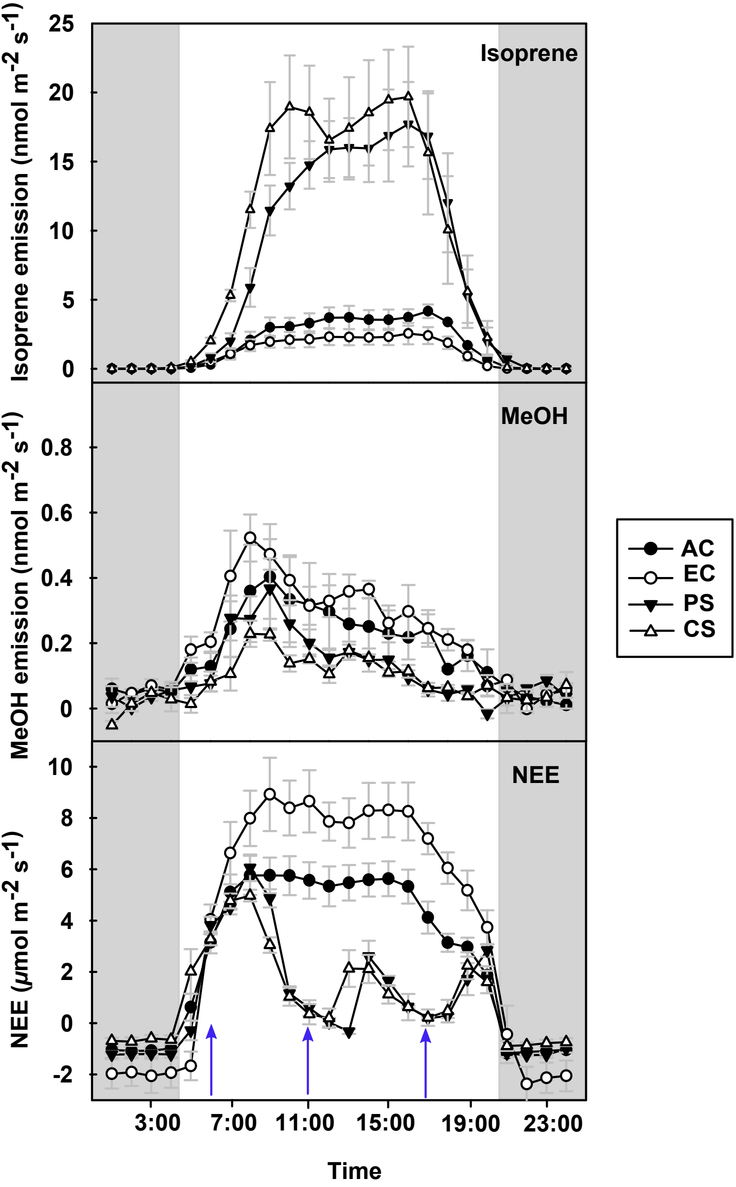

Figure S3. Representative day (d20) showing the canopy isoprene emission, MeOH emission and net ecosystem exchange (NEE) in the four scenarios. Blue arrows indicate time points of irrigation in the 4 scenarios (6:00; 12:00; 18:00, MEZ). Amount of water in AC and EC was higher than in PS and CS. Values for each scenario and treatments are given as mean of 4 sub-chambers (± SE). Dark hours are highlighted in grey. AC = control ambient [CO_2], EC = control elevated [CO_2], PS = periodic stress, CS = chronic stress.

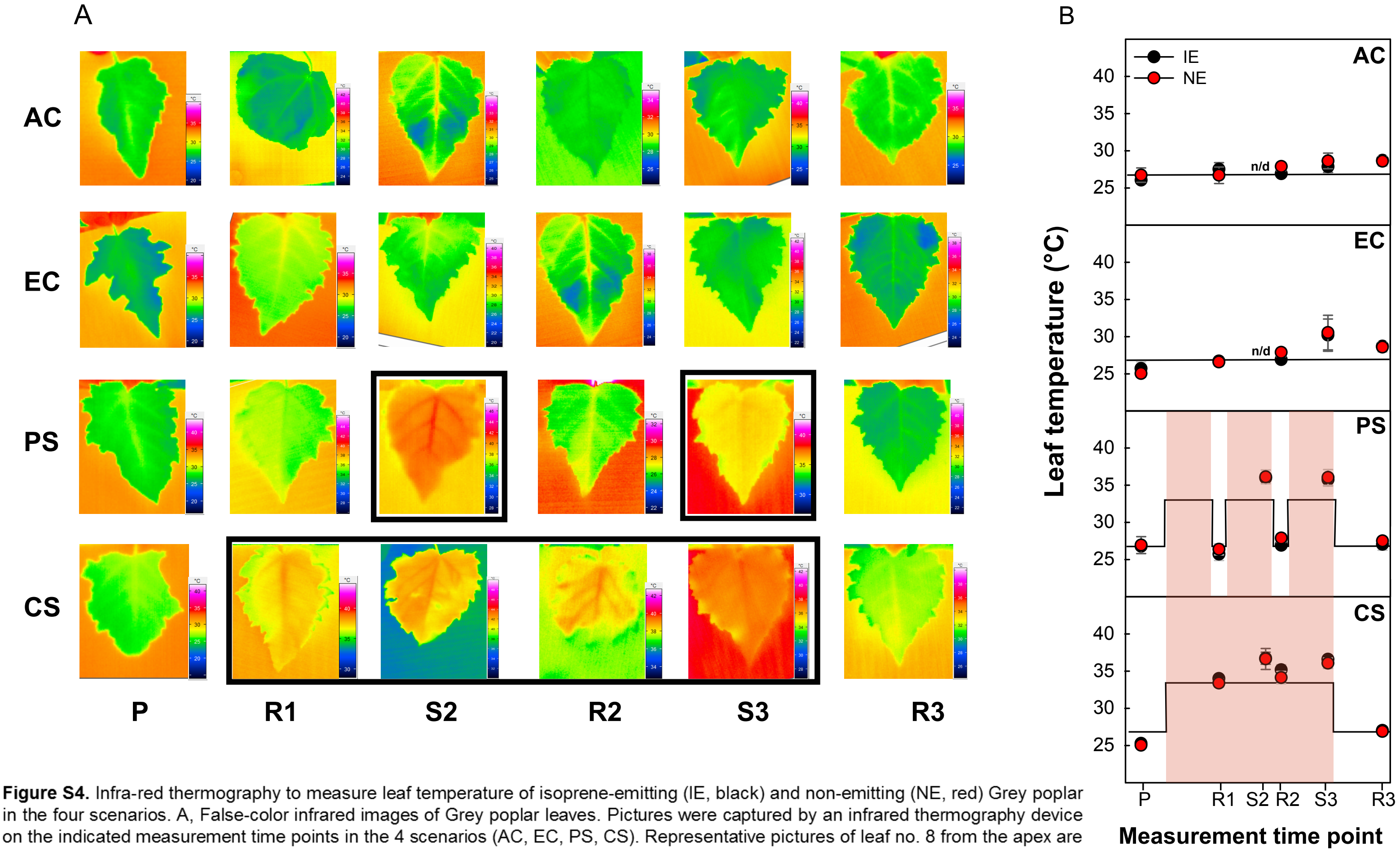

Figure S4. Infra-red thermography to measure leaf temperature of isoprene-emitting (IE, black) and non-emitting (NE, red) Grey poplar in the four scenarios. A, False-color infrared images of Grey poplar leaves. Pictures were captured by an infrared thermography device on the indicated measurement time points in the 4 scenarios (AC, EC, PS, CS). Representative pictures of leaf no. 8 from the apex are given. Black frames indicate heat and drought spells in the PS and CS scenario. B, Effect of 4 scenarios on the leaf temperature of isoprene-emitting (IE, black circles) and non-emitting (NE, red circles) poplar genotypes. Values represent means (± SE) of measurements performed in four sub-chambers; dashed lines denote the maximum air temperature during the light hours in the different scenarios. Thermal images were obtained using a thermographic digital camera (VarioCAM basic, Jenoptic Laser, Jena, Germany); pictures were taken from the adaxial side on the 8th leaf from the top at the time points P, R1, S2, R2, S3 and R3. Digital thermograms were analyzed with the IRBIS Plus software package (v. 2.2 Infratec, Dresden, Germany).

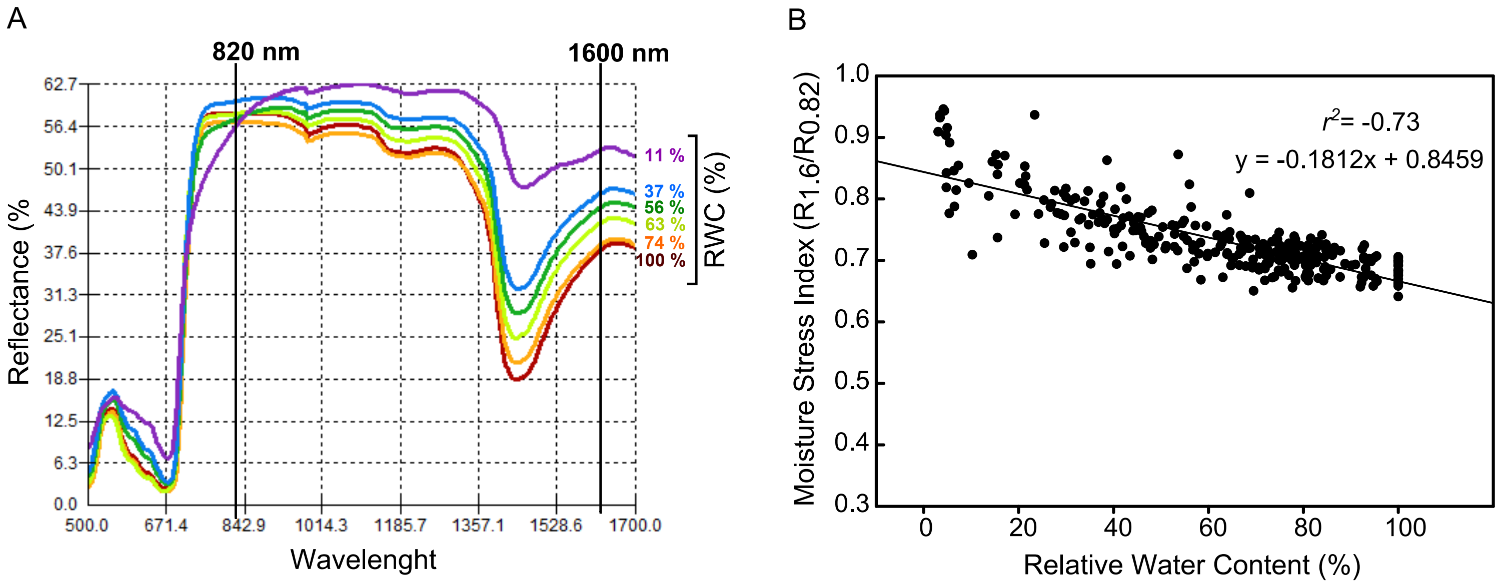

Figure S5. Drying experiment to assess the Moisture Stress Index and the Relative Water Context of Grey poplar leaves. A, Representative spectra of a leaf of Grey poplar during drying. Corresponding relative water contents (RWC) are given. Leaf reflectance was measured by near infrared spectrometry device, RWC was calculated based on the hourly leaf weight according the following equation: (FreshWeight-DryWeight)/(FreshWeight$_0$-DryWeight). Wavelengths of 820 nm and 1600 nm (vertical lines) were used for calculation of the Moisture Stress Index (MSI = Reflectance$_{1600}$/Reflectance$_{820}$). B, Relationship of the MSI to the RWC of drying leaves of Grey poplar. Five plants of each isoprene-emitting and non-emitting poplar genotype were examined hourly by NIR reflectance. Regression equation and coefficient of correlation are given.

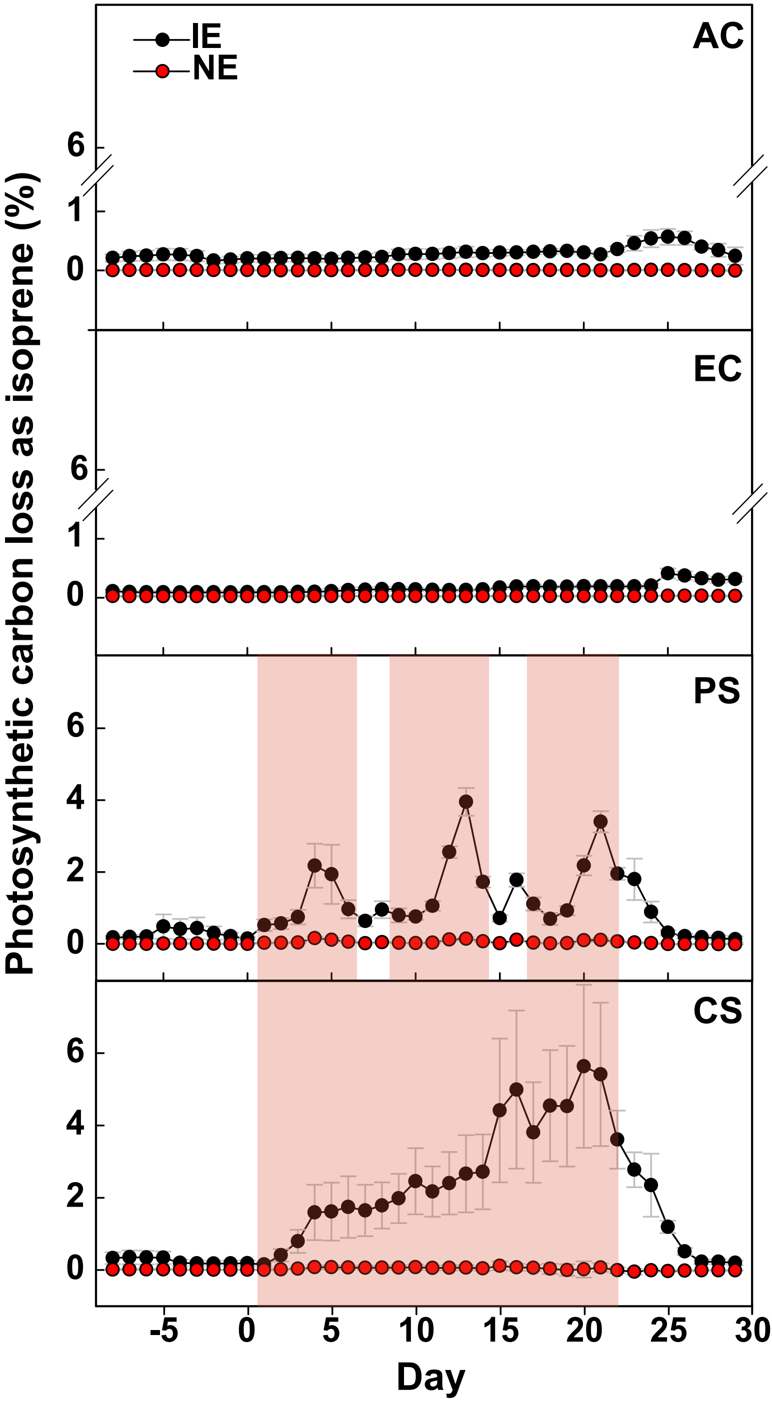

Figure S6. Time course showing the daily percentage of the photosynthetic carbon loss as isoprene in the four scenarios. Calculations are based on canopy CO_2 (NEE) and canopy isoprene emission. Values for each scenario are given as mean of n = 4 (± SE). The scenarios are: AC = control with ambient [CO_2], EC = control with elevated [CO_2], PS = periodic stress, CS = chronic stress. Periods of heat and drought are indicated in red.

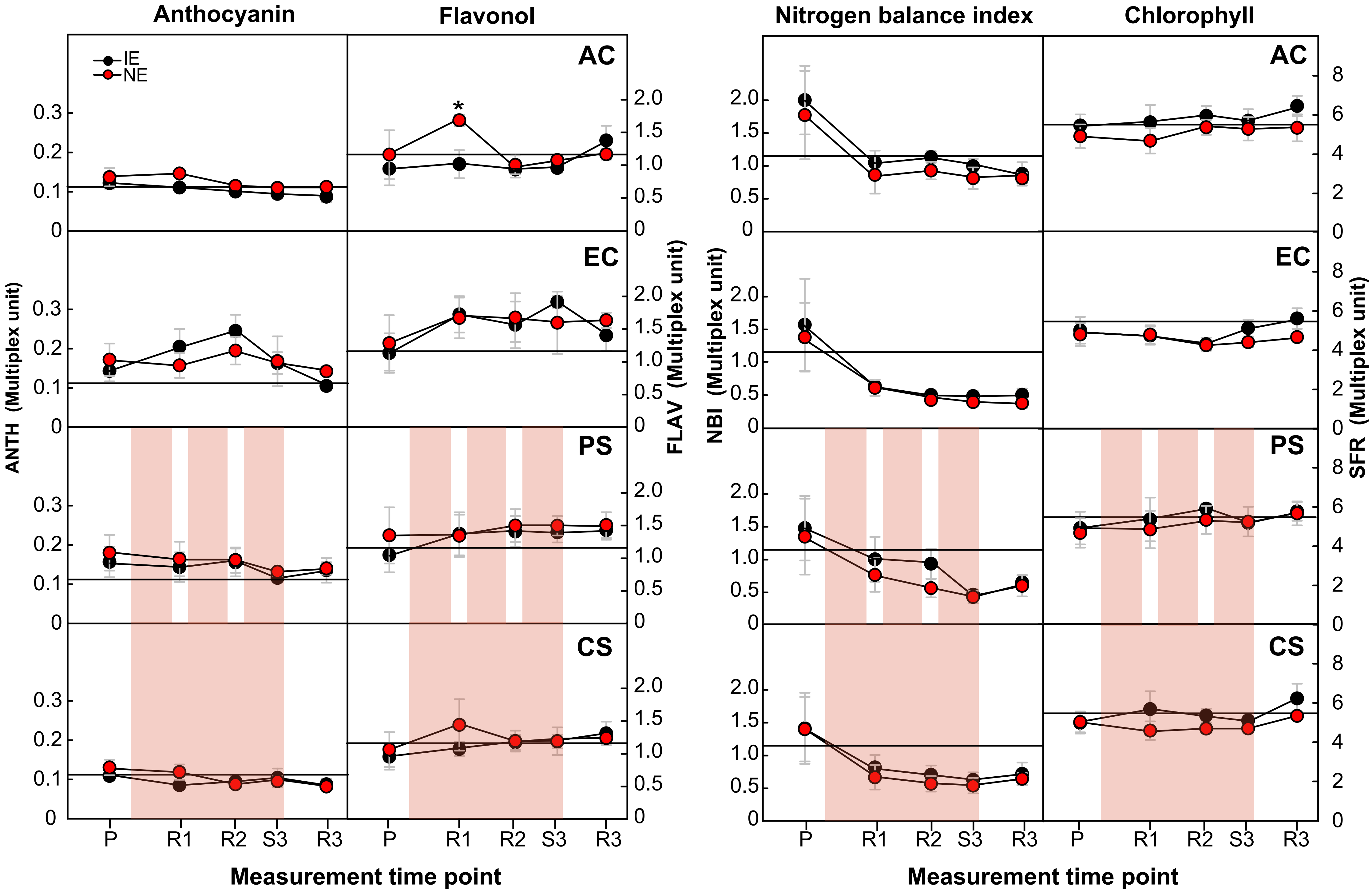

Figure S7. Effect of four scenarios on the anthocyanin index, flavonol index, nitrogen balance index (NBI®) and chlorophyll index of isoprene-emitting (IE, black circles) and non-emitting (NE, red circles) poplar genotypes. Measurement of the pigments was performed weekly by Multiplex® optical sensor (Force-A, Orsay, France). Values represent means (± SE) of measurements performed in 4 sub-chambers; dashed lines indicate an arbitrary reference value. Asterisks indicate significant genotype differences within each scenario and time point (*P* < 0.05).

Multiplex® optical sensor: The fluorescence signals are measured in the red (RF) and far-red (FRF) spectral regions excited under ultraviolet (UV), green (G) or red (R) radiation (in the following equations the subscripted characters indicate the excitation radiation). The simple chlorophyll fluorescence ratio (SFR) of far-red emission (735 nm) divided by red emission (685 nm) is linked to the chlorophyll content of the sample (Lichtenthaler et al., 1986; Buschmann, 2007). The flavonol index (FLAV), calculated according to equation FLAV = $\log(FRF_R/FRF_{UV})$, is proportional to the flavonol content of the leaf (Cerovic et al., 2002). Other fluorescence-based indices like the anthocyanin index ANTH = $\log(FRF_R/FRF_G)$ and the nitrogen balance index NBI = FRF_{UV}/RF_G are also described in literature (Meyer et al., 2006; Agati et al., 2007). Multiplex® measurements were performed in situ under ambient light conditions on the time points pre-stress (P), recovery phase 1 (R1), recovery phase 2 (R2), stress cycle 3 (S3), and recovery phase 3 (R3) on 6 plants per genotype and scenario. A constant distance between sensor and leaves was kept at all measurements using a grid in front of the sensor.

Supplemental Tables

Table S1. Results of two-way ANOVAs and Bonferroni post-hoc tests for all measured parameters. Significant differences are marked in red when $P < 0.05$.

		Main effect genotypes				**Scenario effect**																	
						Main scenario effect (IE + NE)						**IE**						**NE**					
	Time points	AC	EC	PS	CS	AC vs EC	AC vs PS	AC vs CS	EC vs PS	EC vs CS	PS vs CS	AC vs EC	AC vs PS	AC vs CS	EC vs PS	EC vs CS	PS vs CS	AC vs EC	AC vs PS	AC vs CS	EC vs PS	EC vs CS	PS vs CS
		Canopy-level																					
Net ecosystem exchange (NEE)	all time points	0.191	0.320	0.089	0.009	0.001	0.412	0.001	0.010	< 0.001	< 0.001	.	.	.	.	.	.	.	.	.	.	.	.
	P	0.348	0.961	0.205	0.372	1.000	0.172	1.000	0.532	1.000	0.164	1.000	0.988	1.000	1.000	1.000	1.000	1.000	0.517	1.000	0.544	1.000	0.052
	S1	0.338	0.566	0.700	0.542	1.000	< 0.001	< 0.001	< 0.001	< 0.001	1.000	1.000	0.045	0.051	0.004	0.005	1.000	1.000	0.008	< 0.001	0.088	0.009	1.000
	R1	0.531	0.499	0.967	0.605	0.768	0.018	< 0.001	1.000	< 0.001	< 0.001	0.515	0.088	0.019	1.000	< 0.001	< 0.001	1.000	0.441	< 0.001	1.000	0.001	< 0.001
	S2	0.567	0.899	0.425	0.789	1.000	< 0.001	< 0.001	< 0.001	< 0.001	0.961	1.000	0.001	0.014	< 0.001	0.002	1.000	1.000	< 0.001	0.001	< 0.001	0.001	1.000
	R2	0.846	0.516	0.016	0.042	0.278	< 0.001	< 0.001	0.004	0.028	1.000	0.376	< 0.001	< 0.001	0.015	0.082	1.000	1.000	0.005	0.014	0.408	0.705	1.000
	S3	0.985	0.793	0.643	0.511	1.000	< 0.001	< 0.001	< 0.001	< 0.001	1.000	1.000	0.001	0.001	0.001	0.001	1.000	1.000	< 0.001	< 0.001	< 0.001	< 0.001	1.000
	R3	0.846	0.516	0.016	0.042	0.278	< 0.001	< 0.001	0.004	0.028	1.000	0.376	< 0.001	< 0.001	0.015	0.082	1.000	1.000	0.005	0.014	0.408	0.705	1.000
Evapotranspiration	all time points	0.001	0.023	< 0.001	< 0.001	< 0.001	0.466	< 0.001	< 0.001	< 0.001	< 0.001	.	.	.	.	.	.	.	.	.	.	.	.
	P	0.710	< 0.001	0.523	0.011	< 0.001	0.001	0.573	< 0.001	< 0.001	0.186	< 0.001	0.167	0.142	< 0.001	< 0.001	1.000	1.000	0.009	1.000	1.000	1.000	0.012
	S1	< 0.001	< 0.001	< 0.001	0.021	< 0.001	< 0.001	< 0.001	< 0.001	< 0.001	0.240	< 0.001	0.005	< 0.001	< 0.001	< 0.001	< 0.001	1.000	< 0.001	0.092	< 0.001	0.023	0.157
	R1	0.001	< 0.001	< 0.001	0.118	0.002	0.594	< 0.001	0.139	< 0.001	< 0.001	< 0.001	0.528	< 0.001	0.007	< 0.001	< 0.001	1.000	1.000	0.222	1.000	0.187	0.042
	S2	0.012	< 0.001	< 0.001	0.736	0.006	< 0.001	< 0.001	< 0.001	< 0.001	1.000	0.004	0.001	< 0.001	< 0.001	< 0.001	0.726	1.000	< 0.001	0.059	< 0.001	0.005	0.021
	R2	0.525	0.007	0.031	0.836	1.000	1.000	< 0.001	1.000	< 0.001	< 0.001	0.034	0.180	< 0.001	1.000	< 0.001	< 0.001	1.000	1.000	< 0.001	1.000	< 0.001	< 0.001
	S3	0.979	0.012	0.020	0.857	0.267	< 0.001	< 0.001	< 0.001	< 0.001	1.000	0.025	0.013	< 0.001	< 0.001	< 0.001	0.706	1.000	< 0.001	< 0.001	< 0.001	0.002	1.000
	R3	0.901	0.077	0.550	0.138	0.295	< 0.001	< 0.001	0.001	0.900	0.017	0.112	< 0.001	0.002	0.288	1.000	0.544	1.000	< 0.001	0.141	0.003	0.908	0.063
Water use efficiency (WUE), canopy	all time points	< 0.001	0.003	< 0.001	< 0.001	0.099	1.000	1.000	0.007	0.001	1.000	.	.	.	.	.	.	.	.	.	.	.	.
	P	0.133	0.112	0.360	0.465	1.000	1.000	1.000	1.000	1.000	1.000	1.000	1.000	1.000	1.000	1.000	1.000	1.000	1.000	1.000	1.000	1.000	1.000
	S1	0.010	0.059	< 0.001	< 0.001	1.000	0.131	< 0.001	0.004	< 0.001	0.041	1.000	1.000	< 0.001	1.000	< 0.001	< 0.001	1.000	0.003	1.000	< 0.001	1.000	< 0.001
	R1	0.016	0.080	0.405	0.014	1.000	1.000	1.000	1.000	0.423	0.500	1.000	1.000	0.016	1.000	0.005	0.026	1.000	0.924	0.390	1.000	1.000	1.000
	S2	0.041	0.210	< 0.001	0.258	1.000	< 0.001	1.000	< 0.001	1.000	< 0.001	1.000	1.000	0.377	1.000	0.216	0.237	1.000	< 0.001	1.000	< 0.001	1.000	< 0.001
	R2	0.062	0.608	0.970	0.546	1.000	0.863	1.000	1.000	1.000	1.000	1.000	1.000	1.000	1.000	1.000	1.000	0.801	0.312	0.368	1.000	1.000	1.000
	S3	0.248	0.612	0.904	0.556	1.000	1.000	1.000	1.000	1.000	1.000	1.000	1.000	1.000	1.000	1.000	1.000	1.000	1.000	0.652	1.000	1.000	1.000
	R3	0.742	0.729	0.843	0.895	1.000	1.000	1.000	1.000	1.000	1.000	1.000	1.000	1.000	1.000	1.000	1.000	1.000	1.000	1.000	1.000	1.000	1.000
Electron transport rate (ETR) leaf4	all time points	0.677	0.918	0.017	0.344	1.000	0.793	1.000	0.177	1.000	0.063	.	.	.	.	.	.	.	.	.	.	.	.
	P	0.967	0.496	0.984	0.735	1.000	1.000	1.000	1.000	1.000	1.000	1.000	1.000	1.000	1.000	1.000	1.000	1.000	1.000	1.000	1.000	1.000	1.000
	S1	n/d	n/d	0.686	0.755	n/d	n/d	n/d	n/d	n/d	0.496	.	.	.	.	.	0.902	.	.	.	.	.	0.402
	R1	0.927	0.967	0.955	0.842	1.000	0.554	1.000	0.149	1.000	0.380	1.000	1.000	1.000	1.000	0.677	1.000	1.000	1.000	1.000	0.656	1.000	0.892

	S2	n/d	n/d	0.019	0.399	n/d	n/d	n/d	n/d	n/d	0.001	.	.	.	.	.	0.122	.	.	.	.	.	0.003
	R2	0.739	0.422	0.202	0.160	1.000	1.000	1.000	1.000	1.000	1.000	0.779	1.000	0.580	1.000	1.000	1.000	1.000	1.000	1.000	1.000	1.000	1.000
	S3	0.770	0.951	0.051	0.126	1.000	1.000	1.000	1.000	1.000	1.000	1.000	1.000	1.000	1.000	1.000	1.000	1.000	0.936	1.000	1.000	1.000	1.000
	R3	0.307	0.898	0.759	0.667	1.000	1.000	1.000	1.000	1.000	1.000	1.000	1.000	1.000	1.000	1.000	1.000	1.000	1.000	1.000	1.000	1.000	1.000
ETR leaf8	all time points	0.231	0.451	< 0.001	0.001	0.164	< 0.001	0.647	0.044	1.000	0.001	.	.	.	.	.	.	.	.	.	.	.	.
	P	0.735	0.894	0.742	0.629	1.000	1.000	0.374	1.000	1.000	0.850	1.000	1.000	1.000	1.000	1.000	1.000	1.000	1.000	0.504	1.000	1.000	0.893
	S1	.	.	0.024	0.758	n/d	n/d	n/d	n/d	n/d	0.566	.	.	.	.	.	0.565	.	.	.	.	.	0.167
	R1	0.984	0.742	0.735	0.622	1.000	1.000	1.000	1.000	1.000	0.334	1.000	1.000	1.000	1.000	1.000	0.462	1.000	1.000	1.000	1.000	1.000	1.000
	S2	.	.	< 0.001	0.003	n/d	n/d	n/d	n/d	n/d	< 0.001	.	.	.	.	.	0.074	.	.	.	.	.	< 0.001
	R2	0.593	0.926	0.291	0.007	1.000	0.536	0.265	1.000	0.815	1.000	1.000	1.000	1.000	1.000	1.000	1.000	1.000	0.024	0.072	1.000	0.109	1.000
	S3	0.255	0.412	0.014	0.005	0.004	< 0.001	0.001	0.016	1.000	0.048	0.054	0.001	0.353	1.000	1.000	0.242	0.128	< 0.001	0.003	0.020	0.023	0.515
	R3	0.518	0.758	0.681	0.934	0.256	1.000	1.000	0.227	0.544	1.000	0.649	1.000	1.000	0.763	1.000	1.000	1.000	1.000	1.000	0.982	0.982	1.000
ETR leaf12	all time points	0.453	0.746	< 0.001	0.010	1.000	< 0.001	0.113	< 0.001	0.234	0.014	.	.	.	.	.	.	.	.	.	.	.	.
	P	0.969	0.938	0.897	0.796	0.439	1.000	0.743	0.995	1.000	1.000	1.000	1.000	1.000	1.000	1.000	1.000	1.000	1.000	1.000	1.000	1.000	1.000
	S1	n/d	n/d	0.387	0.959	n/d	n/d	n/d	n/d	n/d	0.482	n/d	n/d	n/d	n/d	n/d	0.969	n/d	n/d	n/d	n/d	n/d	0.339
	R1	0.928	0.990	0.642	0.938	1.000	1.000	1.000	0.374	1.000	1.000	1.000	1.000	1.000	0.715	1.000	1.000	1.000	1.000	1.000	1.000	1.000	1.000
	S2	n/d	n/d	< 0.001	0.038	n/d	n/d	n/d	n/d	n/d	< 0.001	n/d	n/d	n/d	n/d	n/d	0.006	n/d	n/d	n/d	n/d	n/d	< 0.001
	R2	0.866	0.948	0.333	0.023	1.000	0.252	0.122	0.338	0.169	1.000	1.000	1.000	1.000	1.000	1.000	1.000	1.000	0.396	0.044	0.374	0.041	1.000
	S3	0.623	0.806	0.001	0.020	0.119	< 0.001	< 0.001	< 0.001	0.009	1.000	0.263	0.004	0.018	0.872	1.000	1.000	1.000	< 0.001	< 0.001	< 0.001	0.003	1.000
	R3	0.251	0.727	0.172	0.679	1.000	1.000	1.000	1.000	1.000	1.000	0.894	1.000	1.000	0.831	1.000	1.000	1.000	1.000	1.000	1.000	1.000	1.000
Isoprene emission, canopy	all time points	< 0.001	0.033	< 0.001	0.000	0.057	< 0.001	< 0.001	< 0.001	< 0.001	0.002	.	.	.	.	.	.	.	.	.	.	.	.
	P	0.112	0.703	0.155	0.159	0.853	1.000	1.000	1.000	1.000	1.000	1.000	1.000	1.000	1.000	1.000	1.000	1.000	1.000	1.000	1.000	1.000	1.000
	S1	0.126	0.577	< 0.001	< 0.001	1.000	0.084	0.100	0.073	0.078	1.000	1.000	0.008	0.004	0.007	0.003	1.000	1.000	1.000	1.000	1.000	1.000	1.000
	R1	0.117	0.473	0.051	< 0.001	1.000	1.000	< 0.001	1.000	0.001	0.001	1.000	1.000	< 0.001	1.000	< 0.001	< 0.001	1.000	1.000	1.000	1.000	1.000	1.000
	S2	0.063	0.503	< 0.001	< 0.001	1.000	< 0.001	< 0.001	< 0.001	< 0.001	1.000	1.000	< 0.001	< 0.001	< 0.001	< 0.001	1.000	1.000	1.000	1.000	1.000	1.000	1.000
	R2	0.065	0.394	0.001	< 0.001	1.000	1.000	< 0.001	1.000	< 0.001	0.002	1.000	0.782	< 0.001	0.419	< 0.001	< 0.001	1.000	1.000	1.000	1.000	1.000	1.000
	S3	0.058	0.412	< 0.001	< 0.001	1.000	0.002	< 0.001	0.004	< 0.001	1.000	1.000	< 0.001	< 0.001	< 0.001	< 0.001	0.366	1.000	1.000	1.000	1.000	1.000	1.000
	R3	0.009	0.094	0.006	0.003	1.000	1.000	1.000	1.000	1.000	1.000	1.000	1.000	1.000	1.000	1.000	1.000	1.000	1.000	1.000	1.000	1.000	1.000
Methanol emission, canopy	all time points	0.048	0.037	0.284	0.466	0.077	< 0.001	< 0.001	< 0.001	< 0.001	1.000	.	.	.	.	.	.	.	.	.	.	.	.
	P	0.040	0.898	0.135	0.885	1.000	1.000	1.000	1.000	0.241	0.351	0.591	1.000	1.000	1.000	1.000	1.000	1.000	1.000	0.437	1.000	0.674	0.188
	S1	0.420	0.789	0.624	0.684	1.000	0.096	0.204	1.000	1.000	1.000	1.000	0.719	1.000	1.000	1.000	1.000	1.000	0.372	0.214	1.000	1.000	1.000
	R1	0.351	0.355	0.595	0.873	1.000	0.798	0.038	0.247	0.014	1.000	0.810	1.000	0.961	0.172	0.053	1.000	1.000	1.000	0.080	1.000	0.532	1.000
	S2	0.493	0.396	0.798	0.515	0.414	0.022	0.067	< 0.001	0.001	1.000	0.243	0.378	1.000	0.003	0.019	1.000	1.000	0.135	0.084	0.105	0.070	1.000
	R2	0.809	0.305	0.876	0.697	1.000	0.140	0.014	0.022	0.002	1.000	0.871	0.701	0.372	0.040	0.019	1.000	1.000	0.591	0.079	0.919	0.210	1.000
	S3	0.957	0.167	0.789	0.920	0.127	0.143	0.286	< 0.001	0.001	1.000	0.088	0.523	1.000	0.001	0.003	1.000	1.000	0.802	0.831	0.250	0.259	1.000
	R3	0.624	0.077	0.715	0.939	0.010	1.000	1.000	0.009	0.011	1.000	0.004	1.000	1.000	0.011	0.009	1.000	1.000	1.000	1.000	0.960	1.000	1.000
Relative water content (RWC) leaf4	all time points	0.406	0.445	0.972	0.888	0.030	0.123	1.000	1.000	0.009	0.027	.	.	.	.	.	.	.	.	.	.	.	.
	P	0.926	1.000	0.577	0.642	0.022	1.000	0.082	0.201	1.000	0.795	0.212	1.000	0.696	0.497	1.000	1.000	0.253	1.000	0.317	1.000	1.000	1.000
	S1	n/d	n/d	0.931	0.853	n/d	n/d	n/d	n/d	n/d	0.659	n/d	n/d	n/d	n/d	n/d	0.731	n/d	n/d	n/d	n/d	n/d	0.780
	R1	0.391	0.895	0.710	0.404	1.000	1.000	0.477	1.000	1.000	0.260	1.000	1.000	1.000	1.000	1.000	0.577	1.000	1.000	1.000	1.000	1.000	1.000
	S2	n/d	n/d	0.780	0.853	n/d	n/d	n/d	n/d	n/d	0.043	n/d	n/d	n/d	n/d	n/d	0.228	n/d	n/d	n/d	n/d	n/d	0.096
	R2	0.458	0.238	0.853	0.642	1.000	0.082	0.137	1.000	0.016	< 0.001	0.423	0.256	1.000	1.000	0.053	0.016	1.000	0.833	0.163	1.000	0.581	0.002
	S3	0.710	0.358	0.516	0.458	0.656	1.000	1.000	1.000	0.066	0.351	0.423	1.000	1.000	1.000	0.253	1.000	1.000	1.000	0.990	1.000	0.677	0.990
	R3	0.780	0.793	0.458	0.780	0.895	0.001	0.000	0.420	0.004	0.260	1.000	0.016	0.001	0.497	0.080	1.000	1.000	0.062	< 0.001	1.000	0.098	0.317

RWC leaf 8	all time points	0.269	0.948	0.848	0.032	0.002	< 0.001	0.386	0.044	0.095	< 0.001	.	.	.	.	.	.	.	.	.	.	.	.
	P	0.919	0.772	0.682	0.414	1.000	1.000	0.588	1.000	0.758	0.898	1.000	1.000	1.000	1.000	1.000	1.000	1.000	1.000	0.760	1.000	0.686	1.000
	S1	n/d	n/d	1.000	0.759	n/d	n/d	n/d	n/d	n/d	0.188	n/d	n/d	n/d	n/d	n/d	0.298	n/d	n/d	n/d	n/d	n/d	0.414
	R1	0.479	0.470	0.838	0.262	1.000	0.005	1.000	0.117	1.000	0.005	1.000	0.026	1.000	1.000	1.000	0.016	1.000	0.313	1.000	0.280	1.000	0.503
	S2	n/d	n/d	1.000	1.000	n/d	n/d	n/d	n/d	n/d	0.010	n/d	n/d	n/d	n/d	n/d	0.067	n/d	n/d	n/d	n/d	n/d	0.067
	R2	0.474	0.772	0.540	0.609	0.073	< 0.001	1.000	0.086	0.027	1.000	0.339	< 0.001	1.000	0.580	0.231	1.000	0.580	< 0.001	1.000	0.408	0.280	< 0.001
	S3	0.838	0.664	0.682	0.682	0.045	0.007	1.000	1.000	0.002	< 0.001	0.231	0.255	1.000	1.000	0.019	0.011	0.488	0.052	1.000	1.000	0.189	0.011
	R3	0.262	0.312	0.084	0.012	0.053	< 0.001	< 0.001	< 0.001	0.027	0.371	0.488	< 0.001	< 0.001	< 0.001	0.686	0.004	0.280	< 0.001	< 0.001	0.408	0.080	1.000
RWC leaf 12	all time points	0.280	0.306	0.071	0.351	0.001	< 0.001	0.015	0.435	0.769	< 0.001	.	.	.	.	.	.	.	.	.	.	.	.
	P	0.938	0.827	0.487	0.487	1.000	1.000	0.618	1.000	1.000	1.000	1.000	1.000	1.000	1.000	1.000	1.000	1.000	1.000	0.863	1.000	1.000	1.000
	S1	n/d	n/d	0.617	0.817	n/d	n/d	n/d	n/d	n/d	0.916	n/d	n/d	n/d	n/d	n/d	0.775	n/d	n/d	n/d	n/d	n/d	0.643
	R1	0.373	0.051	0.106	0.589	1.000	0.980	1.000	1.000	1.000	0.767	1.000	1.000	1.000	1.000	1.000	1.000	1.000	1.000	1.000	1.000	1.000	0.639
	S2	n/d	n/d	0.643	0.817	n/d	n/d	n/d	n/d	n/d	0.035	n/d	n/d	n/d	n/d	n/d	0.166	n/d	n/d	n/d	n/d	n/d	0.106
	R2	0.589	0.743	0.248	1.000	0.502	< 0.001	1.000	0.146	1.000	0.003	0.616	0.011	1.000	1.000	1.000	0.331	1.000	0.001	1.000	0.147	1.000	0.015
	S3	0.643	0.743	0.757	0.699	0.104	0.006	1.000	1.000	0.341	0.036	0.234	0.087	1.000	1.000	1.000	0.639	1.000	0.131	1.000	1.000	1.000	0.131
	R3	0.699	0.445	0.938	0.106	0.116	< 0.001	< 0.001	0.006	1.000	0.016	1.000	< 0.001	0.192	0.038	1.000	0.023	0.314	< 0.001	0.005	0.314	1.000	0.995
Relative leaf expansion rate (RLER)	S3	0.997	n/d	0.881	0.608	n/d	0.001	< 0.001	n/d	n/d	1.000	n/d	0.017	0.003	n/d	n/d	1.000	n/d	0.024	0.010	n/d	n/d	1.000
Area per leaf	S3	0.495	n/d	0.436	0.896	n/d	0.002	0.002	n/d	n/d	1.000	n/d	0.030	0.014	n/d	n/d	1.000	n/d	0.024	0.048	n/d	n/d	1.000
Cell number	S3	0.368	n/d	0.877	0.371	n/d	0.072	0.270	n/d	n/d	1.000	n/d	0.142	0.747	n/d	n/d	1.000	n/d	0.565	0.578	n/d	n/d	1.000
Cell size	S3	0.672	n/d	0.586	0.366	n/d	0.002	< 0.001	n/d	n/d	1.000	n/d	0.027	0.002	n/d	n/d	0.643	n/d	0.021	0.032	n/d	n/d	1.000
Carbon sum	all time points	0.579	0.634	0.391	0.344	0.790	1.000	0.021	0.086	0.002	0.268	0.664	1.000	0.675	0.499	0.041	0.941	1.000	0.819	0.044	0.369	0.024	0.804
Anthocyanin index (ANTH)	all time points	0.216	0.780	0.632	0.690	< 0.001	0.047	1.000	0.336	< 0.001	0.001	.	.	.	.	.	.	.	.	.	.	.	.
	P	0.676	0.426	0.516	0.552	1.000	0.775	1.000	1.000	0.837	0.035	1.000	1.000	1.000	1.000	1.000	1.000	1.000	1.000	1.000	1.000	1.000	1.000
	R1	0.419	0.308	0.565	0.357	0.621	1.000	1.000	1.000	0.050	0.265	0.102	1.000	1.000	0.703	0.016	0.657	1.000	1.000	1.000	1.000	1.000	1.000
	R2	0.693	0.283	0.867	0.850	0.001	0.287	1.000	0.227	< 0.001	0.056	0.008	0.774	1.000	0.263	0.005	0.560	0.244	1.000	1.000	1.000	0.040	0.257
	S3	0.675	0.920	0.685	0.804	0.192	1.000	1.000	0.354	0.157	1.000	0.470	1.000	1.000	1.000	0.775	1.000	1.000	1.000	1.000	0.754	0.602	1.000
	R3	0.491	0.339	0.894	0.889	1.000	0.840	1.000	1.000	1.000	0.345	1.000	1.000	1.000	1.000	1.000	1.000	1.000	1.000	1.000	1.000	0.735	0.820
Flavonol index (FLAV)	all time points	0.203	0.900	0.834	0.591	0.002	0.163	1.000	0.490	0.015	0.848	.	.	.	.	.	.	.	.	.	.	.	.
	P	0.538	0.668	0.393	0.752	1.000	1.000	1.000	1.000	1.000	1.000	1.000	1.000	1.000	1.000	1.000	1.000	1.000	1.000	1.000	1.000	1.000	1.000
	R1	0.049	0.902	0.933	0.295	0.354	1.000	1.000	1.000	0.722	1.000	0.133	0.652	1.000	1.000	0.504	1.000	1.000	1.000	1.000	1.000	1.000	1.000
	R2	0.839	0.807	0.792	0.955	0.156	0.347	1.000	1.000	0.739	1.000	0.886	1.000	1.000	1.000	1.000	1.000	0.489	1.000	1.000	1.000	1.000	1.000
	S3	0.731	0.483	0.471	0.981	0.071	1.000	1.000	0.554	0.286	1.000	0.080	1.000	1.000	1.000	0.326	1.000	1.000	1.000	1.000	1.000	1.000	1.000
	R3	0.549	0.543	0.825	0.860	1.000	1.000	1.000	1.000	1.000	1.000	1.000	1.000	1.000	1.000	1.000	1.000	1.000	1.000	1.000	1.000	1.000	1.000
Nitrogen balance index (NBI)	all time points	0.348	0.512	0.320	0.614	0.066	0.119	0.107	1.000	1.000	1.000	.	.	.	.	.	.	.	.	.	.	.	.
	P	0.585	0.647	0.756	0.974	1.000	0.645	0.616	1.000	1.000	1.000	1.000	1.000	0.948	1.000	1.000	1.000	1.000	1.000	1.000	1.000	1.000	1.000
	R1	0.650	0.942	0.566	0.715	1.000	1.000	1.000	1.000	1.000	1.000	1.000	1.000	1.000	1.000	1.000	1.000	1.000	1.000	1.000	1.000	1.000	1.000
	R2	0.619	0.851	0.370	0.738	0.343	1.000	1.000	1.000	1.000	1.000	0.797	1.000	1.000	1.000	1.000	1.000	1.000	1.000	1.000	1.000	1.000	1.000
	S3	0.658	0.658	0.746	0.829	1.000	0.574	1.000	0.575	1.000	1.000	1.000	1.000	1.000	1.000	1.000	1.000	1.000	1.000	1.000	1.000	1.000	1.000
	R3	0.872	0.758	0.896	0.857	1.000	1.000	1.000	1.000	1.000	1.000	1.000	1.000	1.000	1.000	1.000	1.000	1.000	1.000	1.000	1.000	1.000	1.000
Chlorophyll index (SFR)	all time points	0.049	0.331	0.176	0.123	0.078	1.000	1.000	0.888	0.761	1.000	.	.	.	.	.	.	.	.	.	.	.	.
	P	0.529	0.802	0.771	0.955	1.000	1.000	1.000	1.000	1.000	1.000	1.000	1.000	1.000	1.000	1.000	1.000	1.000	1.000	1.000	1.000	1.000	1.000
	R1	0.284	0.954	0.556	0.209	1.000	1.000	1.000	1.000	1.000	1.000	1.000	1.000	1.000	1.000	1.000	1.000	1.000	1.000	1.000	1.000	1.000	1.000

	R2	0.502	0.950	0.510	0.444	0.167	1.000	1.000	0.172	1.000	1.000	0.375	1.000	1.000	0.388	1.000	1.000	1.000	1.000	1.000	1.000	1.000	1.000
	S3	0.634	0.407	0.185	0.639	1.000	0.938	1.000	1.000	1.000	1.000	1.000	1.000	1.000	1.000	1.000	1.000	1.000	0.770	1.000	1.000	1.000	1.000
	R3	0.203	0.276	0.908	0.308	1.000	1.000	1.000	1.000	1.000	1.000	1.000	1.000	1.000	1.000	1.000	1.000	1.000	1.000	1.000	1.000	1.000	1.000
Temperature (leaf)	all time points	0.659	0.864	0.553	0.559	1.000	0.830	< 0.001	1.000	< 0.001	< 0.001	.	.	.	.	.	.	.	.	.	.	.	.
	P	0.710	0.713	0.933	0.888	1.000	1.000	1.000	1.000	1.000	1.000	1.000	1.000	1.000	1.000	1.000	1.000	1.000	1.000	1.000	1.000	1.000	1.000
	R1	0.531	0.926	0.615	0.638	1.000	1.000	< 0.001	1.000	< 0.001	< 0.001	1.000	1.000	< 0.001	1.000	< 0.001	< 0.001	1.000	1.000	< 0.001	1.000	< 0.001	< 0.001
	S2	n/d	n/d	0.931	0.955	.	.	.	.	.	0.615	.	.	.	.	.	0.669	.	.	.	.	.	0.776
	R2	0.592	0.731	0.680	0.572	1.000	0.657	< 0.001	0.051	< 0.001	< 0.001	1.000	1.000	< 0.001	0.332	0.003	< 0.001	1.000	1.000	0.006	0.385	0.044	< 0.001
	S3	0.548	0.793	n/d.	n/d.	0.022	.	.	.	.	.	0.072	.	.	.	.	.	0.141	.	.	.	.	.
	R3	0.929	0.662	0.724	0.918	1.000	0.805	0.396	1.000	1.000	1.000	1.000	1.000	1.000	1.000	1.000	1.000	1.000	1.000	1.000	1.000	1.000	1.000
Stem water potential (mid-day)	all time points	0.240	0.384	0.656	0.447	0.329	0.011	< 0.001	1.000	< 0.001	0.002	.	.	.	.	.	.	.	.	.	.	.	.
	S3	0.250	0.844	0.650	0.473	1.000	< 0.001	< 0.001	0.006	< 0.001	0.002	1.000	0.002	< 0.001	0.044	< 0.001	0.034	0.808	< 0.001	< 0.001	0.194	< 0.001	0.068
	R3	0.606	0.221	0.860	0.720	0.839	1.000	1.000	0.050	1.000	0.729	1.000	1.000	1.000	1.000	1.000	1.000	0.350	1.000	1.000	0.065	0.651	1.000
Leaf-level																							
Transpiration (E)	all time points	0.002	0.971	< 0.001	< 0.001	0.855	0.001	0.011	0.058	0.450	1.000	.	.	.	.	.	.	.	.	.	.	.	.
	S3	0.055	0.804	0.975	0.695	0.049	< 0.001	< 0.001	0.001	< 0.001	1.000	0.043	< 0.001	< 0.001	0.023	0.019	1.000	1.000	0.002	< 0.001	0.041	0.012	1.000
	R3	0.263	0.184	0.390	0.079	1.000	1.000	0.077	1.000	0.352	0.699	1.000	1.000	0.216	1.000	0.708	0.706	1.000	1.000	0.845	1.000	1.000	1.000
Net assimilation (A)	all time points	0.027	0.016	0.186	0.028	0.649	1.000	1.000	0.219	0.098	1.000	.	.	.	.	.	.	.	.	.	.	.	.
	S3	0.050	0.099	0.531	0.418	1.000	< 0.001	< 0.001	< 0.001	< 0.001	1.000	1.000	0.001	< 0.001	0.002	0.001	1.000	1.000	0.047	0.008	0.046	0.008	1.000
	R3	0.225	0.071	0.212	0.021	0.089	0.001	< 0.001	0.657	0.373	1.000	0.248	0.029	0.003	1.000	0.674	1.000	0.872	0.032	0.081	0.932	1.000	1.000
Water-use efficiency (WUE)	all time points	0.784	0.710	0.123	0.220	0.033	< 0.001	< 0.001	< 0.001	0.001	1.000	.	.	.	.	.	.	.	.	.	.	.	.
	S3	0.749	0.532	0.063	0.241	0.074	< 0.001	< 0.001	< 0.001	< 0.001	1.000	0.150	< 0.001	< 0.001	0.002	0.001	1.000	1.000	0.001	< 0.001	0.071	0.005	1.000
	R3	0.946	0.921	0.755	0.571	0.827	0.016	0.290	0.634	1.000	1.000	1.000	0.115	0.517	1.000	1.000	1.000	1.000	0.280	1.000	1.000	1.000	1.000
Stomatal conductance (g_s)	all time points	0.033	0.270	0.773	0.116	0.812	0.002	0.023	0.164	0.804	1.000	.	.	.	.	.	.	.	.	.	.	.	.
	S3	0.048	0.815	0.981	0.734	0.042	< 0.001	< 0.001	0.002	0.001	1.000	0.035	< 0.001	< 0.001	0.045	0.038	1.000	1.000	0.004	0.001	0.077	0.028	1.000
	R3	0.291	0.186	0.701	0.061	1.000	1.000	0.068	1.000	0.333	1.000	1.000	1.000	0.160	1.000	0.600	0.529	1.000	1.000	0.948	1.000	1.000	1.000
Intracellular [CO_2] (c_i)	all time points	0.847	0.905	0.346	0.985	< 0.001	1.000	1.000	< 0.001	0.002	1.000	.	.	.	.	.	.	.	.	.	.	.	.
	S3	0.875	0.726	0.299	0.576	0.099	0.341	0.119	< 0.001	< 0.001	1.000	0.837	0.318	0.840	0.006	0.025	1.000	0.299	1.000	0.376	0.045	0.002	1.000
	R3	0.909	0.856	0.769	0.558	< 0.001	0.104	0.002	0.410	1.000	1.000	0.020	0.783	0.138	0.756	1.000	1.000	0.024	0.343	0.022	1.000	1.000	1.000
c_i/c_a	all time points	0.495	0.171	< 0.001	< 0.001	1.000	0.002	0.011	< 0.001	< 0.001	1.000	.	.	.	.	.	.	.	.	.	.	.	.
	S3	0.979	0.735	0.253	0.757	1.000	< 0.001	< 0.001	< 0.001	< 0.001	1.000	1.000	< 0.001	0.001	0.001	0.002	1.000	1.000	0.015	< 0.001	0.013	< 0.001	1.000
	R3	0.715	0.576	0.564	0.677	0.395	1.000	0.987	0.331	1.000	0.851	0.956	1.000	1.000	0.334	1.000	1.000	1.000	1.000	1.000	1.000	1.000	1.000
Transpiration dark (E_d)	all time points	0.593	0.798	0.429	0.221	.	.	.	.	.	.	.	.	.	.	.	.	.	.	.	.	.	.
	S3	0.378	0.606	0.769	0.938	0.865	< 0.001	< 0.001	0.023	0.031	1.000	0.515	0.002	0.004	0.280	0.424	1.000	1.000	0.072	0.068	0.168	0.159	1.000
	R3	0.898	0.876	0.409	0.073	0.536	0.001	< 0.001	0.181	< 0.001	0.022	1.000	0.107	< 0.001	< 0.001	< 0.001	0.006	1.000	0.016	0.001	0.261	0.033	1.000
Respiration dark (R_d)	all time points	0.509	0.309	0.456	0.830	0.843	0.361	0.001	1.000	0.061	0.175	.	.	.	.	.	.	.	.	.	.	.	.
	S3	0.060	0.987	0.352	0.920	1.000	1.000	1.000	1.000	1.000	0.607	1.000	1.000	1.000	1.000	1.000	1.000	1.000	0.185	1.000	1.000	1.000	0.695
	R3	0.329	0.148	0.051	0.839	0.112	0.002	< 0.001	0.991	0.032	0.830	0.333	1.000	0.008	1.000	0.957	0.210	0.876	0.001	0.001	0.053	0.058	1.000

Isoprene emission, leaf-level	all time points	< 0.001	0.000	< 0.001	< 0.001	0.039	1.000	1.000	0.064	0.855	1.000	.	.	.	.	.	.	.	.	.	.	.	.
	S3	< 0.001	0.001	< 0.001	< 0.001	0.466	1.000	1.000	0.155	1.000	1.000	0.114	1.000	1.000	0.018	0.950	0.581	1.000	1.000	1.000	1.000	1.000	1.000
	R3	< 0.001	0.002	< 0.001	< 0.001	0.199	1.000	1.000	0.906	1.000	1.000	0.476	1.000	1.000	0.316	0.772	1.000	1.000	1.000	1.000	1.000	1.000	1.000
Photosynthetic carbon lost as isoprene (C%)	all time points	< 0.001	0.044	< 0.001	< 0.001	1.000	0.418	0.318	0.013	0.009	1.000	.	.	.	.	.	.	.	.	.	.	.	.
	S3	0.020	0.124	< 0.001	< 0.001	1.000	0.010	0.002	0.001	< 0.001	1.000	1.000	< 0.001	< 0.001	< 0.001	< 0.001	1.000	1.000	1.000	1.000	1.000	1.000	1.000
	R3	0.004	0.180	0.042	0.091	1.000	1.000	1.000	1.000	1.000	1.000	0.560	1.000	1.000	1.000	1.000	1.000	1.000	1.000	1.000	1.000	1.000	1.000
Net ecosystem productivity	all time points	0.191	0.630	0.687	0.056	0.126	1.000	0.062	1.000	0.010	0.002	.	.	.	.	.	.	.	.	.	.	.	.
	P	0.137	0.840	0.030	0.569	1.000	0.141	1.000	1.000	0.644	0.006	1.000	1.000	1.000	1.000	1.000	1.000	1.000	0.299	0.414	0.637	0.823	0.002
	S3	0.482	0.740	0.711	0.518	1.000	0.002	< 0.001	< 0.001	< 0.001	0.103	1.000	0.216	0.002	0.019	< 0.001	0.696	1.000	0.012	< 0.001	0.023	< 0.001	0.395
	R3	0.943	0.482	0.013	0.035	0.188	< 0.001	< 0.001	0.049	0.183	1.000	0.302	< 0.001	< 0.001	0.076	0.276	1.000	1.000	0.026	0.052	1.000	1.000	1.000
Net isoprene loss	all time points	0.000	0.059	< 0.001	0.000	1.000	0.153	0.003	0.022	0.001	0.930	.	.	.	.	.	.	.	.	.	.	.	.
	P	0.042	0.559	0.030	0.026	1.000	1.000	1.000	1.000	1.000	1.000	1.000	1.000	1.000	1.000	1.000	1.000	1.000	1.000	1.000	1.000	1.000	1.000
	S3	0.022	0.381	0.000	< 0.001	1.000	0.002	< 0.001	0.002	< 0.001	0.964	1.000	< 0.001	< 0.001	< 0.001	< 0.001	0.215	1.000	1.000	1.000	1.000	1.000	1.000
	R3	0.002	0.068	0.003	< 0.001	1.000	1.000	1.000	1.000	1.000	1.000	1.000	1.000	0.460	1.000	0.314	0.295	1.000	1.000	1.000	1.000	1.000	1.000

Table S2. Calculated angles of different stress phases of cumulative net C gain. Phases are: P = pre-stress, S1 = stress cycle 1, R1 = recovery phase 1, S2 = stress cycle 2, R2 = recovery phase 2, S3 = stress cycle 3, R3 = recovery phase 3. In CS scenario, the phases are named as follows: P = pre-stress, S_{IN} = stress initial, S_{SEV} = stress severe, R = recovery. The scenarios are: AC = control with ambient [CO_2], EC = control with elevated [CO_2], PS = periodic stress, CS = chronic stress. IE = isoprene-emitting, NE = non-emitting.

AC			**EC**			**PS**			**CS**		
	IE	**NE**		**IE**	**NE**		**IE**	**NE**		**IE**	**NE**
P	27.5°	30.0°	P	29.0°	29.0°	P	38.0°	38.0°	P	38.0°	37.5°
						S1	20.0°	21.0°	S_{IN}	25.0°	22.0°
						R1	39.0°	39.0°	S_{SEV}	15.5°	12.0°
						S2	9.0°	10.0°	R	43.5°	42.0°
						R2	39.5°	37.0°			
						R3	16.0°	14.0°			
						R3	42.5°	36.0°			

Parsed Citations

Affek HP, Yakir D (2002) Protection by isoprene against singlet oxygen in leaves. Plant Physiol 129: 269-277
Pubmed: Author and Title
CrossRef: Author and Title
Google Scholar: Author Only Title Only Author and Title

Affek HP, Yakir D (2003) Natural abundance carbon isotope composition of isoprene reflects incomplete coupling between isoprene synthesis and photosynthetic carbon flow. Plant Physiol 131: 1727-1736
Pubmed: Author and Title
CrossRef: Author and Title
Google Scholar: Author Only Title Only Author and Title

Ainsworth EA, Yendrek CR, Sitch S, Collins WJ, Emberson LD (2012) The effects of tropospheric ozone on net primary productivity and implications for climate change. Annu Rev Plant Biol 63: 637-661
Pubmed: Author and Title
CrossRef: Author and Title
Google Scholar: Author Only Title Only Author and Title

Alemayehu FR, Frenck G, van der Linden L, Mikkelsen TN, Jorgensen RB (2014) Can barley (Hordeum vulgare L.) adapt to fast climate changes? A controlled selection experiment. Genetic Resources and Crop Evolution 61:151-161
Pubmed: Author and Title
CrossRef: Author and Title
Google Scholar: Author Only Title Only Author and Title

Allen SJ, Hall RL, Rosier PTW (1999) Transpiration by two poplar varieties grown as coppice for biomass production. Tree Physiol 19: 493-501
Pubmed: Author and Title
CrossRef: Author and Title
Google Scholar: Author Only Title Only Author and Title

Andriankaja M, Dhondt S, De Bodt S, Vanhaeren H, Coppens F, De Milde L, Mühlenbock P, Skirycz A, Gonzalez N, Beemster GT, Inzé D (2012) Exit from proliferation during leaf development in Arabidopsis thaliana: a not-so-gradual process. Dev Cell 22: 64-78
Pubmed: Author and Title
CrossRef: Author and Title
Google Scholar: Author Only Title Only Author and Title

Arneth A, Schurgers G, Hickler T, Miller PA (2008) Effects of species composition, land surface cover, CO2 concentration and climate on isoprene emissions from European forests. Plant Biol 10: 150-162
Pubmed: Author and Title
CrossRef: Author and Title
Google Scholar: Author Only Title Only Author and Title

Ashworth K, Folberth G, Hewitt CN, Wild O (2012) Impacts of near-future cultivation of biofuel feedstocks on atmospheric composition and local air quality. ACP 12: 919-939
Pubmed: Author and Title
CrossRef: Author and Title
Google Scholar: Author Only Title Only Author and Title

Aylott MJ, Casella E, Tubby I, Street NR, Smith P, Taylor G (2008) Yield and spatial supply of bioenergy poplar and willow short-rotation coppice in the UK. New Phytol 178: 358-370
Pubmed: Author and Title
CrossRef: Author and Title
Google Scholar: Author Only Title Only Author and Title

Bauwe H, Hagemann M, Fernie AR (2010) Photorespiration: players, partners and origin. Trends Plant Sci 15: 330-336
Pubmed: Author and Title
CrossRef: Author and Title
Google Scholar: Author Only Title Only Author and Title

Beauchamp J, Wisthaler A, Hansel A, Kleist E, Miebach M, Niinemets Ü, Schurr U, Wildt J (2005) Ozone induced emissions of biogenic VOC from tobacco: relationships between ozone uptake and emission of LOX products. Plant Cell Environ 28: 1334-1343
Pubmed: Author and Title
CrossRef: Author and Title
Google Scholar: Author Only Title Only Author and Title

Behnke K, Ehlting B, Teuber M, Bauerfeind M, Louis S, Hänsch R, Polle A, Bohlmann J, Schnitzler J-P (2007) Transgenic, non-isoprene emitting poplars don't like it hot. Plant J 51: 485-499
Pubmed: Author and Title
CrossRef: Author and Title
Google Scholar: Author Only Title Only Author and Title

Behnke K, Grote R, Bruggemann N, Zimmer I, Zhou GW, Elobeid M, Janz D, Polle A, Schnitzler J-P (2012) Isoprene emission-free poplars - a chance to reduce the impact from poplar plantations on the atmosphere. New Phytol 194: 70-82
Pubmed: Author and Title
CrossRef: Author and Title
Google Scholar: Author Only Title Only Author and Title

Behnke K, Ghirardo A, Janz D, Kanawati B, Esperschütz J, Zimmer I, Schmitt-Kopplin P, Niinemets Ü, Polle A, Schnitzler JP, Rosenkranz M (2013) Isoprene function in two contrasting poplars under salt and sunflecks. Tree Physiol 33: 562-578

Pubmed: Author and Title
CrossRef: Author and Title
Google Scholar: Author Only Title Only Author and Title

Behnke K, Kaiser A, Zimmer I, Brüggemann N, Janz D, Polle A, Hampp R, Hänsch R, Popko J, Schmitt-Kopplin P, Ehlting B, Rennenberg H, Barta C, Loreto F, Schnitzler J-P (2010a) RNAi-mediated suppression of isoprene emission in poplar transiently impacts phenolic metabolism under high temperature and high light intensities: a transcriptomic and metabolomic analysis. Plant Mol Biol 74: 61-75
Pubmed: Author and Title
CrossRef: Author and Title
Google Scholar: Author Only Title Only Author and Title

Behnke K, Loivamäki M, Zimmer I, Rennenberg H, Schnitzler J-P, Louis S (2010b) Isoprene emission protects photosynthesis in sunfleck exposed Grey poplar. Photosynth Res 104: 5-17
Pubmed: Author and Title
CrossRef: Author and Title
Google Scholar: Author Only Title Only Author and Title

Bell ML, Goldberg R, Hogrefe C, Kinney PL, Knowlton K, Lynn B, Rosenthal J, Rosenzweig C, Patz JA (2007) Climate change, ambient ozone, and health in 50 US cities. Clim Chang 82: 61-76
Pubmed: Author and Title
CrossRef: Author and Title
Google Scholar: Author Only Title Only Author and Title

Brilli F, Barta C, Fortunati A, Lerdau M, Loreto F, Centritto M (2007) Response of isoprene emission and carbon metabolism to drought in white poplar (Populus alba) saplings. New Phytol 175: 244-254
Pubmed: Author and Title
CrossRef: Author and Title
Google Scholar: Author Only Title Only Author and Title

Brilli F, Hörtnagl L, Bamberger I, Schnitzhofer R, Ruuskanen TM, Hansel A, Loreto F, Wohlfahrt G (2012) Qualitative and quantitative characterization of volatile organic compound emissions from cut grass. Environ Sci Technol 46: 3859-3865
Pubmed: Author and Title
CrossRef: Author and Title
Google Scholar: Author Only Title Only Author and Title

Brilli F, Tsonev T, Mahmood T, Velikova V, Loreto F, Centritto M (2013) Ultradian variation of isoprene emission, photosynthesis, mesophyll conductance, and optimum temperature sensitivity for isoprene emission in water-stressed Eucalyptus citriodora saplings. J Exp Bot 64: 519-528
Pubmed: Author and Title
CrossRef: Author and Title
Google Scholar: Author Only Title Only Author and Title

Brüggemann N, Schnitzler J-P (2002) Comparison of isoprene emission, intercellular isoprene concentration and photosynthetic performance in water-limited oak (Quercus pubescens Willd. and Quercus robur L.) saplings. Plant Biol 4: 456-463
Pubmed: Author and Title
CrossRef: Author and Title
Google Scholar: Author Only Title Only Author and Title

Brunner AM, Busov VB, Strauss SH (2004) Poplar genome sequence: functional genomics in an ecologically dominant plant species. Trends Plant Sci 9: 49-56
Pubmed: Author and Title
CrossRef: Author and Title
Google Scholar: Author Only Title Only Author and Title

Ceccato P, Flasse S, Tarantola S, Jacquemoud S, Gregoire JM (2001) Detecting vegetation leaf water content using reflectance in the optical domain. Remote Sens Environ 77: 22-33
Pubmed: Author and Title
CrossRef: Author and Title
Google Scholar: Author Only Title Only Author and Title

Centritto M, Brilli F, Fodale R, Loreto F (2011) Different sensitivity of isoprene emission, respiration and photosynthesis to high growth temperature coupled with drought stress in black poplar (Populus nigra) saplings. Tree Physiol 31: 275-286
Pubmed: Author and Title
CrossRef: Author and Title
Google Scholar: Author Only Title Only Author and Title

Centritto M, Nascetti P, Petrilli L, Raschi A, Loreto F (2004) Profiles of isoprene emission and photosynthetic parameters in hybrid poplars exposed to free-air CO2 enrichment. Plant Cell Environ 27: 403-412
Pubmed: Author and Title
CrossRef: Author and Title
Google Scholar: Author Only Title Only Author and Title

Chaves MM, Maroco JP, Pereira JS (2003) Understanding plant responses to drought - from genes to the whole plant. Funct Plant Biol 30: 239-264
Pubmed: Author and Title
CrossRef: Author and Title
Google Scholar: Author Only Title Only Author and Title

Cinege G, Louis S, Hänsch R, Schnitzler J-P (2009) Regulation of isoprene synthase promoter by environmental and internal

factors. Plant Mol Biol 69: 593-604
Pubmed: Author and Title
CrossRef: Author and Title
Google Scholar: Author Only Title Only Author and Title

Clausen SK, Frenck G, Linden LG, Mikkelsen TN, Lunde C, Jorgensen RB (2011) Effects of single and multifactor treatments with elevated temperature, CO2 and ozone on oilseed rape and barley. J Agron Crop Sci 197: 442-453
Pubmed: Author and Title
CrossRef: Author and Title
Google Scholar: Author Only Title Only Author and Title

Constable JVH, Guenther AB, Schimel DS, Monson RK (1999) Modelling changes in VOC emission in response to climate change in the continental United States. Global Change Biol 5: 791-806
Pubmed: Author and Title
CrossRef: Author and Title
Google Scholar: Author Only Title Only Author and Title

Copolovici L, Niinemets Ü (2010) Flooding induced emissions of volatile signalling compounds in three tree species with differing waterlogging tolerance. Plant Cell Environ 33: 1582-1594
Pubmed: Author and Title
CrossRef: Author and Title
Google Scholar: Author Only Title Only Author and Title

Copolovici LO, Filella I, Llusia J, Niinemets Ü, Peñuelas J (2005) The capacity for thermal protection of photosynthetic electron transport varies for different monoterpenes in Quercus ilex. Plant Physiol 139: 485-496
Pubmed: Author and Title
CrossRef: Author and Title
Google Scholar: Author Only Title Only Author and Title

Correia B, Pinto-Marijuan M, Neves L, Brossa R, Dias MC, Costa A, Castro BB, Araújo C, Santos C, Chaves MM, Pinto G (2014) Water stress and recovery in the performance of two Eucalyptus globulus clones: physiological and biochemical profiles. Physiol Plant 150: 580-592
Pubmed: Author and Title
CrossRef: Author and Title
Google Scholar: Author Only Title Only Author and Title

Coumou D, Rahmstorf S (2012). A decade of weather extremes. Nature Climate Change 2: 491-496
Pubmed: Author and Title
CrossRef: Author and Title
Google Scholar: Author Only Title Only Author and Title

de Gouw JA, Howard CJ, Custer TG, Fall R (1999) Emissions of volatile organic compounds from cut grass and clover are enhanced during the drying process. Geophys Res Lett 26: 811-814
Pubmed: Author and Title
CrossRef: Author and Title
Google Scholar: Author Only Title Only Author and Title

Eller AS, de Gouw JA, Graus M, Monson RK (2012) Variation among different genotypes of hybrid poplar with regard to leaf volatile organic compound emissions. Ecol Appl 7: 1865-1875
Pubmed: Author and Title
CrossRef: Author and Title
Google Scholar: Author Only Title Only Author and Title

Fall R, Benson AA (1996) Leaf methanol - The simplest natural product from plants. Trends Plant Sci 1: 296-301
Pubmed: Author and Title
CrossRef: Author and Title
Google Scholar: Author Only Title Only Author and Title

Feussner I, Wasternack C (2002) The lipoxygenase pathway. Annu Rev Plant Biol 53: 275-297
Pubmed: Author and Title
CrossRef: Author and Title
Google Scholar: Author Only Title Only Author and Title

Feyen L, Dankers R (2009) Impact of global warming on streamflow drought in Europe. J Geophys Res: Atmospheres 114: D17116
Pubmed: Author and Title
CrossRef: Author and Title
Google Scholar: Author Only Title Only Author and Title

Fischer EM, Schär C (2010) Consistent geographical patterns of changes in high-impact European heatwaves. Nat Geosci 3: 398-403
Pubmed: Author and Title
CrossRef: Author and Title
Google Scholar: Author Only Title Only Author and Title

Fortunati A, Barta C, Brilli F, Centritto M, Zimmer I, Schnitzler J-P, Loreto F (2008) Isoprene emission is not temperature-dependent during and after severe drought-stress: a physiological and biochemical analysis. Plant J 55: 687-697
Pubmed: Author and Title
CrossRef: Author and Title
Google Scholar: Author Only Title Only Author and Title

Gallé A, Feller U (2007) Changes of photosynthetic traits in beech saplings (Fagus sylvatica) under severe drought stress and

during recovery. Physiol Plant 131: 412-421
Pubmed: Author and Title
CrossRef: Author and Title
Google Scholar: Author Only Title Only Author and Title

Genty B, Wonders J, Baker NR (1990) Non-photochemical quenching of Fo in leaves is emission wavelength dependent: consequences for quenching analysis and its interpretation. Photosynth Res 26: 133-139
Pubmed: Author and Title
CrossRef: Author and Title
Google Scholar: Author Only Title Only Author and Title

Ghirardo A, Gutknecht J, Zimmer I, Brüggemann N, Schnitzler J-P (2011) Biogenic volatile organic compound and respiratory CO2 emissions after 13C-labeling: online tracing of C translocation dynamics in poplar plants. PLoS One 6: e17393
Pubmed: Author and Title
CrossRef: Author and Title
Google Scholar: Author Only Title Only Author and Title

Ghirardo A, Heller W, Fladung M, Schnitzler J-P, Schröder H (2012) Function of defensive volatiles in pedunculate oak (Quercus robur) is tricked by the moth Tortrix viridana. Plant Cell Environ 35: 2192-2207
Pubmed: Author and Title
CrossRef: Author and Title
Google Scholar: Author Only Title Only Author and Title

Ghirardo A, Koch K, Taipale R, Zimmer I, Schnitzler J-P, Rinne J (2010) Determination of de novo and pool emissions of terpenes from four common boreal/alpine trees by 13CO2 labelling and PTR-MS analysis. Plant Cell Environ 33: 781-792
Pubmed: Author and Title
CrossRef: Author and Title
Google Scholar: Author Only Title Only Author and Title

Ghirardo A, Wright LP, Bi Z, Rosenkranz M, Pulido P, Rodríguez-Concepción M, Niinemets Ü, Brüggemann N, Gershenzon J, Schnitzler J-P (2014) Metabolic flux analysis of plastidic isoprenoid biosynthesis in poplar leaves emitting and nonemitting isoprene. Plant Physiol 165: 37-51
Pubmed: Author and Title
CrossRef: Author and Title
Google Scholar: Author Only Title Only Author and Title

Graus M, Müller M, Hansel A (2010) High resolution PTR-TOF: quantification and formula confirmation of VOC in real time. J Am Soc Mass Spectrom 21: 1037-1044
Pubmed: Author and Title
CrossRef: Author and Title
Google Scholar: Author Only Title Only Author and Title

Guenther A, Karl T, Harley P, Wiedinmyer C, Palmer PI, Geron C (2006) Estimates of global terrestrial isoprene emissions using MEGAN (Model of Emissions of Gases and Aerosols from Nature). ACP 6: 3181-3210
Pubmed: Author and Title
CrossRef: Author and Title
Google Scholar: Author Only Title Only Author and Title

Hummel I, Pantin F, Sulpice R, Piques M, Rolland G, Dauzat M, Christophe A, Pervent M, Bouteillé M, Stitt M, Gibon Y, Muller B (2010) Arabidopsis plants acclimate to water deficit at low cost through changes of carbon usage: An integrated perspective using growth, metabolite, enzyme, and gene expression analysis. Plant Physiol 154: 357-372
Pubmed: Author and Title
CrossRef: Author and Title
Google Scholar: Author Only Title Only Author and Title

Hunt ERJr, Rock BN (1989) Detection of changes in leaf water content using near- and middle-infrared reflectances. Rem Sens Environ 30: 43-54
Pubmed: Author and Title
CrossRef: Author and Title
Google Scholar: Author Only Title Only Author and Title

Hüve K, Christ MM, Kleist E, Uerlings R, Niinemets Ü, Walter A, Wildt J (2007) Simultaneous growth and emission measurements demonstrate an interactive control of methanol release by leaf expansion and stomata. J Exp Bot 58: 1783-1793
Pubmed: Author and Title
CrossRef: Author and Title
Google Scholar: Author Only Title Only Author and Title

IPCC (2007) Summary for policymakers. In: Climate Change 2007: Impacts, Adaptation and Vulnerability. Contribution of Working Group II to the Fourth Assessment Report of the Intergovernmental Panel on Climate Change (eds Parry ML, Canziani OF, Palutikof JP, Van der Linden PJ, Hanson CE). Cambridge University Press, Cambridge
Pubmed: Author and Title
CrossRef: Author and Title
Google Scholar: Author Only Title Only Author and Title

IPCC (2014) Near-term Climate Change: Projections and Predictability. In: Climate Change 2013: The Physical Science Basis. Contribution of Working Group I to the Fifth Assessment Report of the Intergovernmental Panel on Climate Change (eds Stocker, TF, Qin D, Plattner GK, Tignor M, Allen SK, Boschung J,Nauels A, Xia Y, Bex V, Midgley PM). Cambridge University Press, Cambridge
Pubmed: Author and Title
CrossRef: Author and Title

Google Scholar: Author Only Title Only Author and Title

Jardine KJ, Monson RK, Abrell L, Saleska SR, Arneth A, Jardine A, Ishida FY, Yanez Serrano AM, Artaxo P, Karl T et al. (2012) Within-plant isoprene oxidation confirmed by direct emissions of oxidation products methyl vinyl ketone and methacrolein. Global Change Biol 18: 973-984
Pubmed: Author and Title
CrossRef: Author and Title
Google Scholar: Author Only Title Only Author and Title

Kirschbaum MUF (1988) Recovery of photosynthesis from water stress in Eucalyptus pauciflora - a process in two stages. Plant Cell Environ 11: 685-694
Pubmed: Author and Title
CrossRef: Author and Title
Google Scholar: Author Only Title Only Author and Title

Kreuzwieser J, Scheerer U, Kruse J, Burzlaff T, Honsel A, Alfarraj S, Georgiev P, Schnitzler J-P, Ghirardo A, Kreuzer I, Hedrich R, Rennenberg H (2014) The Venus flytrap attracts insects by the release of volatile organic compounds. J Exp Bot 65: 755-766
Pubmed: Author and Title
CrossRef: Author and Title
Google Scholar: Author Only Title Only Author and Title

Kuokkanen K, Julkunen-Tiitto R, Keinanen M, Niemela P, Tahvanainen J (2001) The effect of elevated CO2 and temperature on the secondary chemistry of Betula pendula seedlings. Trees: Structure and Function 15: 378-384
Pubmed: Author and Title
CrossRef: Author and Title
Google Scholar: Author Only Title Only Author and Title

Leplé J, Brasileiro A, Michel M, Delmotte F, Jouanin L (1992) Transgenic poplars: expression of chimeric genes using four different constructs. Plant Cell Rep 11: 137-141
Pubmed: Author and Title
CrossRef: Author and Title
Google Scholar: Author Only Title Only Author and Title

Levitt J (1980) Stress concepts. In: Kozlowski, TT ed, Responses of plants to environmental stresses, Ed 2, Vol 2. Academic Press, Inc, New York, pp 3 - 20
Pubmed: Author and Title
CrossRef: Author and Title
Google Scholar: Author Only Title Only Author and Title

Lichtenthaler HK (1996) Vegetation stress: An introduction to the stress concept in plants. J Plant Physiol 148: 4-14
Pubmed: Author and Title
CrossRef: Author and Title
Google Scholar: Author Only Title Only Author and Title

Loreto F, Barta C, Brilli F, Nogues I (2006) On the induction of volatile organic compound emissions by plants as consequence of wounding or fluctuations of light and temperature. Plant Cell Environ 29: 1820-1828
Pubmed: Author and Title
CrossRef: Author and Title
Google Scholar: Author Only Title Only Author and Title

Loreto F, Centritto M, Barta C, Calfapietra C, Fares S, Monson RK (2007) The relationship between isoprene emission rate and dark respiration rate in white poplar (Populus alba L.) leaves. Plant Cell Environ 30: 662-669
Pubmed: Author and Title
CrossRef: Author and Title
Google Scholar: Author Only Title Only Author and Title

Loreto F, Schnitzler J-P (2010) Abiotic stresses and induced BVOCs. Trends Plant Sci 15: 154-166
Pubmed: Author and Title
CrossRef: Author and Title
Google Scholar: Author Only Title Only Author and Title

Loreto F, Sharkey TD (1993) Isoprene emission by plants is affected by transmissible wound signals. Plant Cell Environ 16: 563-570
Pubmed: Author and Title
CrossRef: Author and Title
Google Scholar: Author Only Title Only Author and Title

Loreto F, Velikova V (2001) Isoprene produced by leaves protects the photosynthetic apparatus against ozone damage, quenches ozone products, and reduces lipid peroxidation of cellular membranes. Plant Physiol 127: 1781-1787
Pubmed: Author and Title
CrossRef: Author and Title
Google Scholar: Author Only Title Only Author and Title

Mahecha MD, Reichstein M, Carvalhais N, Lasslop G, Lange H, Seneviratne SI, Vargas R, Ammann C, Arain MA, Cescatti A, Janssens IA, Migliavacca M, Montagnani L, Richardson AD (2010) Global convergence in the temperature sensitivity of respiration at ecosystem level. Science 329: 838-840
Pubmed: Author and Title
CrossRef: Author and Title
Google Scholar: Author Only Title Only Author and Title

Mayrhofer S, Teuber M, Zimmer I, Louis S, Fischbach RJ, Schnitzler J-P (2005) Diurnal and seasonal variation of isoprene biosynthesis-related genes in Grey poplar leaves. Plant Physiol 139: 474-484

Pubmed: Author and Title
CrossRef: Author and Title
Google Scholar: Author Only Title Only Author and Title

Mittler R, Zilinskas BA (1994) Regulation of pea cytosolic ascorbate peroxidase and other antioxidant enzymes during the progression of drought stress and following recovery from drought. Plant J 5: 397-405
Pubmed: Author and Title
CrossRef: Author and Title
Google Scholar: Author Only Title Only Author and Title

Monson RK, Grote R, Niinemets Ü, Schnitzler J-P (2012) Modeling the isoprene emission rate from leaves. New Phytol 195: 541-559
Pubmed: Author and Title
CrossRef: Author and Title
Google Scholar: Author Only Title Only Author and Title

Monson RK, Jaeger CH, Adams WW, Driggers EM, Silver GM, Fall R (1992) Relationships among isoprene emission rate, photosynthesis, and isoprene synthase activity as influenced by temperature. Plant Physiol 98: 1175-1180
Pubmed: Author and Title
CrossRef: Author and Title
Google Scholar: Author Only Title Only Author and Title

Monson RK, Trahan N, Rosenstiel TN, Veres P, Moore D, Wilkinson M, Norby RJ, Volder A, Tjoelker MG, Briske DD, Karnosky DF, Fall R (2007) Isoprene emission from terrestrial ecosystems in response to global change: minding the gap between models and observations. Philosophical transactions. Series A, Mathematical, physical, and engineering science 365: 1677-1695
Pubmed: Author and Title
CrossRef: Author and Title
Google Scholar: Author Only Title Only Author and Title

Müller M, Graus M, Ruuskanen TM, Schnitzhofer R, Bamberger I, Kaser L, Titzmann T, Hörtnagl L, Wohlfahrt G, Karl T, Hansel A (2010) First eddy covariance flux measurements PTR-TOF. Atmos Meas Tech 3: 387-395
Pubmed: Author and Title
CrossRef: Author and Title
Google Scholar: Author Only Title Only Author and Title

Murata N, Takahashi S, Nishiyama Y, Allakhverdiev SI (2007) Photoinhibition of photosystem II under environmental stress. Biochim Biophys Acta-Bioenergetics 1767: 414-421
Pubmed: Author and Title
CrossRef: Author and Title
Google Scholar: Author Only Title Only Author and Title

Nemecek-Marshall M, MacDonald RC, Franzen JJ, Wojciechowski CL, Fall R (1995) Methanol Emission from Leaves (Enzymatic Detection of Gas-Phase Methanol and Relation of Methanol Fluxes to Stomatal Conductance and Leaf Development). Plant Physiol 108: 1359-1368
Pubmed: Author and Title
CrossRef: Author and Title
Google Scholar: Author Only Title Only Author and Title

Niinemets Ü, Loreto F, Reichstein M (2004) Physiological and physicochemical controls on foliar volatile organic compound emissions. Trends Plant Sci 9: 180-186
Pubmed: Author and Title
CrossRef: Author and Title
Google Scholar: Author Only Title Only Author and Title

Pegoraro E, Rey A, Bobich EG, Barron-Gafford G, Grieve KA, Malhi Y, Murthy R (2004) Effect of elevated CO2 concentration and vapour pressure deficit on isoprene emission from leaves of Populus deltoides during drought. Funct Plant Biol 31: 1137-1147
Pubmed: Author and Title
CrossRef: Author and Title
Google Scholar: Author Only Title Only Author and Title

Perkins SE, Alexander LV, Naim JR (2012) Increasing frequency, intensity and duration of observed global heatwaves and warm spells. Geophys Res Lett 39: L20714, doi:10.1029/2012GL053361
Pubmed: Author and Title
CrossRef: Author and Title
Google Scholar: Author Only Title Only Author and Title

Possell M, Hewitt CN (2011) Isoprene emissions from plants are mediated by atmospheric CO2 concentrations. Global Change Biol 17: 1595-1610
Pubmed: Author and Title
CrossRef: Author and Title
Google Scholar: Author Only Title Only Author and Title

Potosnak MJ, Lestourgeon L, Nunez O (2014) Increasing leaf temperature reduces the suppression of isoprene emission by elevated CO2 concentration. Sci Total Environ 481: 352-359
Pubmed: Author and Title
CrossRef: Author and Title
Google Scholar: Author Only Title Only Author and Title

Rasulov B, Huve K, Bichele I, Laisk A, Niinemets Ü (2010) Temperature response of isoprene emission in vivo reflects a combined effect of substrate limitations and isoprene synthase activity: a kinetic analysis. Plant Physiol 154: 1558-1570

Pubmed: Author and Title
CrossRef: Author and Title
Google Scholar: Author Only Title Only Author and Title

Rennenberg H, Loreto F, Polle A, Brilli F, Fares S, Beniwal RS, Gessler A (2006) Physiological responses of forest trees to heat and drought. Plant Biol 8: 556-571
Pubmed: Author and Title
CrossRef: Author and Title
Google Scholar: Author Only Title Only Author and Title

Rosenkranz M, Pugh TAM, Schnitzler J-P, Arneth A (2014) Effect of land-use change and management on BVOC emissions - selecting climate-smart cultivars. Plant Cell Environ doi: 10.1111/pce.12453
Pubmed: Author and Title
CrossRef: Author and Title
Google Scholar: Author Only Title Only Author and Title

Rosenstiel TN, Potosnak MJ, Griffin KL, Fall R, Monson RK (2003) Increased CO2 uncouples growth from isoprene emission in an agriforest ecosystem. Nature 421: 256-259
Pubmed: Author and Title
CrossRef: Author and Title
Google Scholar: Author Only Title Only Author and Title

Ryan AC, Hewitt CN, Possell M, Vickers CE, Purnell A, Mullineaux PM, Davies WJ, Dodd IC (2014) Isoprene emission protects photosynthesis but reduces plant productivity during drought in transgenic tobacco (Nicotiana tabacum) plants. New Phytol 201: 205-216
Pubmed: Author and Title
CrossRef: Author and Title
Google Scholar: Author Only Title Only Author and Title

Sales CR, Ribeiro RV, Silveira JA, Machado EC, Martins MO, Lagoa AM (2013) Superoxide dismutase and ascorbate peroxidase improve the recovery of photosynthesis in sugarcane plants subjected to water deficit and low substrate temperature. Plant Physiol Biochem 73: 326-336
Pubmed: Author and Title
CrossRef: Author and Title
Google Scholar: Author Only Title Only Author and Title

Schnitzler J-P, Zimmer I, Bachl A, Arend M, Fromm J, Fischbach RJ (2005) Biochemical properties of isoprene synthase in poplar (Populus x canescens). Planta 222: 777-786
Pubmed: Author and Title
CrossRef: Author and Title
Google Scholar: Author Only Title Only Author and Title

Scholander PF, Bradstreet ED, Hemmingsen EA, Hammel HT (1965) Sap pressure in vascular plants: Negative hydrostatic pressure can be measured in plants. Science 148: 339-346
Pubmed: Author and Title
CrossRef: Author and Title
Google Scholar: Author Only Title Only Author and Title

Seckmeyer GP, Payer HD (1993) A new sunlight simulator for ecological research on plants. J Photochem Photobiol B: Biology 21: 175-181
Pubmed: Author and Title
CrossRef: Author and Title
Google Scholar: Author Only Title Only Author and Title

Sharkey TD, Chen XY, Yeh SS (2001) Isoprene increases thermotolerance of fosmidomycin-fed leaves. Plant Physiol 125: 2001-2006
Pubmed: Author and Title
CrossRef: Author and Title
Google Scholar: Author Only Title Only Author and Title

Sharkey TD, Yeh SS (2001) Isoprene emission from plants. Annu Rev Plant Physiol and Plant Mol Biol 52: 407-436
Pubmed: Author and Title
CrossRef: Author and Title
Google Scholar: Author Only Title Only Author and Title

Singsaas EL, Lerdau M, Winter K, Sharkey TD (1997) Isoprene increases thermotolerance of isoprene-emitting species. Plant Physiol 115: 1413-1420
Pubmed: Author and Title
CrossRef: Author and Title
Google Scholar: Author Only Title Only Author and Title

Singsaas EL, Sharkey TD (1998) The regulation of isoprene emission responses to rapid leaf temperature fluctuations. Plant Cell Environ 21: 1181-1188
Pubmed: Author and Title
CrossRef: Author and Title
Google Scholar: Author Only Title Only Author and Title

Sofo A, Dichio B, Xiloyannis C, Masia A (2004) Effects of different irradiance levels on some antioxidant enzymes and on malondialdehyde content during rewatering in olive tree. Plant Sci 166: 293-302
Pubmed: Author and Title
CrossRef: Author and Title

Google Scholar: Author Only Title Only Author and Title

Sun ZH, Niinemets Ü, Hüve K, Rasulov B, Noe SM (2013) Elevated atmospheric CO2 concentration leads to increased whole-plant isoprene emission in hybrid aspen (Populus tremula x Populus tremuloides). New Phytol 198: 788-800
Pubmed: Author and Title
CrossRef: Author and Title
Google Scholar: Author Only Title Only Author and Title

Takahashi S, Murata N (2008) How do environmental stresses accelerate photoinhibition? Trends Plant Sci 13: 178-182
Pubmed: Author and Title
CrossRef: Author and Title
Google Scholar: Author Only Title Only Author and Title

Tattini M, Velikova V, Vickers C, Brunetti C, Di Ferdinando M, Trivellini A, Fineschi S, Agati G, Ferrini F, Loreto F (2014) Isoprene production in transgenic tobacco alters isoprenoid, non-structural carbohydrate and phenylpropanoid metabolism, and protects photosynthesis from drought stress. Plant Cell Environ 37: 1950-1964
Pubmed: Author and Title
CrossRef: Author and Title
Google Scholar: Author Only Title Only Author and Title

Thiel S, Döhring T, Köfferlein M, Kosak A, Martin P, Seidlitz HK (1996) A phytotron for plant stress research: How far can artificial lighting compare to natural sunlight? J Plant Physiol 148: 456-463
Pubmed: Author and Title
CrossRef: Author and Title
Google Scholar: Author Only Title Only Author and Title

Thornton PK, Ericksen PJ, Herrero M, Challinor AJ (2014) Climate variability and vulnerability to climate change: a review. Glob Change Biol 10: 3313-3328
Pubmed: Author and Title
CrossRef: Author and Title
Google Scholar: Author Only Title Only Author and Title

Trowbridge AM, Asensio D, Eller ASD, Way DA, Wilkinson MJ, Schnitzler J-P, Jackson RB, Monson RK (2012) Contribution of various carbon sources toward isoprene biosynthesis in poplar leaves mediated by altered atmospheric CO2 concentrations. PLoS One 7: e32387
Pubmed: Author and Title
CrossRef: Author and Title
Google Scholar: Author Only Title Only Author and Title

Tschaplinski TJ, Tuskan GA, Gebre GM, Todd DE (1998) Drought resistance of two hybrid Populus clones grown in a large-scale plantation. Tree Physiol 18: 653-658
Pubmed: Author and Title
CrossRef: Author and Title
Google Scholar: Author Only Title Only Author and Title

Tuskan GA, DiFazio S, Jansson S, Bohlmann J, Grigoriev I, Hellsten U, Putnam N, Ralph S, Rombauts S, Salamov A et al. (2006) The genome of black cottonwood, Populus trichocarpa (Torr. and Gray). Science 313: 1596-1604
Pubmed: Author and Title
CrossRef: Author and Title
Google Scholar: Author Only Title Only Author and Title

Velikova V, Ghirardo A, Vanzo E, Merl J, Hauck SM, Schnitzler JP (2014) Genetic manipulation of isoprene emissions in poplar plants remodels the chloroplast proteome. J Prot Res 13: 2005-2018
Pubmed: Author and Title
CrossRef: Author and Title
Google Scholar: Author Only Title Only Author and Title

Velikova V, Müller C, Ghirardo A, Rock TM, Aichler M, Walch A, Schmitt-Kopplin P, Schnitzler J-P (2015) Knocking down of isoprene emission modifies the lipid matrix of thylakoid membranes and influences the chloroplast ultrastructure in poplar. Plant Physiol DOI:10.1104/pp.15.00612, preview
Pubmed: Author and Title
CrossRef: Author and Title
Google Scholar: Author Only Title Only Author and Title

Velikova V, Pinelli P, Loreto F (2005) Consequences of inhibition of isoprene synthesis in Phragmites australis leaves exposed to elevated temperatures. Agric Ecosyst and Environ 106: 209-217
Pubmed: Author and Title
CrossRef: Author and Title
Google Scholar: Author Only Title Only Author and Title

Velikova V, Varkonyi Z, Szabo M, Maslenkova L, Nogues I, Kovács L, Peeva V, Busheva M, Garab G, Sharkey TD, Loreto F et al. (2011) Increased thermostability of thylakoid membranes in isoprene-emitting leaves probed with three biophysical techniques. Plant Physiol 157: 905-916
Pubmed: Author and Title
CrossRef: Author and Title
Google Scholar: Author Only Title Only Author and Title

Vickers CE, Possell M, Cojocariu CI, Velikova VB, Laothawornkitkul J, Ryan A, Mullineaux PM, Hewitt CN (2009) Isoprene synthesis protects transgenic tobacco plants from oxidative stress. Plant Cell Environ 32: 520-531
Pubmed: Author and Title

CrossRef: Author and Title
Google Scholar: Author Only Title Only Author and Title

von Caemmerer S, Farquhar GD (1981) Some relationships between the biochemistry of photosynthesis and the gas exchange of leaves. Planta 153: 376-387
Pubmed: Author and Title
CrossRef: Author and Title
Google Scholar: Author Only Title Only Author and Title

Way DA, Ghirardo A, Kanawati B, Esperschutz J, Monson RK, Jackson RB, Schmitt-Kopplin P, Schnitzler JP (2013) Increasing atmospheric CO2 reduces metabolic and physiological differences between isoprene- and non-isoprene-emitting poplars. New Phytol 200: 534-546
Pubmed: Author and Title
CrossRef: Author and Title
Google Scholar: Author Only Title Only Author and Title

Way DA, Schnitzler J-P, Monson RK, Jackson RB (2011) Enhanced isoprene-related tolerance of heat- and light-stressed photosynthesis at low, but not high, CO2 concentrations. Oecologia 166: 273-282
Pubmed: Author and Title
CrossRef: Author and Title
Google Scholar: Author Only Title Only Author and Title

Way DA, Yamori W (2014) Thermal acclimation of photosynthesis: on the importance of adjusting our definitions and accounting for thermal acclimation of respiration. Photosynth Res 119: 89-100
Pubmed: Author and Title
CrossRef: Author and Title
Google Scholar: Author Only Title Only Author and Title

Wiberley AE, Donohue AR, Westphal MM, Sharkey TD (2009) Regulation of isoprene emission from poplar leaves throughout a day. Plant Cell Environ 32: 939-947
Pubmed: Author and Title
CrossRef: Author and Title
Google Scholar: Author Only Title Only Author and Title

Wiberley AE, Linskey AR, Falbel TG, Sharkey TD (2005) Development of the capacity for isoprene emission in kudzu. Plant Cell Environ 28: 898-905
Pubmed: Author and Title
CrossRef: Author and Title
Google Scholar: Author Only Title Only Author and Title

Wilkinson MJ, Monson RK, Trahan N, Lee S, Brown E, Jackson RB, Polley HW, Fay PA, Fall R (2009) Leaf isoprene emission rate as a function of atmospheric CO2 concentration. Global Change Biol 15: 1189-1200
Pubmed: Author and Title
CrossRef: Author and Title
Google Scholar: Author Only Title Only Author and Title

Wullschleger SD, Jansson S, Taylor G (2002) Genomics and forest biology: Populus emerges as the perennial favorite. Plant Cell 14: 2651-2655
Pubmed: Author and Title
CrossRef: Author and Title
Google Scholar: Author Only Title Only Author and Title

Wuyts N, Palauqui JC, Conejero G, Verdeil JL, Granier C, Massonnet C (2010) High-contrast three-dimensional imaging of the Arabidopsis leaf enables the analysis of cell dimensions in the epidermis and mesophyll. Plant Methods 6: 17
Pubmed: Author and Title
CrossRef: Author and Title
Google Scholar: Author Only Title Only Author and Title

Zhu XG, Song QF, Ort DR (2012) Elements of a dynamic systems model of canopy photosynthesis. Curr Opin Plant Biol 15: 237-244
Pubmed: Author and Title
CrossRef: Author and Title
Google Scholar: Author Only Title Only Author and Title

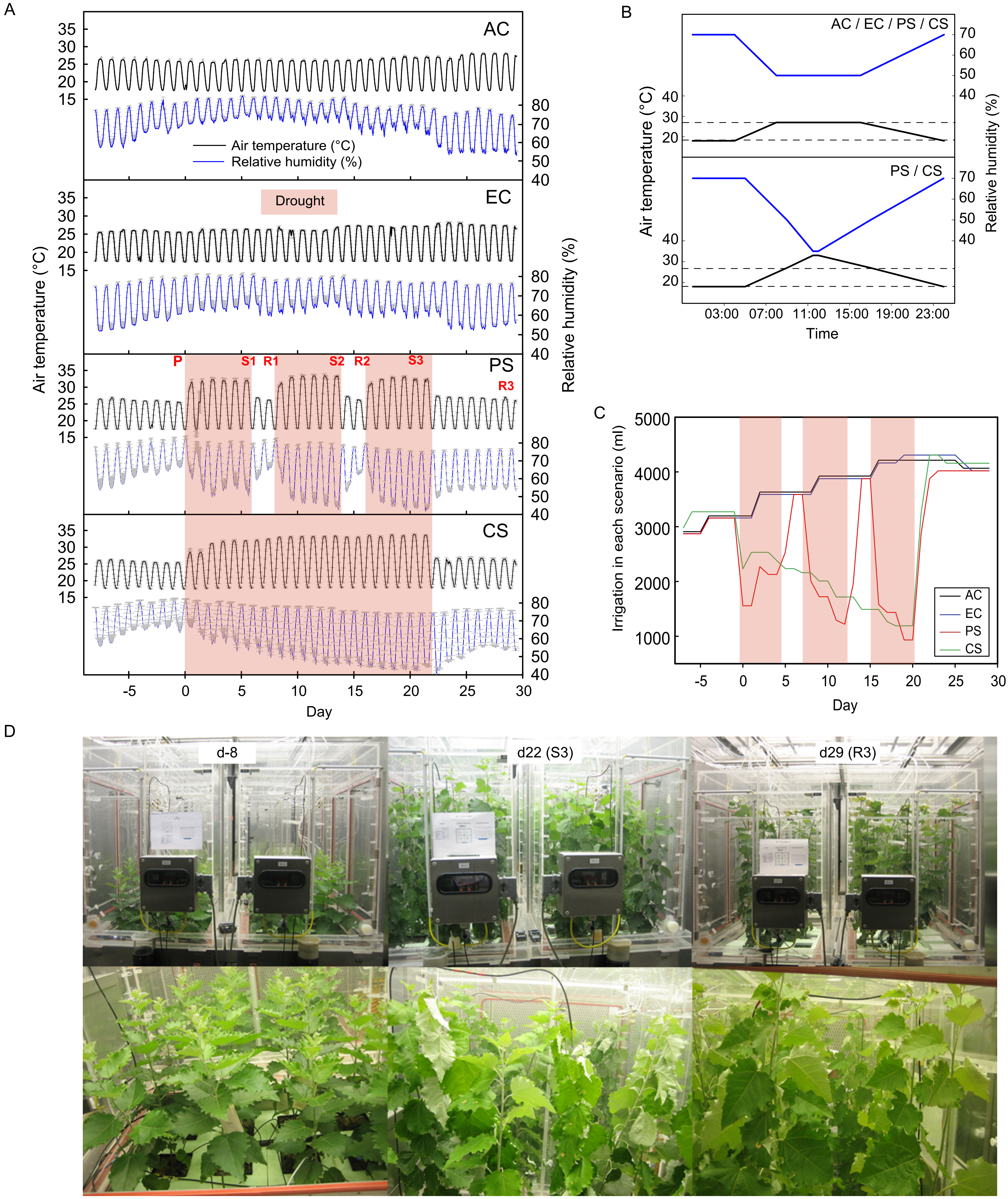

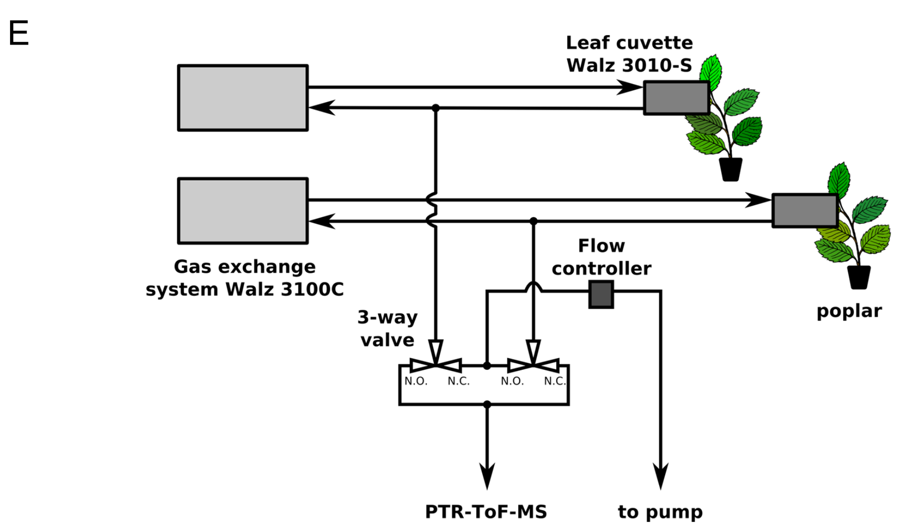

Figure S1. Time courses of air temperature, relative humidity, irrigation and plant appearance in the four scenarios. A, Diurnal course of air temperature and relative humidity during the experiment. The given values are the means of 4 sub-chambers (± SE). B, Theoretical values of daily air temperature and relative humidity when maximum air temperature was set to 27 °C (pre-stress and recovery, above) and to 33 °C during stress in PS and CS (below). Dashed lines indicate mean night temperature (18 °C) and light hour air temperature under unstressed conditions (27 °C). C, Irrigation profile of the experiment. Water amount (in ml) is given to the pots by automated drip irrigation systems. Values represent means of the 4 sub-chambers (representing each genotype) within each scenario (AC, EC, PS, CS). D, Front view of 2 sub-chambers (scenario PS) with12 Grey poplar plants arranged within 1 sub-chamber. E, Schematic of the setup used for the leaf-level gas exchange and VOC emission measurements. The PTR-ToF-MS was sampling from the leaf cuvette back-stream line and could be switched to sample from either gas exchange system. AC = control ambient [CO_2], EC = control elevated [CO_2], PS = periodic stress, CS = chronic stress.

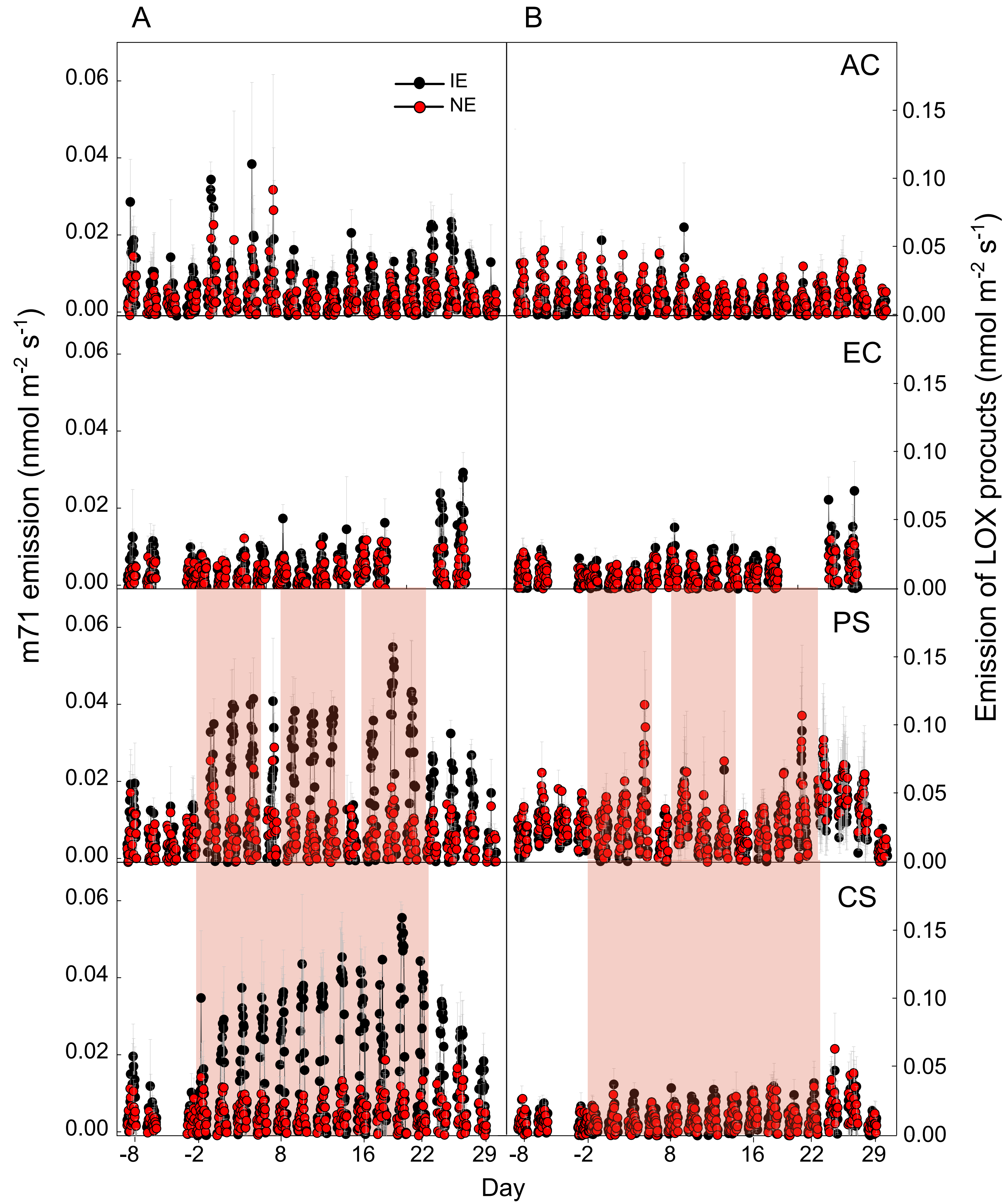

Figure S2. Time course of m71 (A) and LOX (B) products (i.e. m99 + m101) emission rates of isoprene-emitting (IE, black circles) and non-emitting (NE, red circles) Grey poplar genotypes in the four scenarios (AC, EC, PS, CS). Measurements were performed at the canopy-level. Periods of heat and drought spells are highlighted in red. Values represent means of n = 4 ± SE.

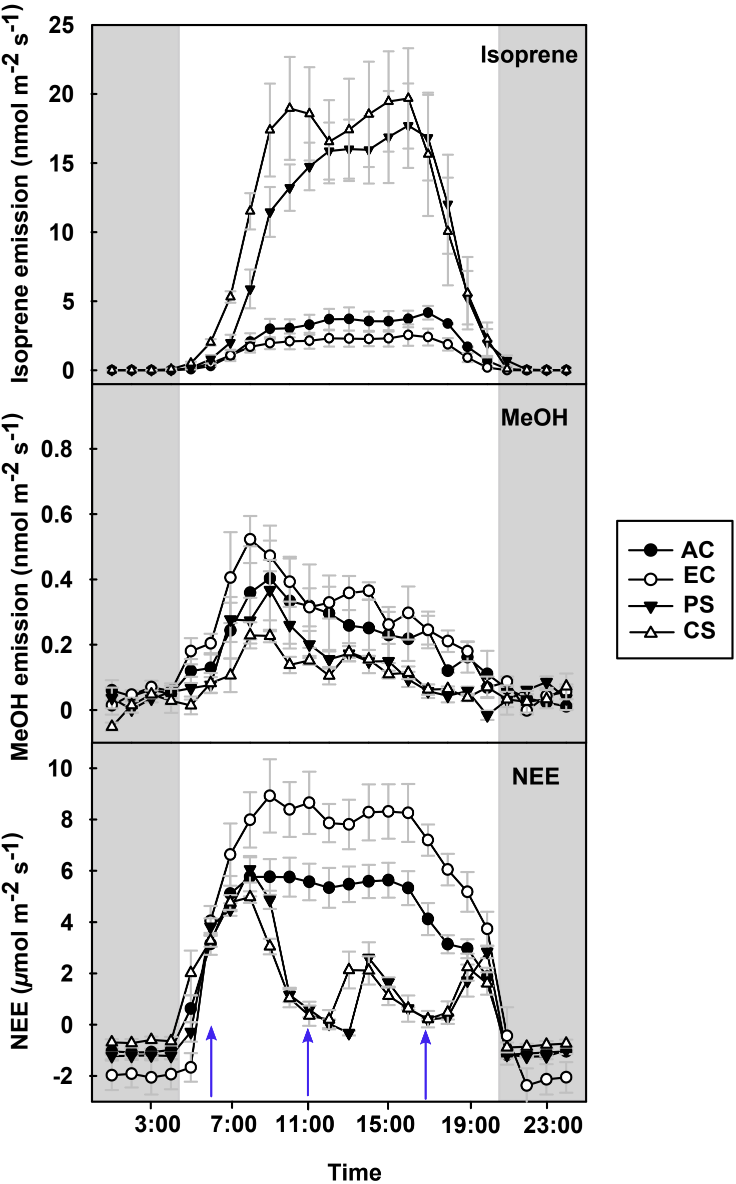

Figure S3. Representative day (d20) showing the canopy isoprene emission, MeOH emission and net ecosystem exchange (NEE) in the four scenarios. Blue arrows indicate time points of irrigation in the 4 scenarios (6:00; 12:00; 18:00, MEZ). Amount of water in AC and EC was higher than in PS and CS. Values for each scenario and treatments are given as mean of 4 sub-chambers (± SE). Dark hours are highlighted in grey. AC = control ambient [CO_2], EC = control elevated [CO_2], PS = periodic stress, CS = chronic stress.

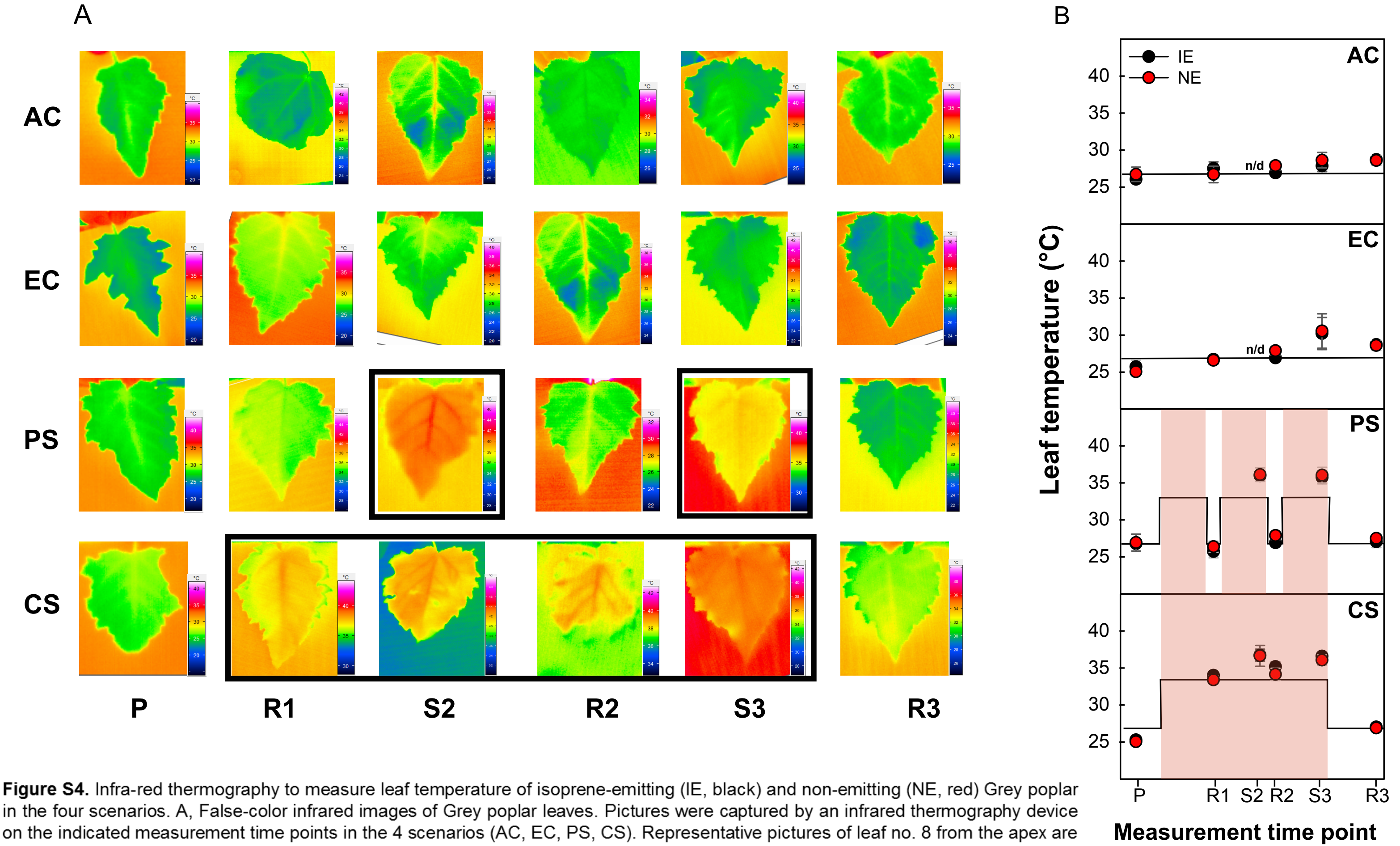

Figure S4. Infra-red thermography to measure leaf temperature of isoprene-emitting (IE, black) and non-emitting (NE, red) Grey poplar in the four scenarios. A, False-color infrared images of Grey poplar leaves. Pictures were captured by an infrared thermography device on the indicated measurement time points in the 4 scenarios (AC, EC, PS, CS). Representative pictures of leaf no. 8 from the apex are given. Black frames indicate heat and drought spells in the PS and CS scenario. B, Effect of 4 scenarios on the leaf temperature of isoprene-emitting (IE, black circles) and non-emitting (NE, red circles) poplar genotypes. Values represent means (± SE) of measurements performed in four sub-chambers; dashed lines denote the maximum air temperature during the light hours in the different scenarios. Thermal images were obtained using a thermographic digital camera (VarioCAM basic, Jenoptic Laser, Jena, Germany); pictures were taken from the adaxial side on the 8th leaf from the top at the time points P, R1, S2, R2, S3 and R3. Digital thermograms were analyzed with the IRBIS Plus software package (v. 2.2 Infratec, Dresden, Germany).

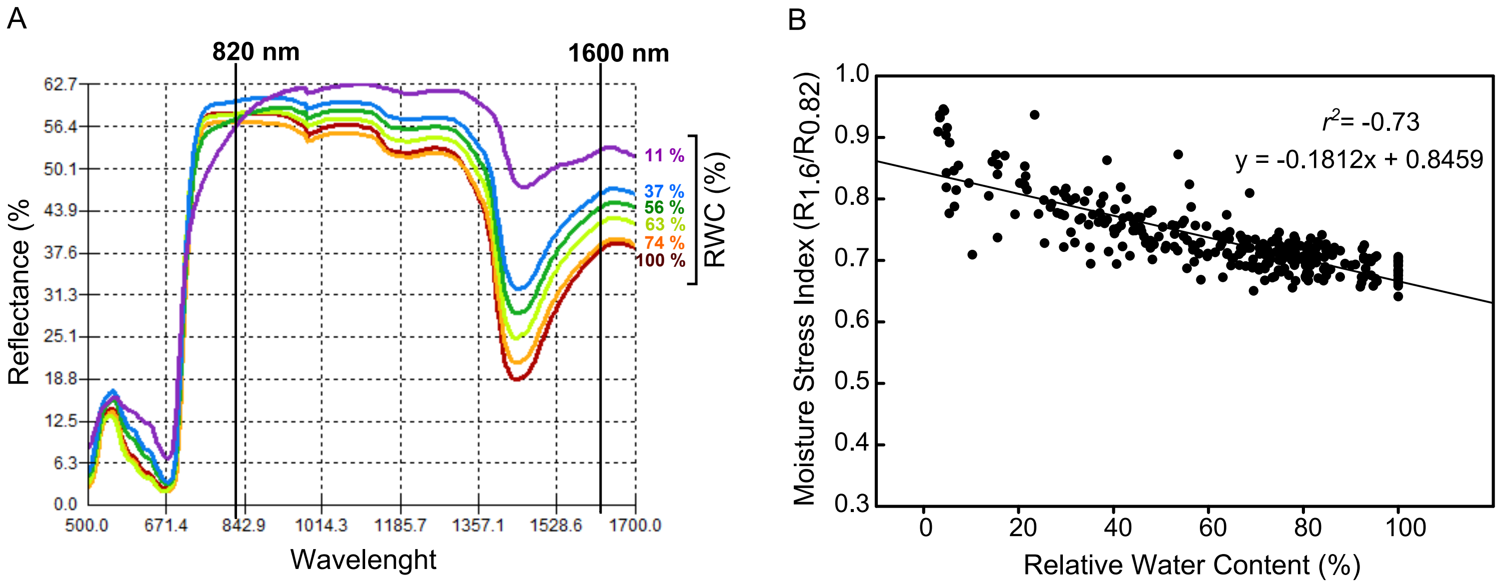

Figure S5. Drying experiment to assess the Moisture Stress Index and the Relative Water Context of Grey poplar leaves. A, Representative spectra of a leaf of Grey poplar during drying. Corresponding relative water contents (RWC) are given. Leaf reflectance was measured by near infrared spectrometry device, RWC was calculated based on the hourly leaf weight according the following equation: (FreshWeight-DryWeight)/($FreshWeight_0$-DryWeight). Wavelengths of 820 nm and 1600 nm (vertical lines) were used for calculation of the Moisture Stress Index (MSI = $Reflectance_{1600}$/$Reflectance_{820}$). B, Relationship of the MSI to the RWC of drying leaves of Grey poplar. Five plants of each isoprene-emitting and non-emitting poplar genotype were examined hourly by NIR reflectance. Regression equation and coefficient of correlation are given.

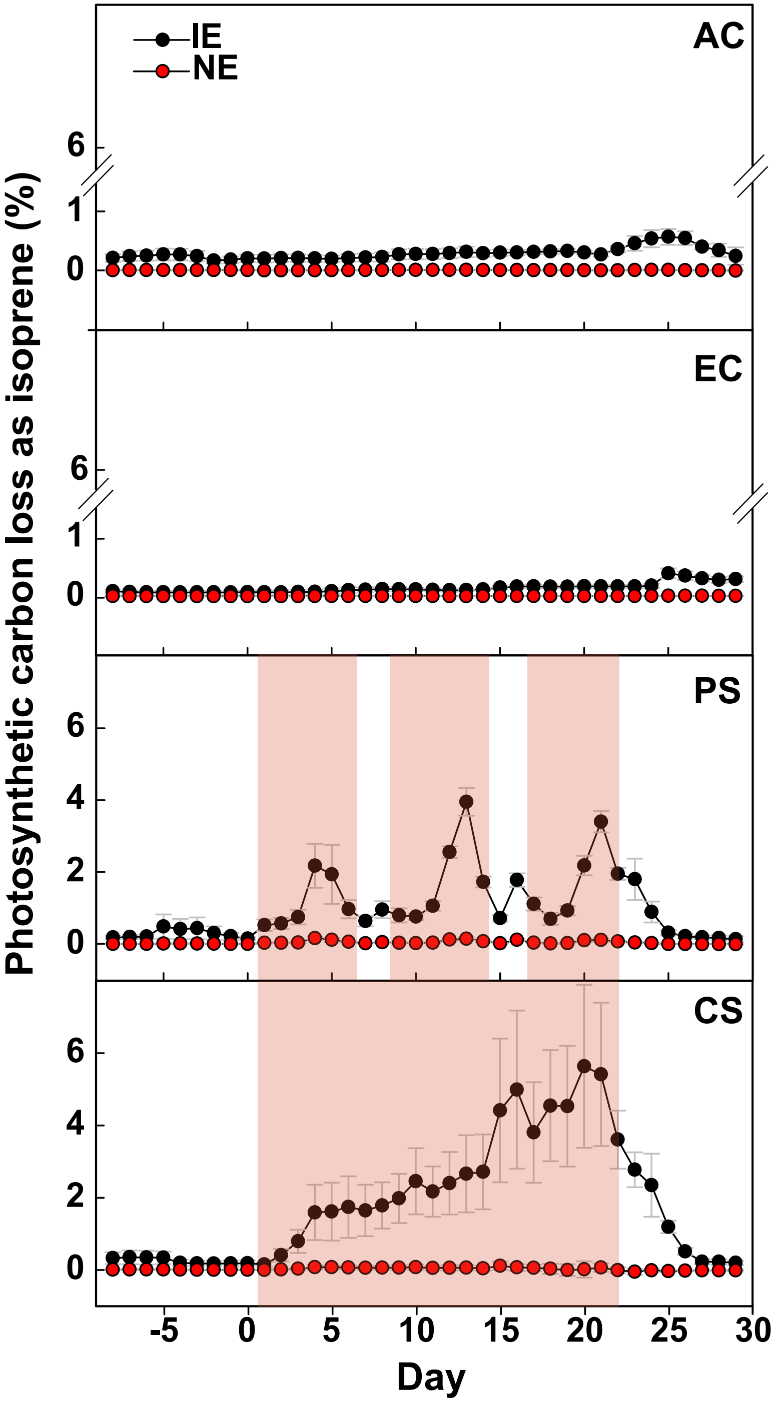

Figure S6. Time course showing the daily percentage of the photosynthetic carbon loss as isoprene in the four scenarios. Calculations are based on canopy CO_2 (NEE) and canopy isoprene emission. Values for each scenario are given as mean of n = 4 (± SE). The scenarios are: AC = control with ambient [CO_2], EC = control with elevated [CO_2], PS = periodic stress, CS = chronic stress. Periods of heat and drought are indicated in red.

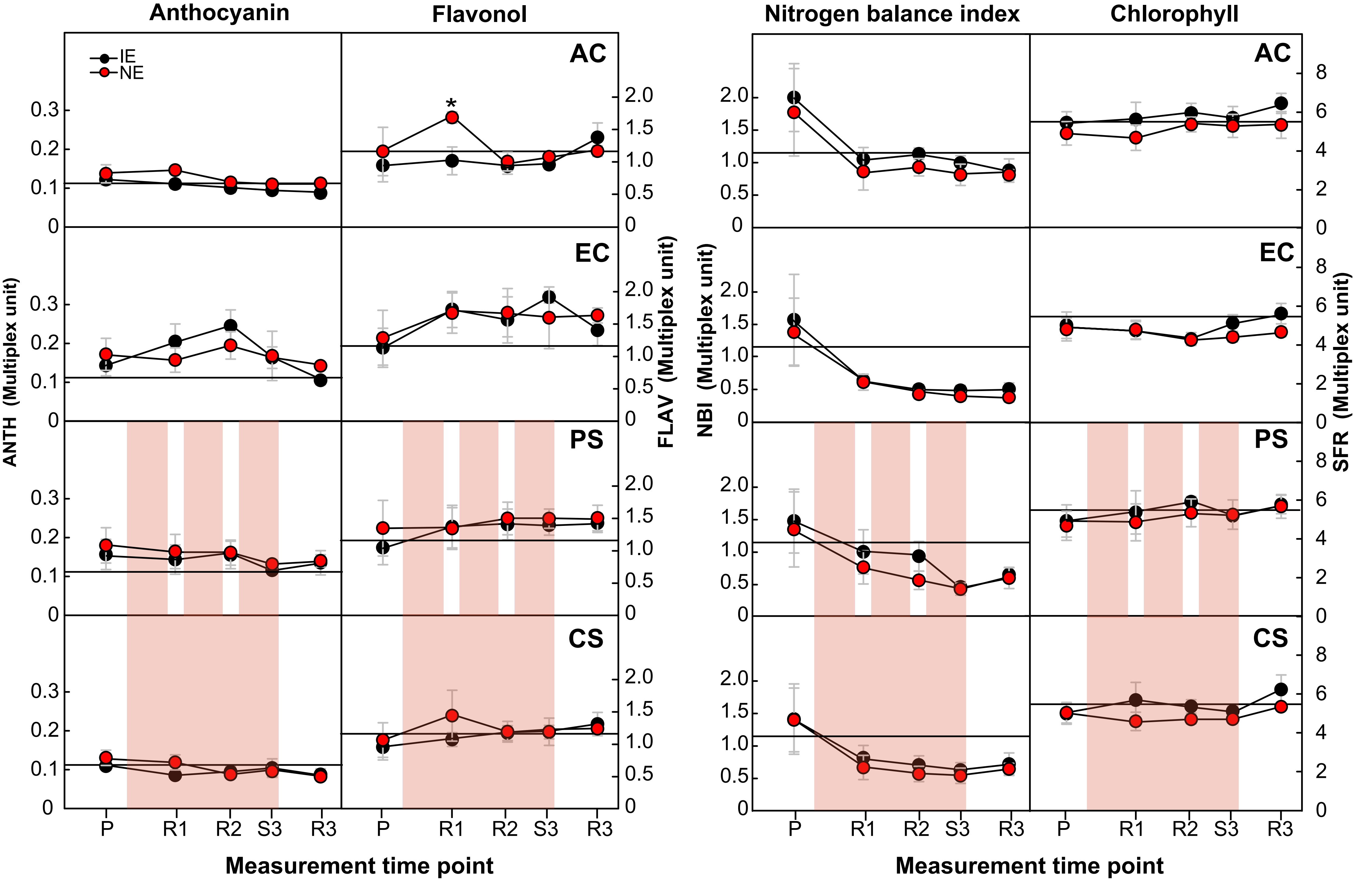

Figure S7. Effect of four scenarios on the anthocyanin index, flavonol index, nitrogen balance index (NBI®) and chlorophyll index of isoprene-emitting (IE, black circles) and non-emitting (NE, red circles) poplar genotypes. Measurement of the pigments was performed weekly by Multiplex® optical sensor (Force-A, Orsay, France). Values represent means (± SE) of measurements performed in 4 sub-chambers; dashed lines indicate an arbitrary reference value. Asterisks indicate significant genotype differences within each scenario and time point ($P < 0.05$).

Multiplex® optical sensor: The fluorescence signals are measured in the red (RF) and far-red (FRF) spectral regions excited under ultraviolet (UV), green (G) or red (R) radiation (in the following equations the subscripted characters indicate the excitation radiation). The simple chlorophyll fluorescence ratio (SFR) of far-red emission (735 nm) divided by red emission (685 nm) is linked to the chlorophyll content of the sample (Lichtenthaler et al., 1986; Buschmann, 2007). The flavonol index (FLAV), calculated according to equation $FLAV = \log(FRF_R/FRF_{UV})$, is proportional to the flavonol content of the leaf (Cerovic et al., 2002). Other fluorescence-based indices like the anthocyanin index $ANTH = \log(FRF_R/FRF_G)$ and the nitrogen balance index $NBI = FRF_{UV}/RF_G$ are also described in literature (Meyer et al., 2006; Agati et al., 2007). Multiplex® measurements were performed in situ under ambient light conditions on the time points pre-stress (P), recovery phase 1 (R1), recovery phase 2 (R2), stress cycle 3 (S3), and recovery phase 3 (R3) on 6 plants per genotype and scenario. A constant distance between sensor and leaves was kept at all measurements using a grid in front of the sensor.

Supplemental Tables

Table S1. Results of two-way ANOVAs and Bonferroni post-hoc tests for all measured parameters. Significant differences are marked in red when $P < 0.05$.

		Main effect genotypes				Scenario effect: Main scenario effect (IE + NE)						IE						NE					
	Time points	AC	EC	PS	CS	AC vs EC	AC vs PS	AC vs CS	EC vs PS	EC vs CS	PS vs CS	AC vs EC	AC vs PS	AC vs CS	EC vs PS	EC vs CS	PS vs CS	AC vs EC	AC vs PS	AC vs CS	EC vs PS	EC vs CS	PS vs CS
		Canopy-level																					
Net ecosystem exchange (NEE)	all time points	0.191	0.320	0.089	0.009	0.001	0.412	0.001	0.010	< 0.001	< 0.001	.	.	.	.	.	.	.	.	.	.	.	.
	P	0.348	0.961	0.205	0.372	1.000	0.172	1.000	0.532	1.000	0.164	1.000	0.988	1.000	1.000	1.000	1.000	1.000	0.517	1.000	0.544	1.000	0.052
	S1	0.338	0.566	0.700	0.542	1.000	< 0.001	< 0.001	< 0.001	< 0.001	1.000	1.000	0.045	0.051	0.004	0.005	1.000	1.000	0.008	< 0.001	0.088	0.009	1.000
	R1	0.531	0.499	0.967	0.605	0.768	0.018	< 0.001	1.000	< 0.001	< 0.001	0.515	0.088	0.019	1.000	< 0.001	< 0.001	1.000	0.441	< 0.001	1.000	0.001	< 0.001
	S2	0.567	0.899	0.425	0.789	1.000	< 0.001	< 0.001	< 0.001	< 0.001	0.961	1.000	0.001	0.014	< 0.001	0.002	1.000	1.000	< 0.001	0.001	< 0.001	0.001	1.000
	R2	0.846	0.516	0.016	0.042	0.278	< 0.001	< 0.001	0.004	0.028	1.000	0.376	< 0.001	< 0.001	0.015	0.082	1.000	1.000	0.005	0.014	0.408	0.705	1.000
	S3	0.985	0.793	0.643	0.511	1.000	< 0.001	< 0.001	< 0.001	< 0.001	1.000	1.000	0.001	0.001	0.001	0.001	1.000	1.000	< 0.001	< 0.001	< 0.001	< 0.001	1.000
	R3	0.846	0.516	0.016	0.042	0.278	< 0.001	< 0.001	0.004	0.028	1.000	0.376	< 0.001	< 0.001	0.015	0.082	1.000	1.000	0.005	0.014	0.408	0.705	1.000
Evapotranspiration	all time points	0.001	0.023	< 0.001	< 0.001	< 0.001	0.466	< 0.001	< 0.001	< 0.001	< 0.001	.	.	.	.	.	.	.	.	.	.	.	.
	P	0.710	< 0.001	0.523	0.011	< 0.001	0.001	0.573	< 0.001	< 0.001	0.186	< 0.001	0.167	0.142	< 0.001	< 0.001	1.000	1.000	0.009	1.000	1.000	1.000	0.012
	S1	< 0.001	< 0.001	< 0.001	0.021	< 0.001	< 0.001	< 0.001	< 0.001	< 0.001	0.240	< 0.001	0.005	< 0.001	< 0.001	< 0.001	< 0.001	1.000	< 0.001	0.092	< 0.001	0.023	0.157
	R1	0.001	< 0.001	< 0.001	0.118	0.002	0.594	< 0.001	0.139	< 0.001	< 0.001	< 0.001	0.528	< 0.001	0.007	< 0.001	< 0.001	1.000	1.000	0.222	1.000	0.187	0.042
	S2	0.012	< 0.001	< 0.001	0.736	0.006	< 0.001	< 0.001	< 0.001	< 0.001	1.000	0.004	0.001	< 0.001	< 0.001	< 0.001	0.726	1.000	< 0.001	0.059	< 0.001	0.005	0.021
	R2	0.525	0.007	0.031	0.836	1.000	1.000	< 0.001	1.000	< 0.001	< 0.001	0.034	0.180	< 0.001	1.000	< 0.001	< 0.001	1.000	1.000	< 0.001	1.000	< 0.001	< 0.001
	S3	0.979	0.012	0.020	0.857	0.267	< 0.001	< 0.001	< 0.001	< 0.001	1.000	0.025	0.013	< 0.001	< 0.001	< 0.001	0.706	1.000	< 0.001	< 0.001	< 0.001	0.002	1.000
	R3	0.901	0.077	0.550	0.138	0.295	< 0.001	< 0.001	0.001	0.900	0.017	0.112	< 0.001	0.002	0.288	1.000	0.544	1.000	< 0.001	0.141	0.003	0.908	0.063
Water use efficiency (WUE), canopy	all time points	< 0.001	0.003	< 0.001	< 0.001	0.099	1.000	1.000	0.007	0.001	1.000	.	.	.	.	.	.	.	.	.	.	.	.
	P	0.133	0.112	0.360	0.465	1.000	1.000	1.000	1.000	1.000	1.000	1.000	1.000	1.000	1.000	1.000	1.000	1.000	1.000	1.000	1.000	1.000	1.000
	S1	0.010	0.059	< 0.001	< 0.001	1.000	0.131	< 0.001	0.004	< 0.001	0.041	1.000	1.000	< 0.001	1.000	< 0.001	< 0.001	1.000	0.003	1.000	< 0.001	1.000	< 0.001
	R1	0.016	0.080	0.405	0.014	1.000	1.000	1.000	1.000	0.423	0.500	1.000	1.000	0.016	1.000	0.005	0.026	1.000	0.924	0.390	1.000	1.000	1.000
	S2	0.041	0.210	< 0.001	0.258	1.000	< 0.001	1.000	< 0.001	1.000	< 0.001	1.000	1.000	0.377	1.000	0.216	0.237	1.000	< 0.001	1.000	< 0.001	1.000	< 0.001
	R2	0.062	0.608	0.970	0.546	1.000	0.863	1.000	1.000	1.000	1.000	1.000	1.000	1.000	1.000	1.000	1.000	0.801	0.312	0.368	1.000	1.000	1.000
	S3	0.248	0.612	0.904	0.556	1.000	1.000	1.000	1.000	1.000	1.000	1.000	1.000	1.000	1.000	1.000	1.000	1.000	1.000	0.652	1.000	1.000	1.000
	R3	0.742	0.729	0.843	0.895	1.000	1.000	1.000	1.000	1.000	1.000	1.000	1.000	1.000	1.000	1.000	1.000	1.000	1.000	1.000	1.000	1.000	1.000
Electron transport rate (ETR) leaf4	all time points	0.677	0.918	0.017	0.344	1.000	0.793	1.000	0.177	1.000	0.063	.	.	.	.	.	.	.	.	.	.	.	.
	P	0.967	0.496	0.984	0.735	1.000	1.000	1.000	1.000	1.000	1.000	1.000	1.000	1.000	1.000	1.000	1.000	1.000	1.000	1.000	1.000	1.000	1.000
	S1	n/d	n/d	0.686	0.755	n/d	n/d	n/d	n/d	n/d	0.496	.	.	.	.	.	0.902	.	.	.	.	.	0.402
	R1	0.927	0.967	0.955	0.842	1.000	0.554	1.000	0.149	1.000	0.380	1.000	1.000	1.000	1.000	0.677	1.000	1.000	1.000	1.000	0.656	1.000	0.892

	S2	n/d	n/d	0.019	0.399	n/d	n/d	n/d	n/d	n/d	0.001	.	.	.	.	.	0.122	.	.	.	.	.	0.003
	R2	0.739	0.422	0.202	0.160	1.000	1.000	1.000	1.000	1.000	1.000	0.779	1.000	0.580	1.000	1.000	1.000	1.000	1.000	1.000	1.000	1.000	1.000
	S3	0.770	0.951	0.051	0.126	1.000	1.000	1.000	1.000	1.000	1.000	1.000	1.000	1.000	1.000	1.000	1.000	1.000	0.936	1.000	1.000	1.000	1.000
	R3	0.307	0.898	0.759	0.667	1.000	1.000	1.000	1.000	1.000	1.000	1.000	1.000	1.000	1.000	1.000	1.000	1.000	1.000	1.000	1.000	1.000	1.000
ETR leaf8	all time points	0.231	0.451	< 0.001	0.001	0.164	< 0.001	0.647	0.044	1.000	0.001	.	.	.	.	.	.	.	.	.	.	.	.
	P	0.735	0.894	0.742	0.629	1.000	1.000	0.374	1.000	1.000	0.850	1.000	1.000	1.000	1.000	1.000	1.000	1.000	1.000	0.504	1.000	1.000	0.893
	S1	.	.	0.024	0.758	n/d	n/d	n/d	n/d	n/d	0.566	.	.	.	.	.	0.565	.	.	.	.	.	0.167
	R1	0.984	0.742	0.735	0.622	1.000	1.000	1.000	1.000	1.000	0.334	1.000	1.000	1.000	1.000	1.000	0.462	1.000	1.000	1.000	1.000	1.000	1.000
	S2	.	.	< 0.001	0.003	n/d	n/d	n/d	n/d	n/d	< 0.001	.	.	.	.	.	0.074	.	.	.	.	.	< 0.001
	R2	0.593	0.926	0.291	0.007	1.000	0.536	0.265	1.000	0.815	1.000	1.000	1.000	1.000	1.000	1.000	1.000	1.000	0.024	0.072	1.000	0.109	1.000
	S3	0.255	0.412	0.014	0.005	0.004	< 0.001	0.001	0.016	1.000	0.048	0.054	0.001	0.353	1.000	1.000	0.242	0.128	< 0.001	0.003	0.020	0.023	0.515
	R3	0.518	0.758	0.681	0.934	0.256	1.000	1.000	0.227	0.544	1.000	0.649	1.000	1.000	0.763	1.000	1.000	1.000	1.000	1.000	0.982	0.982	1.000
ETR leaf12	all time points	0.453	0.746	< 0.001	0.010	1.000	< 0.001	0.113	< 0.001	0.234	0.014	.	.	.	.	.	.	.	.	.	.	.	.
	P	0.969	0.938	0.897	0.796	0.439	1.000	0.743	0.995	1.000	1.000	1.000	1.000	1.000	1.000	1.000	1.000	1.000	1.000	1.000	1.000	1.000	1.000
	S1	n/d	n/d	0.387	0.959	n/d	n/d	n/d	n/d	n/d	0.482	n/d	n/d	n/d	n/d	n/d	0.969	n/d	n/d	n/d	n/d	n/d	0.339
	R1	0.928	0.990	0.642	0.938	1.000	1.000	1.000	0.374	1.000	1.000	1.000	1.000	1.000	0.715	1.000	1.000	1.000	1.000	1.000	1.000	1.000	1.000
	S2	n/d	n/d	< 0.001	0.038	n/d	n/d	n/d	n/d	n/d	< 0.001	n/d	n/d	n/d	n/d	n/d	0.006	n/d	n/d	n/d	n/d	n/d	< 0.001
	R2	0.866	0.948	0.333	0.023	1.000	0.252	0.122	0.338	0.169	1.000	1.000	1.000	1.000	1.000	1.000	1.000	1.000	0.396	0.044	0.374	0.041	1.000
	S3	0.623	0.806	0.001	0.020	0.119	< 0.001	< 0.001	< 0.001	0.009	1.000	0.263	0.004	0.018	0.872	1.000	1.000	1.000	< 0.001	< 0.001	< 0.001	0.003	1.000
	R3	0.251	0.727	0.172	0.679	1.000	1.000	1.000	1.000	1.000	1.000	0.894	1.000	1.000	0.831	1.000	1.000	1.000	1.000	1.000	1.000	1.000	1.000
Isoprene emission, canopy	all time points	< 0.001	0.033	< 0.001	0.000	0.057	< 0.001	< 0.001	< 0.001	< 0.001	0.002	.	.	.	.	.	.	.	.	.	.	.	.
	P	0.112	0.703	0.155	0.159	0.853	1.000	1.000	1.000	1.000	1.000	1.000	1.000	1.000	1.000	1.000	1.000	1.000	1.000	1.000	1.000	1.000	1.000
	S1	0.126	0.577	< 0.001	< 0.001	1.000	0.084	0.100	0.073	0.078	1.000	1.000	0.008	0.004	0.007	0.003	1.000	1.000	1.000	1.000	1.000	1.000	1.000
	R1	0.117	0.473	0.051	< 0.001	1.000	1.000	< 0.001	1.000	0.001	0.001	1.000	1.000	< 0.001	1.000	< 0.001	< 0.001	1.000	1.000	1.000	1.000	1.000	1.000
	S2	0.063	0.503	< 0.001	< 0.001	1.000	< 0.001	< 0.001	< 0.001	< 0.001	1.000	1.000	< 0.001	< 0.001	< 0.001	< 0.001	1.000	1.000	1.000	1.000	1.000	1.000	1.000
	R2	0.065	0.394	0.001	< 0.001	1.000	1.000	< 0.001	1.000	< 0.001	0.002	1.000	0.782	< 0.001	0.419	< 0.001	< 0.001	1.000	1.000	1.000	1.000	1.000	1.000
	S3	0.058	0.412	< 0.001	< 0.001	1.000	0.002	< 0.001	0.004	< 0.001	1.000	1.000	< 0.001	< 0.001	< 0.001	< 0.001	0.366	1.000	1.000	1.000	1.000	1.000	1.000
	R3	0.009	0.094	0.006	0.003	1.000	1.000	1.000	1.000	1.000	1.000	1.000	1.000	1.000	1.000	1.000	1.000	1.000	1.000	1.000	1.000	1.000	1.000
Methanol emission, canopy	all time points	0.048	0.037	0.284	0.466	0.077	< 0.001	< 0.001	< 0.001	< 0.001	1.000	.	.	.	.	.	.	.	.	.	.	.	.
	P	0.040	0.898	0.135	0.885	1.000	1.000	1.000	1.000	0.241	0.351	0.591	1.000	1.000	1.000	1.000	1.000	1.000	1.000	0.437	1.000	0.674	0.188
	S1	0.420	0.789	0.624	0.684	1.000	0.096	0.204	1.000	1.000	1.000	1.000	0.719	1.000	1.000	1.000	1.000	1.000	0.372	0.214	1.000	1.000	1.000
	R1	0.351	0.355	0.595	0.873	1.000	0.798	0.038	0.247	0.014	1.000	0.810	1.000	0.961	0.172	0.053	1.000	1.000	1.000	0.080	1.000	0.532	1.000
	S2	0.493	0.396	0.798	0.515	0.414	0.022	0.067	< 0.001	0.001	1.000	0.243	0.378	1.000	0.003	0.019	1.000	1.000	0.135	0.084	0.105	0.070	1.000
	R2	0.809	0.305	0.876	0.697	1.000	0.140	0.014	0.022	0.002	1.000	0.871	0.701	0.372	0.040	0.019	1.000	1.000	0.591	0.079	0.919	0.210	1.000
	S3	0.957	0.167	0.789	0.920	0.127	0.143	0.286	< 0.001	0.001	1.000	0.088	0.523	1.000	0.001	0.003	1.000	1.000	0.802	0.831	0.250	0.259	1.000
	R3	0.624	0.077	0.715	0.939	0.010	1.000	1.000	0.009	0.011	1.000	0.004	1.000	1.000	0.011	0.009	1.000	1.000	1.000	1.000	0.960	1.000	1.000
Relative water content (RWC) leaf4	all time points	0.406	0.445	0.972	0.888	0.030	0.123	1.000	1.000	0.009	0.027	.	.	.	.	.	.	.	.	.	.	.	.
	P	0.926	1.000	0.577	0.642	0.022	1.000	0.082	0.201	1.000	0.795	0.212	1.000	0.696	0.497	1.000	1.000	0.253	1.000	0.317	1.000	1.000	1.000
	S1	n/d	n/d	0.931	0.853	n/d	n/d	n/d	n/d	n/d	0.659	n/d	n/d	n/d	n/d	n/d	0.731	n/d	n/d	n/d	n/d	n/d	0.780
	R1	0.391	0.895	0.710	0.404	1.000	1.000	0.477	1.000	1.000	0.260	1.000	1.000	1.000	1.000	1.000	0.577	1.000	1.000	1.000	1.000	1.000	1.000
	S2	n/d	n/d	0.780	0.853	n/d	n/d	n/d	n/d	n/d	0.043	n/d	n/d	n/d	n/d	n/d	0.228	n/d	n/d	n/d	n/d	n/d	0.096
	R2	0.458	0.238	0.853	0.642	1.000	0.082	0.137	1.000	0.016	< 0.001	0.423	0.256	1.000	1.000	0.053	0.016	1.000	0.833	0.163	1.000	0.581	0.002
	S3	0.710	0.358	0.516	0.458	0.656	1.000	1.000	1.000	0.066	0.351	0.423	1.000	1.000	1.000	0.253	1.000	1.000	1.000	0.990	1.000	0.677	0.990
	R3	0.780	0.793	0.458	0.780	0.895	0.001	0.000	0.420	0.004	0.260	1.000	0.016	0.001	0.497	0.080	1.000	1.000	0.062	< 0.001	1.000	0.098	0.317

RWC leaf 8	all time points	0.269	0.948	0.848	0.032	0.002	< 0.001	0.386	0.044	0.095	< 0.001	.	.	.	.	.	.	.	.	.	.	.	.
	P	0.919	0.772	0.682	0.414	1.000	1.000	0.588	1.000	0.758	0.898	1.000	1.000	1.000	1.000	1.000	1.000	1.000	1.000	0.760	1.000	0.686	1.000
	S1	n/d	n/d	1.000	0.759	n/d	n/d	n/d	n/d	n/d	0.188	n/d	n/d	n/d	n/d	n/d	0.298	n/d	n/d	n/d	n/d	n/d	0.414
	R1	0.479	0.470	0.838	0.262	1.000	0.005	1.000	0.117	1.000	0.005	1.000	0.026	1.000	1.000	1.000	0.016	1.000	0.313	1.000	0.280	1.000	0.503
	S2	n/d	n/d	1.000	1.000	n/d	n/d	n/d	n/d	n/d	0.010	n/d	n/d	n/d	n/d	n/d	0.067	n/d	n/d	n/d	n/d	n/d	0.067
	R2	0.474	0.772	0.540	0.609	0.073	< 0.001	1.000	0.086	0.027	1.000	0.339	< 0.001	1.000	0.580	0.231	1.000	0.580	< 0.001	1.000	0.408	0.280	< 0.001
	S3	0.838	0.664	0.682	0.682	0.045	0.007	1.000	1.000	0.002	< 0.001	0.231	0.255	1.000	1.000	0.019	0.011	0.488	0.052	1.000	1.000	0.189	0.011
	R3	0.262	0.312	0.084	0.012	0.053	< 0.001	< 0.001	< 0.001	0.027	0.371	0.488	< 0.001	< 0.001	< 0.001	0.686	0.004	0.280	< 0.001	< 0.001	0.408	0.080	1.000
RWC leaf 12	all time points	0.280	0.306	0.071	0.351	0.001	< 0.001	0.015	0.435	0.769	< 0.001	.	.	.	.	.	.	.	.	.	.	.	.
	P	0.938	0.827	0.487	0.487	1.000	1.000	0.618	1.000	1.000	1.000	1.000	1.000	1.000	1.000	1.000	1.000	1.000	1.000	0.863	1.000	1.000	1.000
	S1	n/d	n/d	0.617	0.817	n/d	n/d	n/d	n/d	n/d	0.916	n/d	n/d	n/d	n/d	n/d	0.775	n/d	n/d	n/d	n/d	n/d	0.643
	R1	0.373	0.051	0.106	0.589	1.000	0.980	1.000	1.000	1.000	0.767	1.000	1.000	1.000	1.000	1.000	1.000	1.000	1.000	1.000	1.000	1.000	0.639
	S2	n/d	n/d	0.643	0.817	n/d	n/d	n/d	n/d	n/d	0.035	n/d	n/d	n/d	n/d	n/d	0.166	n/d	n/d	n/d	n/d	n/d	0.106
	R2	0.589	0.743	0.248	1.000	0.502	< 0.001	1.000	0.146	1.000	0.003	0.616	0.011	1.000	1.000	1.000	0.331	1.000	0.001	1.000	0.147	1.000	0.015
	S3	0.643	0.743	0.757	0.699	0.104	0.006	1.000	1.000	0.341	0.036	0.234	0.087	1.000	1.000	1.000	0.639	1.000	0.131	1.000	1.000	1.000	0.131
	R3	0.699	0.445	0.938	0.106	0.116	< 0.001	< 0.001	0.006	1.000	0.016	1.000	< 0.001	0.192	0.038	1.000	0.023	0.314	< 0.001	0.005	0.314	1.000	0.995
Relative leaf expansion rate (RLER)	S3	0.997	n/d	0.881	0.608	n/d	0.001	< 0.001	n/d	n/d	1.000	n/d	0.017	0.003	n/d	n/d	1.000	n/d	0.024	0.010	n/d	n/d	1.000
Area per leaf	S3	0.495	n/d	0.436	0.896	n/d	0.002	0.002	n/d	n/d	1.000	n/d	0.030	0.014	n/d	n/d	1.000	n/d	0.024	0.048	n/d	n/d	1.000
Cell number	S3	0.368	n/d	0.877	0.371	n/d	0.072	0.270	n/d	n/d	1.000	n/d	0.142	0.747	n/d	n/d	1.000	n/d	0.565	0.578	n/d	n/d	1.000
Cell size	S3	0.672	n/d	0.586	0.366	n/d	0.002	< 0.001	n/d	n/d	1.000	n/d	0.027	0.002	n/d	n/d	0.643	n/d	0.021	0.032	n/d	n/d	1.000
Carbon sum	all time points	0.579	0.634	0.391	0.344	0.790	1.000	0.021	0.086	0.002	0.268	0.664	1.000	0.675	0.499	0.041	0.941	1.000	0.819	0.044	0.369	0.024	0.804
Anthocyanin index (ANTH)	all time points	0.216	0.780	0.632	0.690	< 0.001	0.047	1.000	0.336	< 0.001	0.001	.	.	.	.	.	.	.	.	.	.	.	.
	P	0.676	0.426	0.516	0.552	1.000	0.775	1.000	1.000	0.837	0.035	1.000	1.000	1.000	1.000	1.000	1.000	1.000	1.000	1.000	1.000	1.000	1.000
	R1	0.419	0.308	0.565	0.357	0.621	1.000	1.000	1.000	0.050	0.265	0.102	1.000	1.000	0.703	0.016	0.657	1.000	1.000	1.000	1.000	1.000	1.000
	R2	0.693	0.283	0.867	0.850	0.001	0.287	1.000	0.227	< 0.001	0.056	0.008	0.774	1.000	0.263	0.005	0.560	0.244	1.000	1.000	1.000	0.040	0.257
	S3	0.675	0.920	0.685	0.804	0.192	1.000	1.000	0.354	0.157	1.000	0.470	1.000	1.000	1.000	0.775	1.000	1.000	1.000	1.000	0.754	0.602	1.000
	R3	0.491	0.339	0.894	0.889	1.000	0.840	1.000	1.000	1.000	0.345	1.000	1.000	1.000	1.000	1.000	1.000	1.000	1.000	1.000	1.000	0.735	0.820
Flavonol index (FLAV)	all time points	0.203	0.900	0.834	0.591	0.002	0.163	1.000	0.490	0.015	0.848	.	.	.	.	.	.	.	.	.	.	.	.
	P	0.538	0.668	0.393	0.752	1.000	1.000	1.000	1.000	1.000	1.000	1.000	1.000	1.000	1.000	1.000	1.000	1.000	1.000	1.000	1.000	1.000	1.000
	R1	0.049	0.902	0.933	0.295	0.354	1.000	1.000	1.000	0.722	1.000	0.133	0.652	1.000	1.000	0.504	1.000	1.000	1.000	1.000	1.000	1.000	1.000
	R2	0.839	0.807	0.792	0.955	0.156	0.347	1.000	1.000	0.739	1.000	0.886	1.000	1.000	1.000	1.000	1.000	0.489	1.000	1.000	1.000	1.000	1.000
	S3	0.731	0.483	0.471	0.981	0.071	1.000	1.000	0.554	0.286	1.000	0.080	1.000	1.000	1.000	0.326	1.000	1.000	1.000	1.000	1.000	1.000	1.000
	R3	0.549	0.543	0.825	0.860	1.000	1.000	1.000	1.000	1.000	1.000	1.000	1.000	1.000	1.000	1.000	1.000	1.000	1.000	1.000	1.000	1.000	1.000
Nitrogen balance index (NBI)	all time points	0.348	0.512	0.320	0.614	0.066	0.119	0.107	1.000	1.000	1.000	.	.	.	.	.	.	.	.	.	.	.	.
	P	0.585	0.647	0.756	0.974	1.000	0.645	0.616	1.000	1.000	1.000	1.000	1.000	0.948	1.000	1.000	1.000	1.000	1.000	1.000	1.000	1.000	1.000
	R1	0.650	0.942	0.566	0.715	1.000	1.000	1.000	1.000	1.000	1.000	1.000	1.000	1.000	1.000	1.000	1.000	1.000	1.000	1.000	1.000	1.000	1.000
	R2	0.619	0.851	0.370	0.738	0.343	1.000	1.000	1.000	1.000	1.000	0.797	1.000	1.000	1.000	1.000	1.000	1.000	1.000	1.000	1.000	1.000	1.000
	S3	0.658	0.658	0.746	0.829	1.000	0.574	1.000	0.575	1.000	1.000	1.000	1.000	1.000	1.000	1.000	1.000	1.000	1.000	1.000	1.000	1.000	1.000
	R3	0.872	0.758	0.896	0.857	1.000	1.000	1.000	1.000	1.000	1.000	1.000	1.000	1.000	1.000	1.000	1.000	1.000	1.000	1.000	1.000	1.000	1.000
Chlorophyll index (SFR)	all time points	0.049	0.331	0.176	0.123	0.078	1.000	1.000	0.888	0.761	1.000	.	.	.	.	.	.	.	.	.	.	.	.
	P	0.529	0.802	0.771	0.955	1.000	1.000	1.000	1.000	1.000	1.000	1.000	1.000	1.000	1.000	1.000	1.000	1.000	1.000	1.000	1.000	1.000	1.000
	R1	0.284	0.954	0.556	0.209	1.000	1.000	1.000	1.000	1.000	1.000	1.000	1.000	1.000	1.000	1.000	1.000	1.000	1.000	1.000	1.000	1.000	1.000

	R2	0.502	0.950	0.510	0.444	0.167	1.000	1.000	0.172	1.000	1.000	0.375	1.000	1.000	0.388	1.000	1.000	1.000	1.000	1.000	1.000	1.000	1.000
	S3	0.634	0.407	0.185	0.639	1.000	0.938	1.000	1.000	1.000	1.000	1.000	1.000	1.000	1.000	1.000	1.000	1.000	0.770	1.000	1.000	1.000	1.000
	R3	0.203	0.276	0.908	0.308	1.000	1.000	1.000	1.000	1.000	1.000	1.000	1.000	1.000	1.000	1.000	1.000	1.000	1.000	1.000	1.000	1.000	1.000
Temperature (leaf)	all time points	0.659	0.864	0.553	0.559	1.000	0.830	< 0.001	1.000	< 0.001	< 0.001	.	.	.	.	.	.	.	.	.	.	.	.
	P	0.710	0.713	0.933	0.888	1.000	1.000	1.000	1.000	1.000	1.000	1.000	1.000	1.000	1.000	1.000	1.000	1.000	1.000	1.000	1.000	1.000	1.000
	R1	0.531	0.926	0.615	0.638	1.000	1.000	< 0.001	1.000	< 0.001	< 0.001	1.000	1.000	< 0.001	1.000	< 0.001	< 0.001	1.000	1.000	< 0.001	1.000	< 0.001	< 0.001
	S2	n/d	n/d	0.931	0.955	.	.	.	.	.	0.615	.	.	.	.	.	0.669	.	.	.	.	.	0.776
	R2	0.592	0.731	0.680	0.572	1.000	0.657	< 0.001	0.051	< 0.001	< 0.001	1.000	1.000	< 0.001	0.332	0.003	< 0.001	1.000	1.000	0.006	0.385	0.044	< 0.001
	S3	0.548	0.793	n/d.	n/d.	0.022	.	.	.	.	.	0.072	.	.	.	.	.	0.141	.	.	.	.	.
	R3	0.929	0.662	0.724	0.918	1.000	0.805	0.396	1.000	1.000	1.000	1.000	1.000	1.000	1.000	1.000	1.000	1.000	1.000	1.000	1.000	1.000	1.000
Stem water potential (mid-day)	all time points	0.240	0.384	0.656	0.447	0.329	0.011	< 0.001	1.000	< 0.001	0.002	.	.	.	.	.	.	.	.	.	.	.	.
	S3	0.250	0.844	0.650	0.473	1.000	< 0.001	< 0.001	0.006	< 0.001	0.002	1.000	0.002	< 0.001	0.044	< 0.001	0.034	0.808	< 0.001	< 0.001	0.194	< 0.001	0.068
	R3	0.606	0.221	0.860	0.720	0.839	1.000	1.000	0.050	1.000	0.729	1.000	1.000	1.000	1.000	1.000	1.000	0.350	1.000	1.000	0.065	0.651	1.000
Leaf-level																							
Transpiration (E)	all time points	0.002	0.971	< 0.001	< 0.001	0.855	0.001	0.011	0.058	0.450	1.000	.	.	.	.	.	.	.	.	.	.	.	.
	S3	0.055	0.804	0.975	0.695	0.049	< 0.001	< 0.001	0.001	< 0.001	1.000	0.043	< 0.001	< 0.001	0.023	0.019	1.000	1.000	0.002	< 0.001	0.041	0.012	1.000
	R3	0.263	0.184	0.390	0.079	1.000	1.000	0.077	1.000	0.352	0.699	1.000	1.000	0.216	1.000	0.708	0.706	1.000	1.000	0.845	1.000	1.000	1.000
Net assimilation (A)	all time points	0.027	0.016	0.186	0.028	0.649	1.000	1.000	0.219	0.098	1.000	.	.	.	.	.	.	.	.	.	.	.	.
	S3	0.050	0.099	0.531	0.418	1.000	< 0.001	< 0.001	< 0.001	< 0.001	1.000	1.000	0.001	< 0.001	0.002	0.001	1.000	1.000	0.047	0.008	0.046	0.008	1.000
	R3	0.225	0.071	0.212	0.021	0.089	0.001	< 0.001	0.657	0.373	1.000	0.248	0.029	0.003	1.000	0.674	1.000	0.872	0.032	0.081	0.932	1.000	1.000
Water-use efficiency (WUE)	all time points	0.784	0.710	0.123	0.220	0.033	< 0.001	< 0.001	< 0.001	0.001	1.000	.	.	.	.	.	.	.	.	.	.	.	.
	S3	0.749	0.532	0.063	0.241	0.074	< 0.001	< 0.001	< 0.001	< 0.001	1.000	0.150	< 0.001	< 0.001	0.002	0.001	1.000	1.000	0.001	< 0.001	0.071	0.005	1.000
	R3	0.946	0.921	0.755	0.571	0.827	0.016	0.290	0.634	1.000	1.000	1.000	0.115	0.517	1.000	1.000	1.000	1.000	0.280	1.000	1.000	1.000	1.000
Stomatal conductance (g_s)	all time points	0.033	0.270	0.773	0.116	0.812	0.002	0.023	0.164	0.804	1.000	.	.	.	.	.	.	.	.	.	.	.	.
	S3	0.048	0.815	0.981	0.734	0.042	< 0.001	< 0.001	0.002	0.001	1.000	0.035	< 0.001	< 0.001	0.045	0.038	1.000	1.000	0.004	0.001	0.077	0.028	1.000
	R3	0.291	0.186	0.701	0.061	1.000	1.000	0.068	1.000	0.333	1.000	1.000	1.000	0.160	1.000	0.600	0.529	1.000	1.000	0.948	1.000	1.000	1.000
Intracellular [CO_2] (c_i)	all time points	0.847	0.905	0.346	0.985	< 0.001	1.000	1.000	< 0.001	0.002	1.000	.	.	.	.	.	.	.	.	.	.	.	.
	S3	0.875	0.726	0.299	0.576	0.099	0.341	0.119	< 0.001	< 0.001	1.000	0.837	0.318	0.840	0.006	0.025	1.000	0.299	1.000	0.376	0.045	0.002	1.000
	R3	0.909	0.856	0.769	0.558	< 0.001	0.104	0.002	0.410	1.000	1.000	0.020	0.783	0.138	0.756	1.000	1.000	0.024	0.343	0.022	1.000	1.000	1.000
c_i/c_a	all time points	0.495	0.171	< 0.001	< 0.001	1.000	0.002	0.011	< 0.001	< 0.001	1.000	.	.	.	.	.	.	.	.	.	.	.	.
	S3	0.979	0.735	0.253	0.757	1.000	< 0.001	< 0.001	< 0.001	< 0.001	1.000	1.000	< 0.001	0.001	0.001	0.002	1.000	1.000	0.015	< 0.001	0.013	< 0.001	1.000
	R3	0.715	0.576	0.564	0.677	0.395	1.000	0.987	0.331	1.000	0.851	0.956	1.000	1.000	0.334	1.000	1.000	1.000	1.000	1.000	1.000	1.000	1.000
Transpiration dark (E_d)	all time points	0.593	0.798	0.429	0.221	.	.	.	.	.	.	.	.	.	.	.	.	.	.	.	.	.	.
	S3	0.378	0.606	0.769	0.938	0.865	< 0.001	< 0.001	0.023	0.031	1.000	0.515	0.002	0.004	0.280	0.424	1.000	1.000	0.072	0.068	0.168	0.159	1.000
	R3	0.898	0.876	0.409	0.073	0.536	0.001	< 0.001	0.181	< 0.001	0.022	1.000	0.107	< 0.001	< 0.001	< 0.001	0.006	1.000	0.016	0.001	0.261	0.033	1.000
Respiration dark (R_d)	all time points	0.509	0.309	0.456	0.830	0.843	0.361	0.001	1.000	0.061	0.175	.	.	.	.	.	.	.	.	.	.	.	.
	S3	0.060	0.987	0.352	0.920	1.000	1.000	1.000	1.000	1.000	0.607	1.000	1.000	1.000	1.000	1.000	1.000	1.000	0.185	1.000	1.000	1.000	0.695
	R3	0.329	0.148	0.051	0.839	0.112	0.002	< 0.001	0.991	0.032	0.830	0.333	1.000	0.008	1.000	0.957	0.210	0.876	0.001	0.001	0.053	0.058	1.000

Isoprene emission, leaf-level	all time points	< 0.001	0.000	< 0.001	< 0.001	0.039	1.000	1.000	0.064	0.855	1.000	.	.	.	.	.	.	.	.	.	.	.	.
	S3	< 0.001	0.001	< 0.001	< 0.001	0.466	1.000	1.000	0.155	1.000	1.000	0.114	1.000	1.000	0.018	0.950	0.581	1.000	1.000	1.000	1.000	1.000	1.000
	R3	< 0.001	0.002	< 0.001	< 0.001	0.199	1.000	1.000	0.906	1.000	1.000	0.476	1.000	1.000	0.316	0.772	1.000	1.000	1.000	1.000	1.000	1.000	1.000
Photosynthetic carbon lost as isoprene (C%)	all time points	< 0.001	0.044	< 0.001	< 0.001	1.000	0.418	0.318	0.013	0.009	1.000	.	.	.	.	.	.	.	.	.	.	.	.
	S3	0.020	0.124	< 0.001	< 0.001	1.000	0.010	0.002	0.001	< 0.001	1.000	1.000	< 0.001	< 0.001	< 0.001	< 0.001	1.000	1.000	1.000	1.000	1.000	1.000	1.000
	R3	0.004	0.180	0.042	0.091	1.000	1.000	1.000	1.000	1.000	1.000	0.560	1.000	1.000	1.000	1.000	1.000	1.000	1.000	1.000	1.000	1.000	1.000
Net ecosystem productivity	all time points	0.191	0.630	0.687	0.056	0.126	1.000	0.062	1.000	0.010	0.002	.	.	.	.	.	.	.	.	.	.	.	.
	P	0.137	0.840	0.030	0.569	1.000	0.141	1.000	1.000	0.644	0.006	1.000	1.000	1.000	1.000	1.000	1.000	1.000	0.299	0.414	0.637	0.823	0.002
	S3	0.482	0.740	0.711	0.518	1.000	0.002	< 0.001	< 0.001	< 0.001	0.103	1.000	0.216	0.002	0.019	< 0.001	0.696	1.000	0.012	< 0.001	0.023	< 0.001	0.395
	R3	0.943	0.482	0.013	0.035	0.188	< 0.001	< 0.001	0.049	0.183	1.000	0.302	< 0.001	< 0.001	0.076	0.276	1.000	1.000	0.026	0.052	1.000	1.000	1.000
Net isoprene loss	all time points	0.000	0.059	< 0.001	0.000	1.000	0.153	0.003	0.022	0.001	0.930	.	.	.	.	.	.	.	.	.	.	.	.
	P	0.042	0.559	0.030	0.026	1.000	1.000	1.000	1.000	1.000	1.000	1.000	1.000	1.000	1.000	1.000	1.000	1.000	1.000	1.000	1.000	1.000	1.000
	S3	0.022	0.381	0.000	< 0.001	1.000	0.002	< 0.001	0.002	< 0.001	0.964	1.000	< 0.001	< 0.001	< 0.001	< 0.001	0.215	1.000	1.000	1.000	1.000	1.000	1.000
	R3	0.002	0.068	0.003	< 0.001	1.000	1.000	1.000	1.000	1.000	1.000	1.000	1.000	0.460	1.000	0.314	0.295	1.000	1.000	1.000	1.000	1.000	1.000

Table S2. Calculated angles of different stress phases of cumulative net C gain. Phases are: P = pre-stress, S1 = stress cycle 1, R1 = recovery phase 1, S2 = stress cycle 2, R2 = recovery phase 2, S3 = stress cycle 3, R3 = recovery phase 3. In CS scenario, the phases are named as follows: P = pre-stress, S_{IN} = stress initial, S_{SEV} = stress severe, R = recovery. The scenarios are: AC = control with ambient [CO_2], EC = control with elevated [CO_2], PS = periodic stress, CS = chronic stress. IE = isoprene-emitting, NE = non-emitting.

AC			**EC**			**PS**			**CS**		
	IE	**NE**		**IE**	**NE**		**IE**	**NE**		**IE**	**NE**
P	27.5°	30.0°	P	29.0°	29.0°	P	38.0°	38.0°	P	38.0°	37.5°
						S1	20.0°	21.0°	S_{IN}	25.0°	22.0°
						R1	39.0°	39.0°	S_{SEV}	15.5°	12.0°
						S2	9.0°	10.0°	R	43.5°	42.0°
						R2	39.5°	37.0°			
						R3	16.0°	14.0°			
						R3	42.5°	36.0°			